May 2019

Behavior and Design of Post-Installed Anchors in Thin Concrete Members

Ahmad Nawaf Tarawneh
Clemson University, eng.tarawneh.90@gmail.com

BEHAVIOR AND DESIGN OF POST-INSTALLED ANCHORS IN THIN CONCRETE MEMBERS

A Dissertation
Presented to
the Graduate School of
Clemson University

In Partial Fulfillment
of the Requirements for the Degree
Doctor of Philosophy
Civil Engineering

---

by
Ahmad Nawaf Tarawneh
May 2019

Accepted by:
Dr. Brandon E. Ross, Committee Chair
Dr. Thomas E. Cousins, Co-Committee Chair
Dr. Weichiang Pang
Dr. Laura Redmond

ABSTRACT

This dissertation evaluates the behavior and capacity of single screw and adhesive anchors in thin concrete members that do not meet the minimum thickness requirements of current standards for anchorage. This dissertation focuses on the concept of full thickness embedment, wherein anchors are embedded through the entire thickness of the concrete member, and its implications. This is the first exclusive study on the concept of full thickness embedment anchors. In addition, this dissertation provides design models for single anchors in thin concrete members subjected to tension and shear loads.

Three experimental programs were conducted to investigate the tensile and shear capacity of screw and adhesive anchors with a total of 350 tests. Variables included are concrete compressive strength, concrete thickness, anchor type, anchor diameter, screw and adhesive manufacturer, and edge distance for shear tests. Experimental data were used to develop the aforementioned design models for anchors in tension and shear. Consistent with modern standards for anchor design, the proposed design models are based on the 5% lower fractile and 90% confidence.

It is shown that drilling through the concrete thickness causes the concrete to blowout at the back-face. The blowout is conical in shape with the depth of the blowout ranging from 0.65 to 0.96. This blowout affects the tensile capacity of screw anchors as the embedment depth is reduced by the depth of the blowout. However, back-face blowout effect was not noticeable in adhesive anchors as the adhesive fills the crack and fractures due to drilling. As a result, adhesive anchors have substantially higher tensile capacity

compared to screw anchors. For example, typical adhesive anchor capacity in a 2-in. thick concrete member is almost four times larger than typical screw anchor capacity. In addition, adhesive anchors showed consistent performance independent of the adhesive supplier, unlike screw anchors wherein the failure mode and capacity were dependent on the product itself.

Back-face blowout also affects shear capacity of screw anchors. However, the effect is less significant than on tension capacity. The reduction in the capacity (relative to adhesive anchors) is attributed to the reduction of the anchor stiffness due to the blowout.

Modifications to the Concrete Capacity Design method are proposed to extend the method to full thickness embedment anchors in thin concrete members. To include the effect of back-face blowout on screw anchors in tension and shear, a reduced embedment depth and shear transfer length is proposed. In addition, a revised thickness modification factor is proposed for anchors subjected to shear loads.

DEDICATION

This dissertation is dedicated to my parents Randa Burjak and Nawaf Tarawneh for their endless love and support throughout my whole life. Without their loving support, I could not have made it this far. Words cannot express my feelings and gratitude.

I would like also to dedicate this dissertation to my beautiful and supportive wife Ruaa Alawadi for her support and her love. I love you all.

ACKNOWLEDGMENTS

First and foremost, I would like to thank Allah for giving me the opportunity, hope, strength, and patient to complete this dissertation. Without his blessing, this work would not have been completed.

I would like to thank and acknowledge my advisors Dr. Brandon Ross and Dr. Thomas Cousins for their continuous guidance, patient, and support throughout my study. Their guidance improved the quality of my research and led to writing this manuscript. In addition to my advisors, I would like to thank my committee members Dr. Weichiang Pang and Dr. Laura Redmond for their helpful comments and guidance.

I would like to thank the lab technicians Daniel Metz and Scott Black for their help in the experimental program. In addition, I would like to thank Marcos Martínez and Haitham Zaidan for their assistance in conducting the experimental work.

Furthermore, I would like to thank Metromont Corporation for providing a research topic and concrete panel specimens; and Dewalt, Redhead ITW, and Simpson strong-tie for sponsoring this research. Moreover, I am thankful for the Hashemite University in Jordan for providing financial support.

Last but not least, I would like to thank my parents and my wife for believing in me and supporting me to turn my dream into reality.

TABLE OF CONTENTS

Table of Contents (Continued) Page

LIST OF TABLES

LIST OF FIGURES

CHAPTER ONE

INTRODUCTION

1.1 Research Motivation

Precast concrete sandwich wall panel systems have been used in the construction industry in the past 50 years (Losch et al. 2011) for their structural and thermal insulation efficiency. Precast sandwich panels consist of two thin concrete layers separated by a thermal insulation layer (Fig. 1-1). The concrete layers are commonly made structurally composite using shear connecters. Precast concrete sandwich wall panels are used as exterior and interior walls as partitions in different types of buildings. The concrete layer thicknesses in sandwich panels are made to be as thin as possible, but within the practical limits of panel usage and design (Losch et al. 2011). Typically, concrete layers thickness range from 2 to 5 in. (50.8-127 mm).

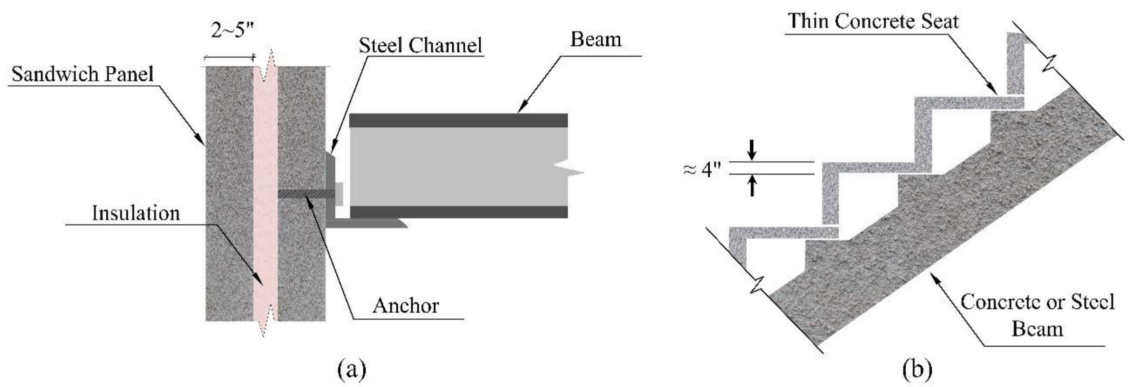

Fig. 0-1. Thin concrete layers (a) Sandwich panels (b) Stadium seating.

Connecting precast sandwich panels to other concrete or steel members can be attained using anchors. Concrete anchors come in many categories (Fig. 1-2). The general categories are cast-in place anchors which are installed before the concrete cures, and post-installed anchors which are installed into cured concrete (Cook et al. 2003). Post-installed anchors can be divided into subcategories based on load transfer mechanism (Fig. 1-1). Mechanical anchors transfer loads through mechanical interlock; bonded anchors transfer load through a bonding agent between the anchor and the concrete.

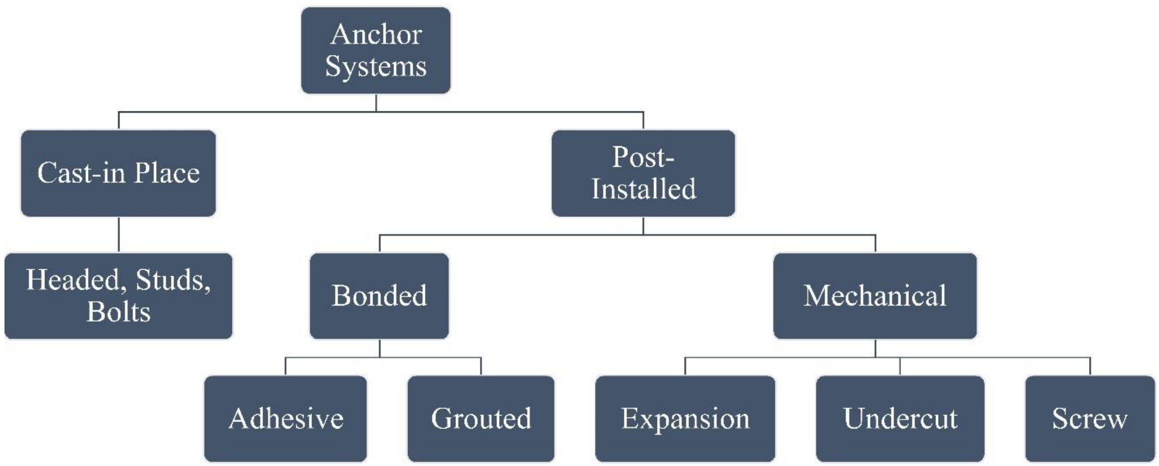

Fig. 0-2. Anchorage systems.

Post-installed anchorage systems have seen increased use due to the growing demand for more flexible planning and construction (PCI design manual 2017). Post-installed anchors have the advantage to be more flexible in job sites because the installation location can be easily adjusted to ensure proper alignment of connecting members and retrofits. However, anchorage to sandwich panels can be challenging precisely because of their thinness and lack of information regarding anchorage in such members. Code and specification impose limitations on the minimum concrete member thickness and minimum anchor embedment depth that prevents engineers from designing anchors in sandwich panels and in thin concrete members in general. These limitations will be discussed in greater detail later in this dissertation.

The continuing use of sandwich wall panels and the benefits of flexible post-installed anchorage systems motivates the investigation of capacity and behavior of post-installed anchorage systems in thin concrete members. The behavior and capacity of screw and adhesive anchors including experimental variables have been chosen for the current study based on recommendation from concrete and anchors suppliers. In this manner the results can be readily applied to conditions encountered in precast sandwich panel buildings.

1.2 Dissertation Contributions

This research presents the results and the analysis of three experimental programs that describe the behavior and capacity of screw and adhesive post-installed anchors in thin concrete members under tensile and shear loads. The first two experimental programs investigated the tensile behavior and capacity of screw and adhesive anchors through series of unconfined pullout tests. Variables included in the experimental programs: concrete thickness, concrete compressive strength, anchor diameter, and anchor manufacturer. In this research, the anchors were embedded through the full concrete layer thickness. The effects of full thickness drilling (penetration) on back-face and its implications on anchor tensile capacity are also investigated.

The third experimental program investigated the shear capacity of screw and adhesive anchors in thin concrete members. Variables included in the experimental programs: edge distance, concrete thickness, concrete compressive strength, and anchor diameter. The effect of back-face blowout on shear capacity is also investigated

Based on the experimental results, a behavioral and design models are proposed for screw and adhesive anchors under tensile and shear loads. The design models are based on the 5% fractile of the behavioral models as required by design codes.

Each of the three experimental programs adds to the body of knowledge on post-installed anchors. In particular, this research fills a gap on the use of anchors that are embedded through the entire thickness of thin concrete members. Additionally, this is one of the first programs to study the capacity and behavior of screw anchors.

1.3 Dissertation Organization

The remainder of this dissertation is organized into five chapters. Chapter two presents a background on anchorage systems and the load transfer mechanism for each of the considered systems. In addition, chapter two describes the potential failure modes for anchors under tensile and shear forces, and the design approach taken for each failure mode. Finally, chapter two reviews the codes and specifications limitations that affect the design of anchors in thin concrete members.

Chapters three and four present two experimental programs investigating the tensile behavior and capacity of screw and adhesive anchors respectively. These two chapters also propose behavioral and design models for screw and adhesive anchors under tensile loading. The effects and implications of full thickness drilling on back-face blowout are also addressed.

Chapter five presents an experimental program that investigates the shear behavior and capacity of screw and adhesive anchors. Behavioral and design models for screw and adhesive anchors are proposed.

Finally, chapter six summarizes the key points of the experimental programs and recommends future work to expand the current work. The proposed design procedures for screw and adhesive anchors with full thickness embedment are also summarized.

1.4 References

ACI Committee 318. "Building Code Requirements for Structural Concrete (ACI 318-14): An ACI Standard: Commentary on Building Code Requirements for Structural Concrete (ACI 318R-14), an ACI Report." American Concrete Institute, 2015.

Cook, R. A.; Burtz, J. L.; and Ansley, M. H., "Design Guidelines and Specifications for Engineered Grouts," FDOT Research Report BC354RPWO, No. 48, Aug. 2003, available at http://www.dot.state.fl.us/researchcenter/Completed_Structures.htm.

Eligehausen, R.; Cook, R. A.; and Appl, J., 2006a, "Behavior and Design of Adhesive Bonded Anchors," ACI Structural Journal, V. 103, No. 6, Nov.-Dec., pp. 822-831.

ICC Evaluation Services AC193, "Acceptance Criteria for Mechanical Anchors in Concrete Elements," Whittier, CA, Feb. 2010.

ICC Evaluation Services AC308, "Acceptance Criteria for Post Installed Adhesive Anchors in Concrete.", Inc., Whittier, CA (2008).

Losch, Edward D., Patrick W. Hynes, Ray Andrews Jr, Ryan Browning, Paul Cardone, Ravi Devalapura, Rex Donahey et al. "State of the art of precast/prestressed concrete sandwich wall panels." PCI Journal 56, no. 2 (2011): 131-176.

Olsen, Jacob, Thilo Pregartner, and Anthony J. Lamanna. "Basis for design of screw anchors in concrete." ACI Structural Journal 109, no. 4 (2012): 559.

PCI Design Handbook - Precast and Prestressed Concrete, eighth Edition, Precast/Prestressed Concrete Institute, Chicago, IL, 2017.

CHAPTER TWO

BACKGROUND

2.1 Anchorage Systems

Anchors are commonly used in precast concrete industry to connect structural members and transmit loads. In sandwich wall panel systems cast-in place anchors, which are installed in the panels during fabrication but before the concrete hardens, are used for different connection purposes such as load bearing for metal roof (Fig. 2-1(a)) and panel to intermediate floor connections (Fig. 2-1(b)).

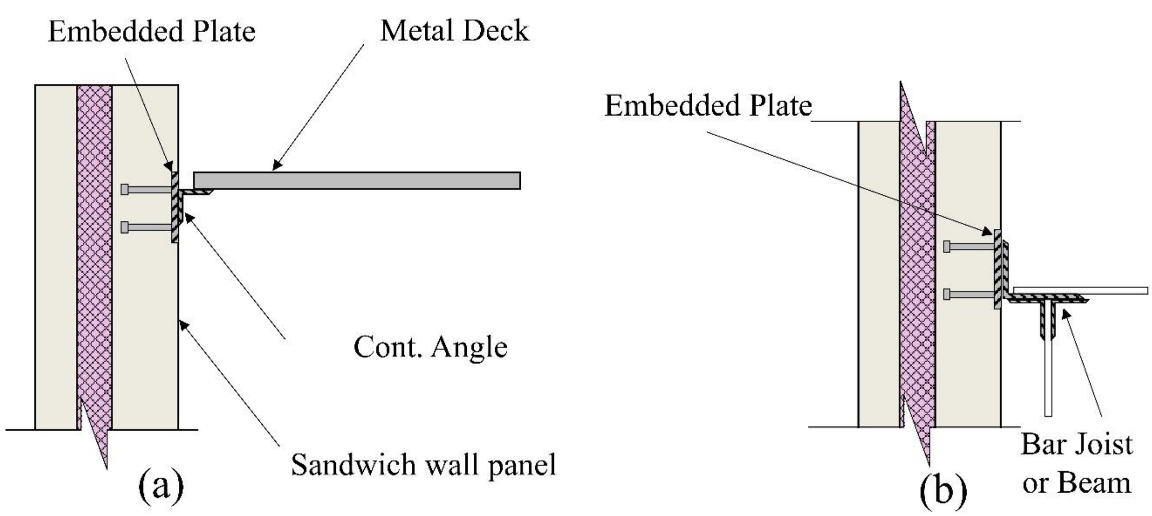

Fig. 2-1. Sandwich panel wall connections (a) load bearing for metal roof (b) panel to intermediate floor connections.

Cast-in place headed studs are fastened to the framework of panel and cast into the concrete. The headed stud generates capacity through mechanical interlock with the concrete (Fuchs et al., 1995) as shown in Fig. 2-2.

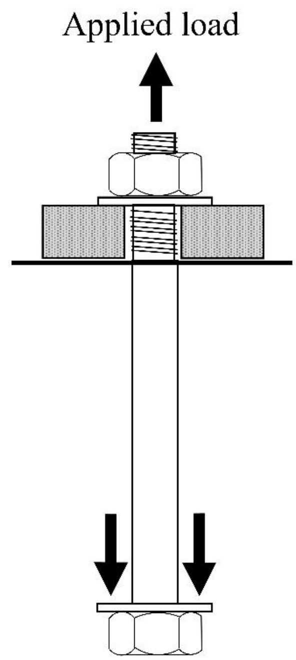

Fig. 2-2. Load transfer mechanism for headed stud anchors.

However, the use of post-installed anchors, in which the anchors are installed into harden concrete, is desirable because the location of connections can be determined to suit field conditions. Post-installed anchors can be used for different purposes such as providing a beam support, repair alignment, and post-installed features (i.e. fixing canopies). Post-installed anchors are more flexible in job site because its location can be easily adjusted to ensure proper alignment.

Post-installed anchors are divided into two sub-categories: 1) mechanical anchors which the anchor develop its capacity by the mechanical interlock with the concrete or friction, and 2) bonded anchors which develop its capacity using a bonding agent that form the bond between the anchor and the concrete. This dissertation focuses on investigating the behavior or adhesive bonded anchors and mechanical screw anchors.

2.2 Screw Anchors

Post-installed anchors are available in several types, a relatively new type being screw anchors. Screw anchors are attractive because of their efficient installation procedure and reliable performance (Oslen et al. 2012). Compared to other types of post-installed anchors that require several installation steps including torque application, multistep cleaning, and hammering, screw anchors can be installed in a drilled hole in one-step using an impact wrench. Screw anchors are seeing increasing acceptance in the construction industry (Oslen et al. 2012). These post-installed anchors transfer loads through the mechanical interlocking of the threads and concrete as shown in Fig. 2-3 below.

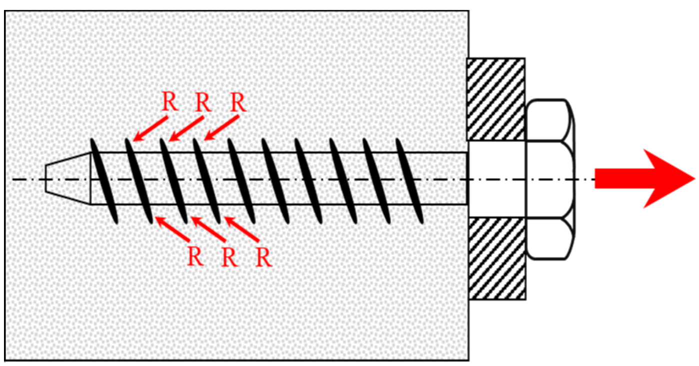

Fig. 2-3. Load transfer mechanism in screw anchors.

Similar to other anchor types, screw anchor capacity is a function of such factors as anchor diameter, embedment depth, and concrete compressive strength. Screw anchors are not explicitly mentioned in ACI 318-14 Chapter 17; currently their design is typically based on manufacturer product testing or according to ICC-ES Acceptance Criteria AC193. Because of their construction efficiency, there is a desire to evaluate the tensile behavior and capacity of screw anchors embedded in thin concrete members.

2.3 Adhesive Anchors

Adhesive-bonded anchors are commonly used as structural fasteners for connections to hardened concrete (Cook and Konz 2001). An adhesive anchor is a threaded rod or rebar inserted into a drilled hole with a bonding agent that bonds the anchor to the concrete. Fig. 2-4 shows the use of adhesive anchor for beam-column connection. The applied load transfers to the adhesive through mechanical interlocking between the threads and the adhesive, and then to the concrete through the adhesion and/or micro interlock between the adhesive and the concrete (Eligehausen et al. 2006), as shown in Fig. 2-5.

Fig. 2-4. Beam-column adhesive anchor connection.

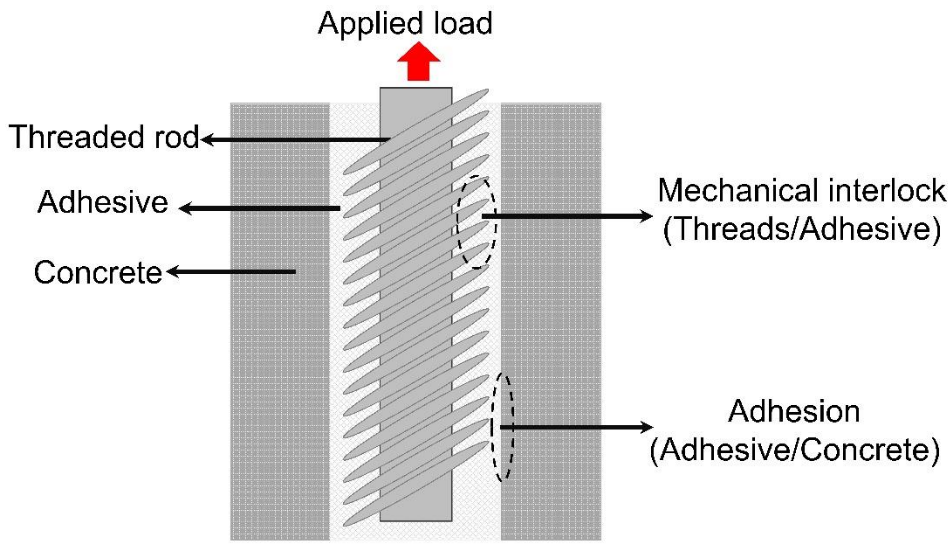

Fig. 2-5. Adhesive anchor load transfer mechanism.

Adhesive anchors are generally installed with a caulking type gun, with the adhesive being mixed in the nozzle. Adhesive anchors are sensitive to the installation procedure, which requires a multistep hole cleaning using compressed air and brush. Because of their reliance on chemical and mechanical bond adhesive anchors are uniquely susceptible to potentially adverse factors. These different factors can occur during installation procedure and/or throughout the service life of the anchor (Cook and Konz 2001). For example, improper hole cleaning can result in a significant reduction in the capacity.

2.4 Anchor Design and Failure Modes

The capacity of an anchor in concrete is a function of its failure mode. More specifically, post-installed anchors can exhibit several failure modes under tension load, including steel anchor failure, concrete cone breakout, bond (pullout) failure, or a combination of bond and concrete cone breakout failure. Fig. 2-6 shows schematic representations of these failure modes for anchors embedded in one layer of a sandwich panel system. In the design process of an anchor, the capacity for each failure mode is calculated; the mode with the lowest capacity governs the design.

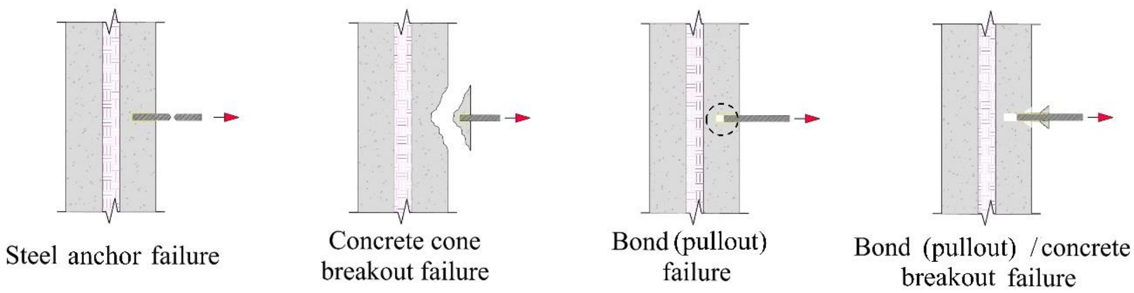

Fig. 2-6. Different failure modes of anchors.

2.4.1 Anchor Steel Failure

Steel anchor failure model is typically a ductile failure more due to the ductile nature of steel. The nominal capacity of an anchor governed by anchor steel failure (N_{sa}) is given in the ACI 318-14 by Eq.2-1. The tensile strength is limited to 1.9 times the yield strength or 125,000 psi (860 MPa), whichever is smaller.

$$N_{sa} = A_{se,N}\ f_{uta} \qquad \text{Eq. 2-1}$$

Where

$A_{se,N}$ = anchor effective cross-sectional area

f_{uta} = tensile strength of the steel.

2.4.2 Concrete Cone Breakout Failure

The capacity of anchors failing in full concrete cone breakout is determined using the Concrete Capacity Design model (CCD), proposed by Fuchs et al. in 1995. It is based on concrete failure of a 35^o cone failure originating at the end of the anchor as shown in Fig. 2-7, where h_{ef} is the effective embedment depth. This model has been extended to include the effect of multiple anchor and edge effects, and was adopted by ACI 318 as the design model for concrete breakout failures. The calculated capacity of an anchor based on the CCD is a function of the embedment depth and the compressive strength of concrete. The CCD is applicable for cast-in place headed studs anchors and post-instlled anchors that fail in concrete cone breakout.

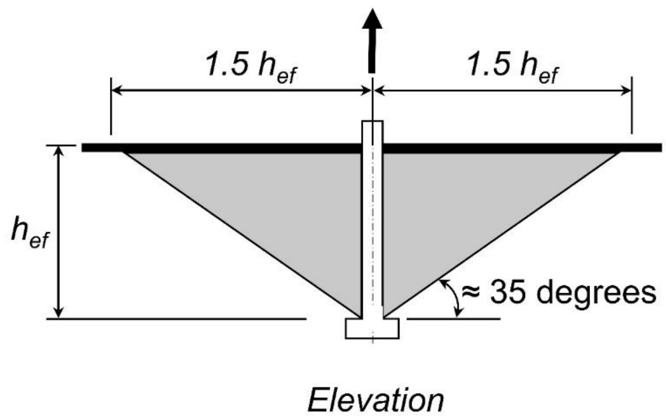

Fig. 2-7. Concrete capacity design model.

The CCD strength of post-installed anchors in uncracked concrete is given by Eq. 2-2

$$N_{cb} = k_c\sqrt{f'_c}\, h_{ef}^{1.5} \qquad \text{Eq. 2-2}$$

Where

k_c = factor evaluated for experimental data at 5% fractile as per ACI 355.

f'_c = concrete compressive strength

h_{ef} = effective embedment depth

Eq. 2-2 is derived by multiplying the surface area of concrete cone breakout (function of h_{ef}^2) by the concrete tensile strength (function of $\sqrt{f'_c}$) and accounting for the size effect phenomenon by linear mechanics (function of $\frac{1}{\sqrt{f'_c}}$). The derivation is illustrated in Fig. 2-8.

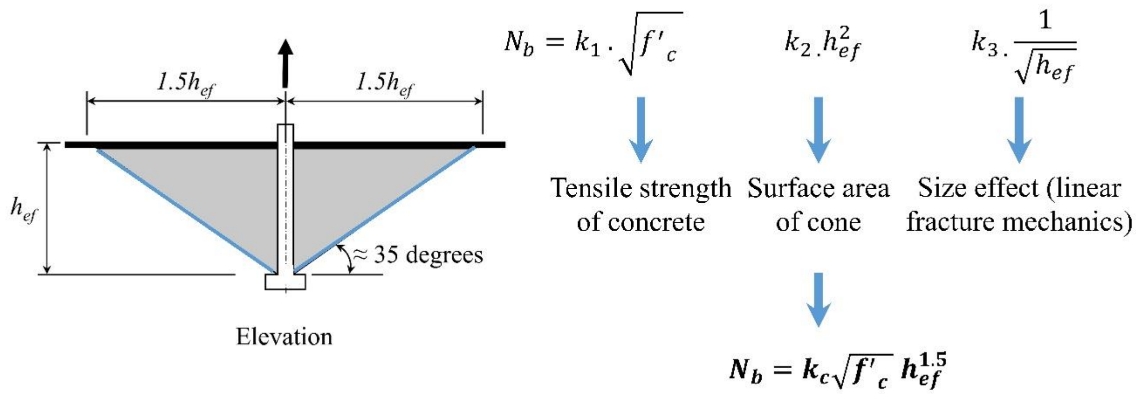

Fig. 2-8. CCD equation derivation.

Anchors loaded in shear toward a free edge may fail in the form of semi-conical surface. Concrete breakout capacity under shear loads are also calculated based on the CCD, fracture mechanics theory, and test results utilizing a 35^o angle failure surface as shown in Fig. 2-8. The shear breakout capacity is given by Eq. 2-3a as reported in Fuchs et al. (1995).

$$V_b = \left(7\left(\frac{\ell_e}{d_a}\right)^{0.2}\sqrt{d_a}\right)\lambda_a\sqrt{f'_c}\,(c_{a1})^{1.5} \qquad \text{(Eq. 2-3a)}$$

$$V_b = 9\lambda_a\sqrt{f'_c}\,(c_{a1})^{1.5} \qquad \text{(Eq. 2-3b)}$$

Where:

ℓ_e = the effective load transfer length and is equal to the embedment depth for anchors with constant stiffness along the length of the anchor.

d_a = outside diameter of the post-installed anchor.

c_{a1} = edge distance measured from the center of the anchor to the concrete edge.

λ_a = modification factor for light weight concrete.

The constant 7 = Constant determined based on the 5 percent fractile.

According to Eq. 2-3a, the shear load is proportional to $c_{a1}^{1.5}$ instead of c_{a1}^{2}. This is again due to considering the size effect. In shear-loaded anchors, c_{a1} is analogous to h_{ef} in tension. In addition, Eq. 2-3a consider the diameter effect and the anchor stiffness by the term$\left(\frac{\ell_e}{d_a}\right)^{0.2}$.

The CCD model indicates that the shear capacity of an anchor is mainly a function of the edge distance since this parameter controls the failure surface size as shown in Fig. 2-8. Anchor diameter and stiffness effects are represented in the (l/d) term. These effects are not apparent in large diameter anchors, thus an upper limit on the breakout shear capacity is provided by Eq. (2-3b). For anchors far from the edge, concrete breakout typically will not govern.

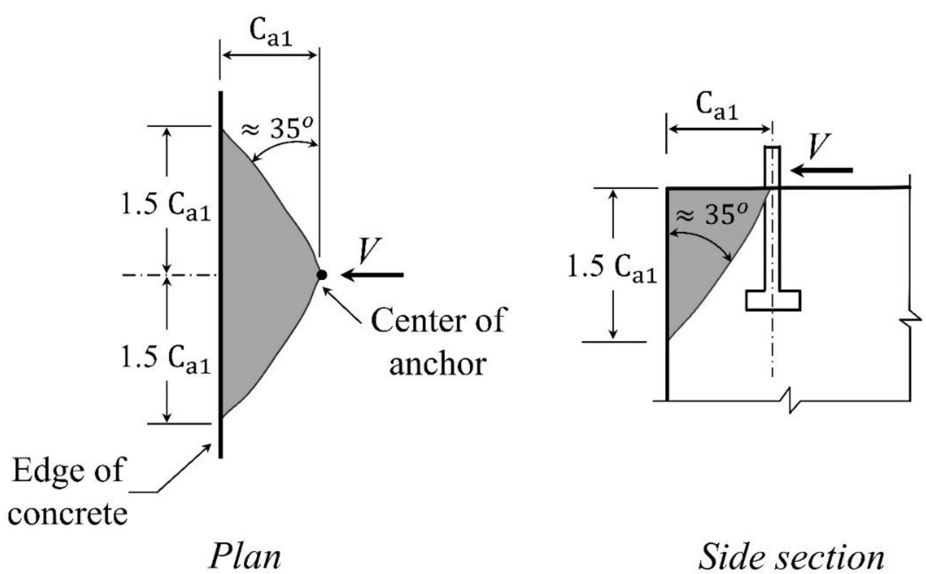

Fig. 2-9. Concrete capacity design model for anchors loaded in shear towards free edge.

2.4.3 Bond Failure

Concrete cone failure is common for shallow embedment depths; however, with deeper embedment depth bond failure may occur3. Experimental results discussed in Eligehausen et al. (2004) shows that bond stress distribution along the embedment depth is non-linear. However, based on work by Cook et al. (1998) a uniform bond stress can be practically used in design. Assuming a uniform stress distribution, bond failure capacity can be calculated as in Eq. 2-4.

$$N_\tau = \tau \pi d h_{ef} \qquad \text{Eq. 2-4}$$

Where

τ = mean bond stress associated with each product

d= anchor diameter

h_{ef}=embedment depth.

2.4.4 Screw Anchors Design

While ACI 318 code has adopted the CCD for designing cast-in and post-installed anchors, screw anchors are not included in ACI 318-14 (Oslen et al. 2012). In 2004, Kuenzlen presented a design procedure for screw anchors using Eq. 2-2, but with the reduced effective embedment depth given by Eq. 2-5 and shown in Fig. 2-9.

$$h_{ef} = 0.85\,(h_{nom} - 0.5h_t - h_s) \qquad \text{Eq. 2-5}$$

where h_{nom} is the nominal length of the anchor, h_t is the thread spacing, and h_s is the tip length after the last thread. When using this reduced embedment length in Eq. 2-1, k_c is specified as 13.5 (SI units) or k_c=32 (U.S. Customary units, computed by the author), a value similar to the expansion anchor model. The diameter of a screw anchor was not included in the equation because its effect is considered negligible compared to the influence of other variables (Eligehausen et al. 2006).

Eq. 2-5 was validated by Kuenzlen using data from 500 tests of screw anchors. Olsen et al. expanded the data from Kuenzlen with an additional 353 tests which were conducted by independent laboratories in accordance with ICC-ES AC 193. The results from Olsen confirmed the applicability of the reduced effective embedment depth equation (Eq. 2-5).

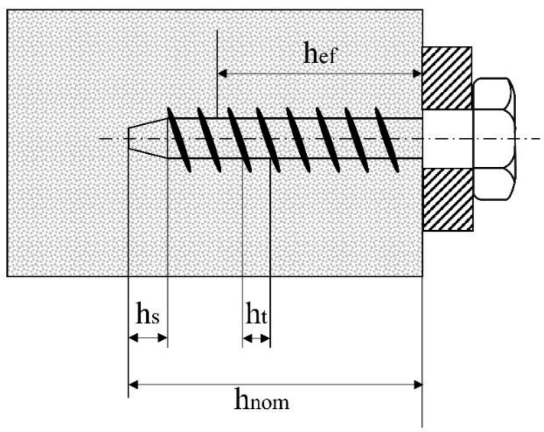

$$\boxed{h_{ef} = 0.85(h_{nom} - 0.5h_t - h_s)}$$

Fig. 2-10. Reduced embedment depth for screw anchors.

2.5 Limitations on Anchoring to Thin Concrete Members

limitations that limit the use of anchors in thin concrete members. According to ICC-ES AC193 Acceptance *Criteria for Mechanical Anchors in Concrete Elements*, the minimum allowable concrete thickness required for the use of mechanical anchors is twice the effective embedment depth unless acceptable test data are provided. In addition, both acceptance criteria for mechanical and adhesive anchors (ICC-ES AC308) specify minimum member thickness should not be less than the hole depth plus twice the hole diameter or 1.25 in., whichever is larger. Product design tables from anchor suppliers also specify minimum member thickness values larger than the embedment depth. These limitations prohibit the use of full thickness embedment.

Acceptance criteria for mechanical and adhesive anchors also require a minimum embedment depth of 1.5 in. while manufacturers specifications require minimum embedment depths larger than 2 in. These provisions on minimum member thickness and minimum embedment depth prevent the use of anchors in thin concrete layers and in applications with full-thickness embedment.

According to chapter 17, Anchoring to Concrete, in ACI 318-14 *Building Code Requirements for Structural Concrete and Commentary*, the embedment depth for expansion and undercut post-installed anchors must not exceed the greater of 2/3 of the member thickness or the member thickness minus 4 in. Limitations on the maximum embedment depth are intended to prevent splitting failures during loading and concrete back-face blowout during drilling (ACI 318-14). These limitations restrict full-thickness embedment, which effectively prevents engineers from designing post-installed anchors in thin concrete members. Fig. 2-10 summarizes the limitations by different codes and specifications.

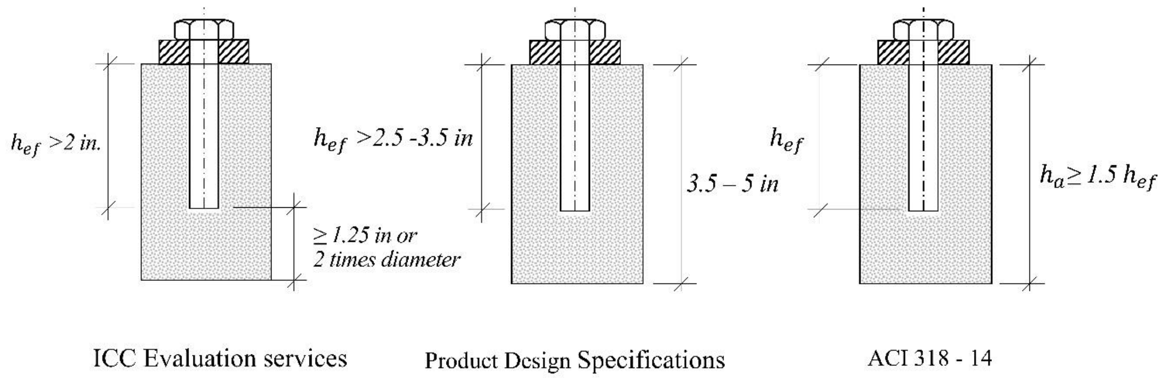

Fig. 2-11. Different limitations on anchorage in thin concrete members.

2.6 References

ACI Committee 318. "Building Code Requirements for Structural Concrete (ACI 318-14): An ACI Standard: Commentary on Building Code Requirements for Structural Concrete (ACI 318R-14), an ACI Report." American Concrete Institute, 2015.

Cook, Ronald A., and Robert C. Konz. "Factors influencing bond strength of adhesive anchors." *Structural Journal* 98, no. 1 (2001): 76-86.

Cook, R. A.; Kunz, J.; Fuchs, W.; and Konz, R. C., 1998, "Behavior and Design of Single Adhesive Anchors under Tensile Load in Uncracked Concrete," ACI Structural Journal, V. 95, No. 1, Jan.-Feb., pp. 9-26.

Eligehausen, R.; Mallee, R.; and Silva, J., Anchorage in Concrete Construction, Ernst & Sohn, Berlin, Germany, 2006, 391 pp.

Eligehausen, R.,Appl, J. J., Lehr, B., Meszaros, J., and Fuchs, W.: "Tragverhalten und Bemessung von Befestigungen mit Verbunddübeln unter Zugbeanspruchung, Part 1: Einzeldübel mit großem Achs- und Randabstand" (Load-bearing Behavior and Design of Fastenings with

Adhesive Anchors under Tension Loading – Part 1: Single Anchors with Large Axial and Edge Spacing), Beton und Stahlbetonbau 99, No. 7, July 2004, pp. 561–571

Fuchs, W.; Eligehausen, R.; and Breen, J., "Concrete Capacity Design (CCD) Approach for Fastening to Concrete," ACI Structural Journal, V. 92, No. 1, Jan.-Feb. 1995, pp. 73-94.

ICC Evaluation Service AC193, "Acceptance Criteria for Mechanical Anchors in Concrete Elements," Whittier, CA, Feb. 2010.

ICC Evaluation Services AC308, "Acceptance Criteria for Post Installed Adhesive Anchors in Concrete.", Inc., Whittier, CA (2008).

Kuenzlen, J. H., "Load-Bearing Behavior of Screw Anchors under Axial Tension," doctoral thesis, the University of Stuttgart, Stuttgart, Germany, 2004. (in German).

Olsen, Jacob, Thilo Pregartner, and Anthony J. Lamanna. "Basis for design of screw anchors in concrete." ACI Structural Journal 109, no. 4 (2012): 559.

CHAPTER THREE

TENSILE BEHAVIOR AND DESIGN OF SCREW ANCHORS IN THIN CONCRETE MEMBERS

3.1 Introduction

Post-installed anchors are available in several types, a relatively new type being screw anchors. Screw anchors, are attractive because of their efficient installation procedure and reliable performance (Oslen et al. 2012). Although screw anchors are seeing increasing acceptance in the construction industry (Oslen et al. 2012), screw anchors are not explicitly mentioned in ACI 318-14 Chapter 17 and their current design is typically based on manufacturer product testing or according to ICC-ES Acceptance Criteria AC193. Since current codes and specifications have limitations that affect the use of anchors in thin concrete members as mentioned in section 2.5, there is a desire to evaluate the tensile behavior and capacity of screw anchors embedded in thin concrete members.

Accordingly, this chapter presents an experimental program that evaluates the effects of concrete member thickness, anchor diameter, concrete compressive strength, and anchor brand on screw anchor tensile capacity and behavior. The effects of full thickness drilling (penetration) on back-face and its implications on anchor tensile capacity are also investigated. The experimental results are then used to develop behavioral and design models for screw anchors in thin concrete members. The models, which are based on previous work by Kuenzlen (Kuenzlen 2004;Oslen et al. 2012), are applicable to screw anchors installation in holes drilled through the entire thickness of a concrete member.

3.2 Experimental Program

An experimental program of 100 screw anchor pullout tests performed in seven precast concrete sandwich panel specimens was conducted to evaluate the behavior, capacity and failure modes of tension-loaded single screw anchors embedded in thin concrete members. All tests were conducted in plain uncracked concrete away from concrete edge. Variables included in the experimental program are concrete thickness, anchor diameter, concrete compressive strength, embedment depth, and three ICC certified anchor brands (Table 3-1). Three or four repetitions were tested for each combination of variables considered. Values of the variables were chosen based on common industry practice and on recommendations from precast concrete and anchor suppliers. In each test, the embedment depth of the screw anchor was equal to the thickness of the concrete member. Of the 100 tests, 44 were conducted using 2-in. thick concrete, 48 using 4-in. thick concrete, and 8 using 3-in. thick concrete.

Table 3-1. Test variables

Tested concrete compressive strength	5.3 k, 6.7 ksi, 8.7 ksi
Brands (unique threads)	(A, B, C)
Nominal diameters	3/8 in., 1/2 in.
Embedment depth	2 in., 3 in., 4 in.
Repetitions	3-4
Total number of tests	100

Note: 1 in. = 25.4 mm.;
1 ksi = 6.895 MPa.

After the screw anchor tests were completed a small study on back-face blowout was also conducted. The study included 31 holes drilled with 5 different bit sizes. The depth and width of the blowout cones were measured in the study.

3.3 Test Specimens

Seven concrete sandwich panels were fabricated by a precast concrete manufacturer. Each panel consisted of two layers of concrete separated by a 2-in. insulation layer. The concrete layers were 2 in., 3 in. or 4 in. thick. The concrete layer thicknesses were chosen based on a recommendation from precast concrete supplier as practical thicknesses used in the field and that do not meet the thickness requirement for anchorage. Screw anchors were installed and tested in each of the sandwich panel concrete layers. After the tests on one side of a panel were completed, the panel was flipped and anchors were installed and tested on the other side. The testing area in the panels was unreinforced; however, reinforcement was provided at the perimeter to support the lifting points. Fig. 3-1, 3-2 show the panels fabrication process and the testing area. Three concrete mixes were used for the panels, resulting in a three well-separated concrete compressive strengths tested according to ASTM C39 protocol (Table 3-2). Maximum aggregate size in all panels was 3/4" (i.e. #67 stone).

Fig. 3-1. Sandwich panel fabrication.

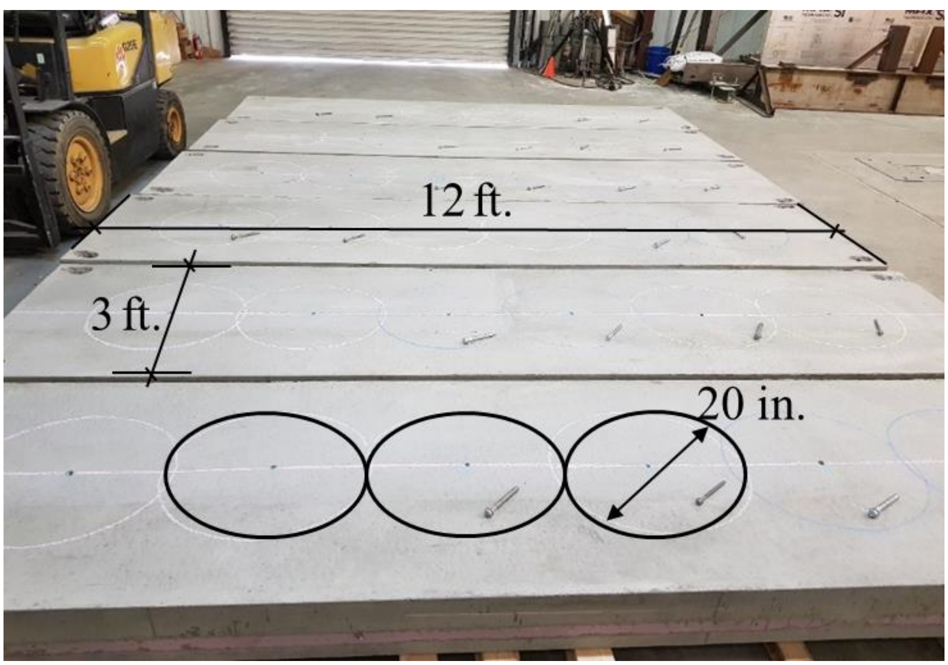

Fig. 3-2. Anchors pullout test locations.

Table 3-2. Concrete strength

Specified compressive strength	Tested compressive strength	Tested splitting tensile strength
4 ksi	5.5 ksi	-
4 ksi	6.7 ksi	0.55 ksi
6 ksi	8.7 ksi	0.64 ksi

Note: 1 in. = 25.4 mm.;

1 ksi = 6.895 MPa.

Sandwich panels were 12 ft. long by 3 ft. wide. Typically, seven tests were conducted on each side of each panel. To prevent interaction between adjacent tests, the clear distance between tested anchors was at least five times the embedment depth. Thus, this distance exceeded the minimum distance specified by ASTM E488 *Standard Test Methods for Strength of Anchors in Concrete Elements* for unconfined pullout tests. The distance between the anchors and the perimeter reinforcement also complied with ASTM E488. Based on information provided by the manufacturers screw anchors tensile strength was approximately 110 ksi (760 MPa).

3.4 Setup, Procedure and Measurements

Holes for anchors were drilled using carbide drill bits and a rotary-hammer drill. Because rotary-hammer drills combine the rotary mechanism of a drill bit with a hammering action that produces a pounding force, they are efficient and effective for drilling in concrete and masonry. Rotary-hammer drills also lead to the back-face blowout, a phenomena that is discussed in more detail in the next section. Holes were drilled through the entire thickness of the concrete layer. The diameter of the drilled holes, hole cleaning, and anchor placement followed the manufacturer's installation instructions.

The testing apparatus is shown in Fig. 3-3, and was designed to comply with ASTM E488, including the required distance between supporting points for unconfined pullout tests. The tension load was applied perpendicular to the panel by a hand operated hydraulic jack. Load was recorded using a calibrated load cell and checked using a pressure gage. The loading rate was adjusted to ensure that failure occurred within 1 to 3 minutes after the beginning of the test as specified by ASTM E488.

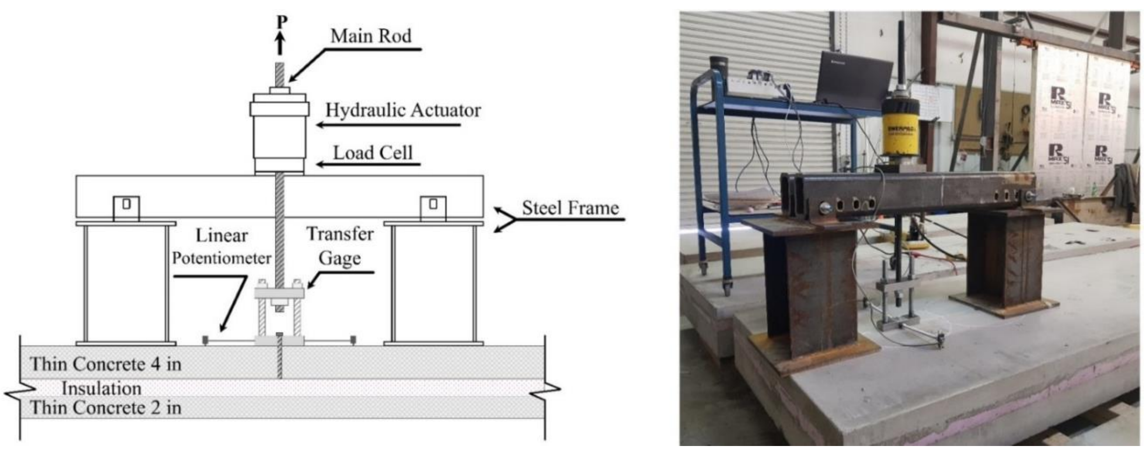

Fig. 3-3. Test Apparatus.

Two calibrated displacement transducers recorded the displacement of the anchor relative to the concrete surface and the average displacement was considered as recommended by ASTM E488. Data were continuously monitored using a computer-based data acquisition system.

3.5 Concrete Back-Face Blowout Results

Back-face blowout is cited as a reason for prohibiting the embedding of anchors in the full thickness of a concrete member (ACI 318-14). This phenomenon occurs when the hammering action of a rotary-hammer drill breaks a cone out of the concrete as the drill bit approaches the back-face (Fig. 3-4). In this study, the effect of back-face blowout was investigated by drilling thirty-one holes in thin concrete panels with 5 drill bit sizes (5/16, 3/8, 1/2, 7/16, 9/16 inches) and then autopsying the panels to measure the size of the blowout cone. Back-face concrete blowout was found at each hole location.

It was observed that holes drilled with smaller drill bits tended to have narrower blowout cones. Blowout widths range from 3.5-5.0 in. (89-127 mm). Depth of the blowout cones ranged from 0.70 to 0.95 in. (17.78-24.13 mm). Critically, it was observed that for these tests blowout depth and was not a function of the drill bit diameter (Table 3-1).

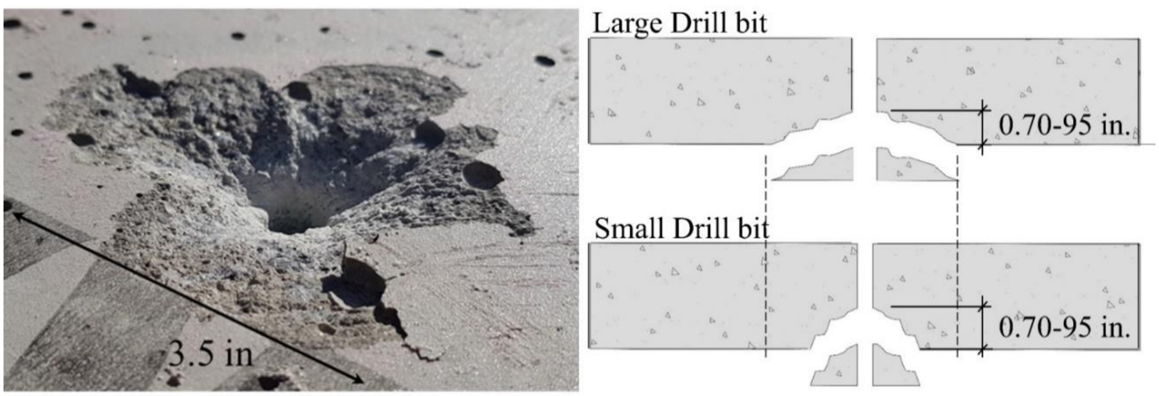

Fig. 3-4. Back-face concrete blowout due to drilling.

Attempts were made to reduce or eliminate the back-face blowout by changing the drilling mode to rotary-only when the bit approached the back face. This approach was deemed to be impractical as drilling in rotary-only mode was time consuming. Even after minutes of rotary-only drilling the bit did not advance through the concrete.

Table 3-3. Back-face blowout correlation coefficient

Correlations			
		Spall Depth	Spall Diameter
Drill bit Diameter	Pearson Correlation	-.138	.487**
	Sig. (2-tailed)	.457 (Not significant)	.005 (Significant)
Concrete Strength	Pearson Correlation	-.046	-.077
	Sig. (2-tailed)	.805 (Not significant)	.679 (Not significant)
Concrete Thickness	Pearson Correlation	-.104	-.194
	Sig. (2-tailed)	.578 (Not significant)	.294 (Not significant)

3.6 Pullout Test Results

Results of the pullout tests are presented according to the thickness of the concrete test specimens. This is because failure modes and the effects of the variables were dependent on concrete thickness. To illustrate the extremes in behavior the discussion focuses on the tests in 4-in. concrete (maximum thickness in the program) and 2-in. concrete (minimum thickness in the program). As noted previously, holes were drilled and screw anchors were embedded though the entire thickness of the concrete.

3.7 Tests Results for Anchors Embedded in 4-in. Thick Concrete

3.7.1 Failure Modes

Three types of failure modes were observed: cone breakout, shallow cone, and pullout (Fig. 3-5). Steel failure did not occur during the testing since the stresses developed were well below the tensile strength of the anchors. The average applied stress in the anchors was as high as 70 ksi; the steel tensile strength was approximately 110 ksi.

Breakout cone and shallow cone failures did not extend for the entire thickness of the concrete layer (Fig. 3-6). This is because the lower portion of the anchor could not be fully engaged due to damaged that occurred in the concrete from back-face blowout. Depth of breakout cone failures was typically two to three inches. In contrast, shallow cone failures were more superficial and extended approximately one inch into the concrete.

Different failure modes were observed in replicate tests that had the same concrete strength, embedment depth, and diameter. This observation suggests that these variables had minimal effect on the type of failure mode. Anchor brand, however, was observed to have strong correlation with failure mode. Breakout cone failure was the most common mode observed in Brand B anchors, while the majority of the failures for Brands A and C were shallow cone and pullout, respectively. It was also observed that anchor capacity was correlated with failure mode. Brand B (typically concrete breakout failures) had a higher average capacity than the other two brands. The effects of brand on anchor capacity will be discussed later in the paper.

Transverse cracks were observed in some of the tests of the anchors in the 4-in. concrete layers. These cracks were attributed to flexural tension in the concrete layer. Reinforcement around the perimeter of the sandwich panels controlled the cracks and prevented splitting failures.

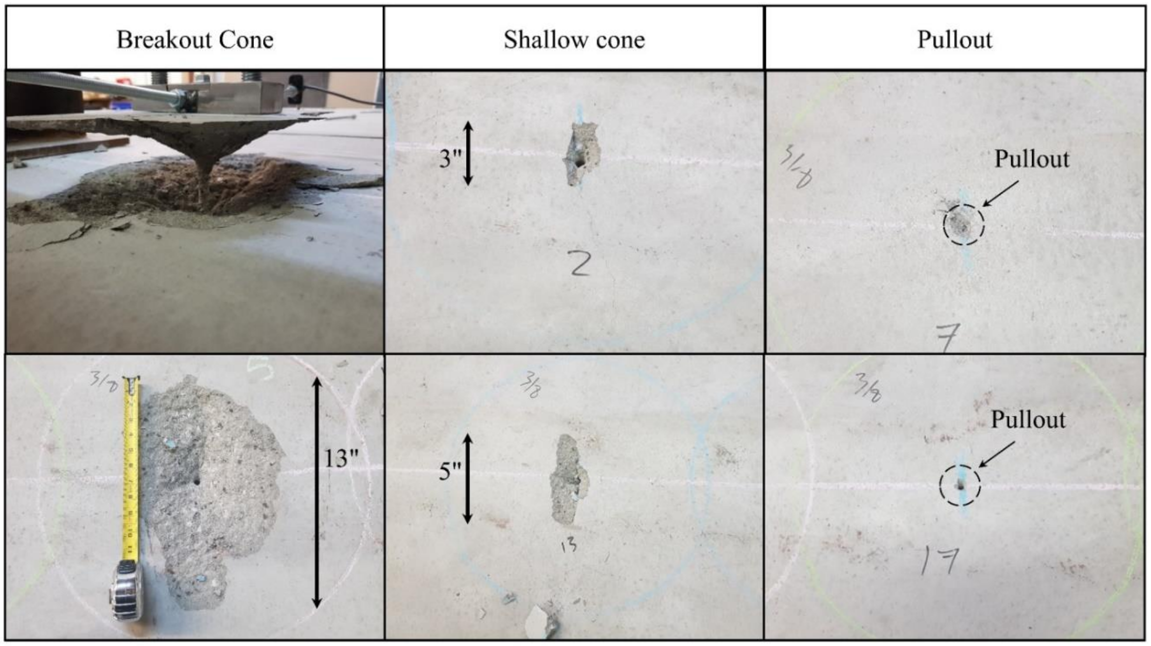

Fig. 3-5. Observed failure modes in 4 in. thick concrete.

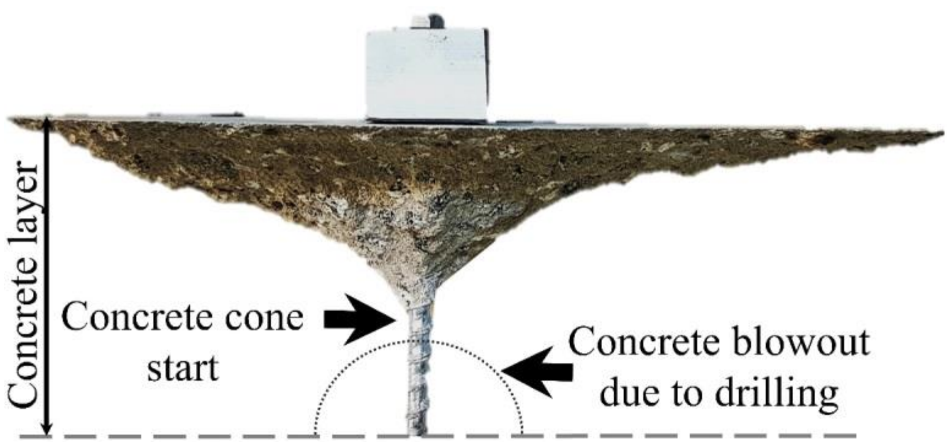

Fig. 3-6. Breakout cone failure.

3.7.2 Load-Displacement Response

Fig. 3-7 shows a typical load-displacement response for a typical screw anchor in 4-in. concrete. The overall load-displacement behavior demonstrated in the figure was similar regardless of failure mode. Load and displacement increased linearly until cracks began to form in the concrete failure cone and/or anchor-concrete interface. For the anchor in Fig. 3-7 cracks formed when the displacement reached approximately 0.010 in. (0.254 mm). Initial cracking in the concrete led to a reduction of stiffness but not to immediate failure. In the example, the load continued to increase until the load reached a peak near 9.8 kip. The experimental capacities used in the subsequent analysis were taken as the peak load measures in the experiment.

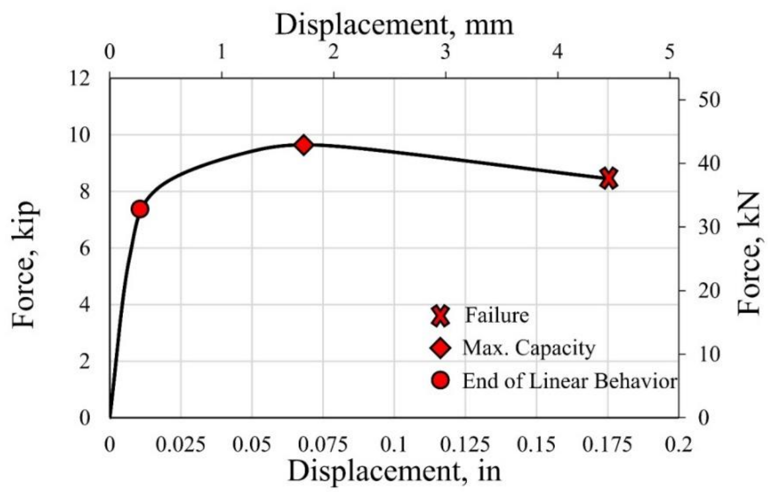

Fig. 3-7. Typical Load-displacement response for screw anchor in 4 in. thick concrete.

Because of the nature of hydraulic loading the failure mechanism in the experiment allowed for post-peak load carrying capacity. The anchor shown in Fig. 3-7 retained post-peak capacity until the maximum displacement reached approximately 0.150 in. to 0.200 in. (3.80-5.00 mm). Post-peak capacity was attributed to the residual friction between the threads and the concrete after the primary breakout or pullout mechanism occurred. An example of a shallow cone failure is shown in Fig. 3-8. The threads below the breakout cone remained engaged with the concrete, as the displacement increased in the post-peak portion of the test. The threads below the breakout cone sheared the concrete to create post-peak capacity.

Fig. 3-8. Shallow cone failure in 4 in. thick concrete.

3.7.3 Statistical Analysis

A three-way ANOVA with a 95% confidence level was conducted to evaluate the effect of anchor diameter, concrete compressive strength, and brand on anchor capacity. There were no outliers in the data as assessed by inspection of a boxplot. The anchor capacities were normally distributed ($p > .05$) as assessed by Shapiro-Wilk's test of normality. The analysis indicated no statistically significant three-way nor two-way interaction between screw anchor diameter, concrete compressive strength, and brand. However, there was a statistically significant main effect for anchor diameter ($p < .001$), concrete compressive strength ($p < 0.001$), and brand ($p < .001$) on the anchor capacity. The results also show a statistically significant mean difference between brands B and A, and brands B and C, but not between brands A and C. Table 3 shows the mean capacity corresponding to each of the variables.

Table 3-4. Anchor pullout mean capacity in 4 in. thick concrete

Variable		*Mean Tested Capacity*
Diameter	*3/8 in.*	9.0 kip
	1/2 in.	10.2 kip
Concrete Compressive Strength	*6.7 ksi*	9.1 kip
	8.7 ksi	10.2 kip
Brand	*A*	9.3 kip
	B	10.7 kip
	C	8.9 kip

Note: 1 in. = 25.4 mm.;
1 ksi = 6.895 MPa.

3.7.4 Effect of Concrete Compressive Strength

To evaluate the effect of concrete compressive strength, each of the anchor brands and diameters were installed and tested in concrete layers with 6.7 and 8.7 ksi concrete strengths. Fig. 3-9 shows the relationships between concrete compressive strength and anchor capacity for each of the brands and diameters embedded in 4-in. thick concrete. The general trend of all brands and diameters is increased capacity as the concrete compressive strength increases.

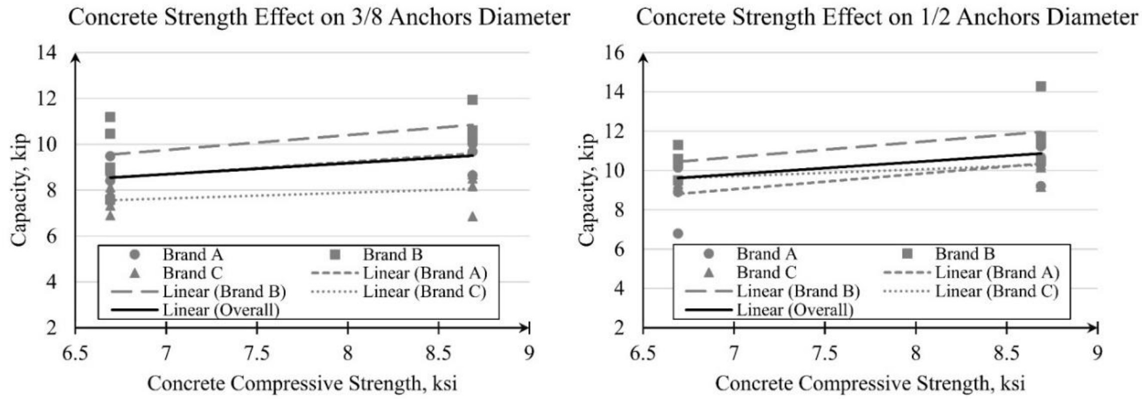

Fig. 3-9. Effect of concrete compressive strength on anchor capacity embedded in 4-in. thick concrete (Note: 1 in. = 25.4 mm; 1 ksi = 6.895 MPa).

3.7.5 Effect of Anchor Diameter

The experimental program includes two anchor diameters, 3/8 in. and 1/2 in. Fig. 3-10 presents the relationships between the capacity and the anchor diameter for each of the brands and concrete strengths. The trend is that capacity increases for the larger diameter anchors; however, the strength of the trend is different for each brand as seen by the slope of the trend lines shown in Fig. 3-10. For example, the trend lines for Brand A are relatively flat compared to those of Brand C.

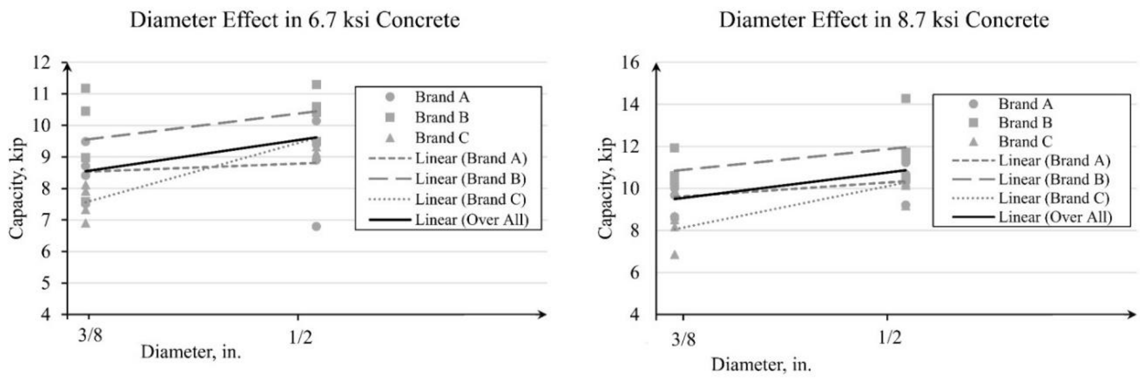

Fig. 3-10. Effect of screw anchor diameter on anchor capacity embedded in 4-in. thick concrete. (Note: 1 in. = 25.4 mm.; 1 ksi = 6.895 MPa).

3.7.6 Effect of Brand

Fig. 3-11 shows box and whisker plots comparing capacity of the brands. Brand A and C have similar capacities, while Brand B gives the highest average capacity as confirmed by the statistical analysis. Average capacity for Brand B is 15% to 20% greater than for Brands A and C.

The difference in failure modes and capacities among brands is attributed to thread configuration and the ability of threads to provide mechanical interlock with the concrete. If the threads produce high interlocking resistance, a cone or pullout-cone failure results; otherwise, the interlocking between the threads and the concrete breaks and a pullout failure develops.

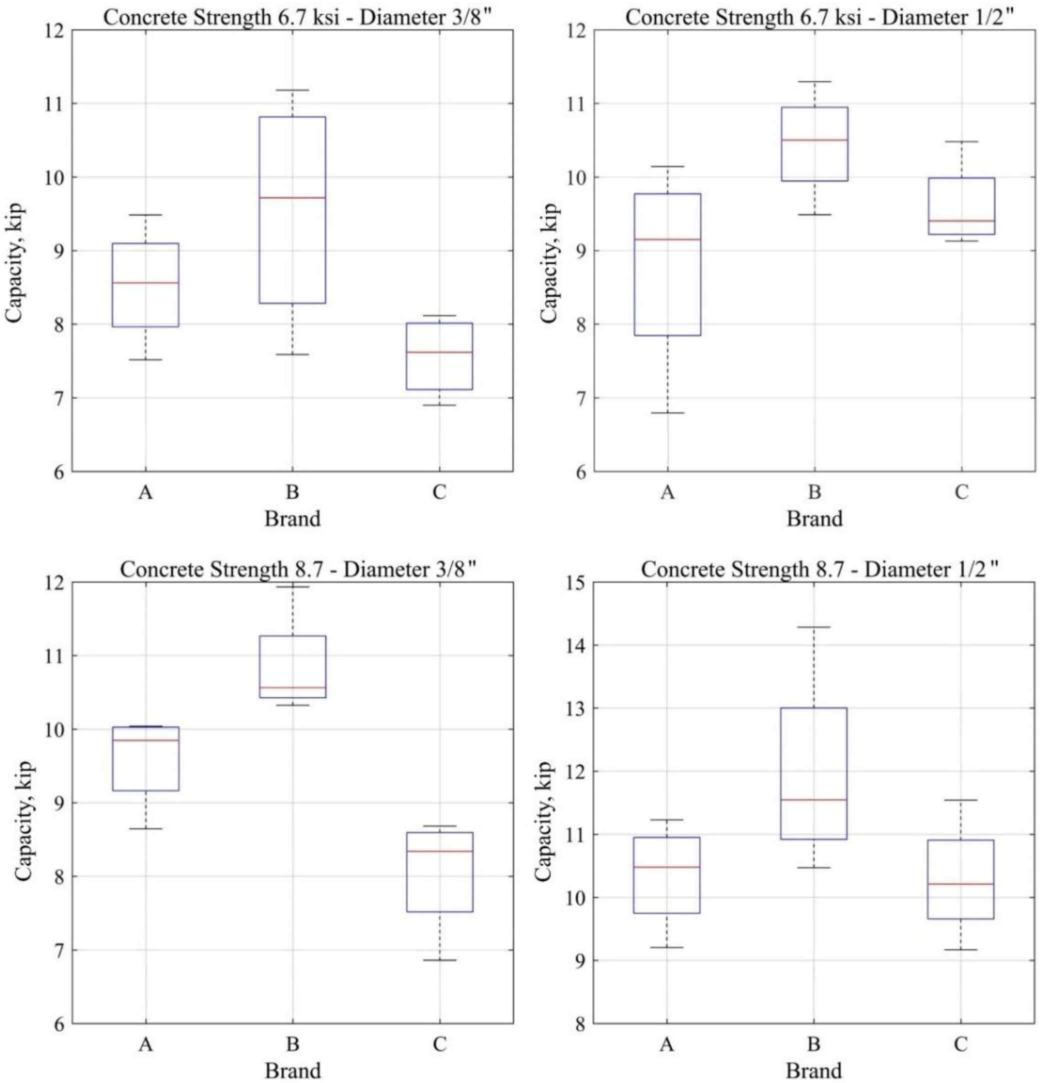

Fig. 3-11. Effect of screw anchor brand on anchor capacity embedded in 4-in. thick concrete. (Note: 1 ksi = 6.895 MPa).

The degree of mechanical interlock of a screw anchor can be expressed as the undercut dimension. Undercut is defined as the difference between the outer diameter of the screw anchor (d_{sc}) and the diameter of the hole that the anchor is installed in (d_{hole}). Fig. 3-12 shows the effect of undercut dimension on anchor capacity. The brands and hole diameters used in the experiment resulted in six different values of undercut. As shown in the figure, anchor capacity increases with the degree of undercut. In each anchors size, anchors with the highest undercut tended have breakout cone failures whereas anchors with the lowest undercut values tended to fail in pullout or shallow cones. It is reasoned that smaller undercuts are associated with higher stresses at the thread-to-concrete interface. The increased concrete stress leads to shearing of the concrete adjacent to the threads which leads to pullout failure.

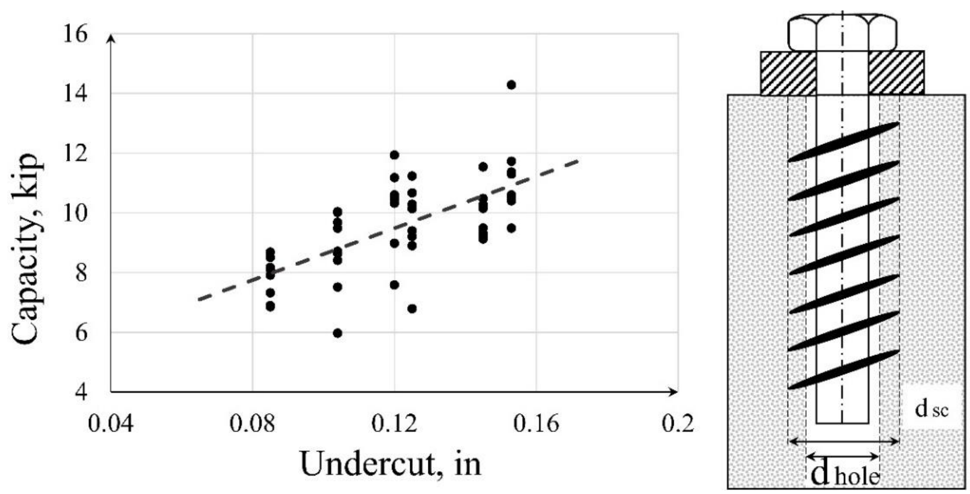

Fig. 3-12. Effect of undercut degree on the capacity of anchors embedded in 4-in. thick concrete. (Note: 1 in. = 25.4 mm.; 1 ksi = 6.895 MPa).

3.8 Tests Results for Anchors Embedded in 2-in. Thick Concrete

3.8.1 Load-Displacement Response and Failure Mode

The behavior of screw anchors embedded in 2-in. thick concrete was different from the behavior of anchors embedded in a 4-in. thickness. The thinner concrete led to difference in failure behavior and in the effect of the variables on anchor capacity. The distinction between the behavior between anchor in 2-in. and 4-in. is attributed to surface effects and the relative impact of blowout during drilling.

Fig. 3-13 shows a typical load-displacement relationship for anchors embedded in 2-in. thick concrete. Comparing Fig. 3-7 and 3-13 it can be observed that the capacity of anchors in 2-in. thick concrete were approximately 20% of the capacity of anchors in 4-in. thick concrete. The maximum displacement was approximately 10% of the displacement of anchors in 4-in. concrete. For the anchor represented in Fig. 3-13, linear response was observed until displacement reached approximately 0.0015in. (0.0381mm), followed by a stiffness reduction. The load increased until brittle failure occurred at a displacement of approximately 0.0025 in. (3.8-5mm) and load of approximately 2 kip. Post-peak capacity was not observed in the test with 2-in. thick concrete because there was no thread engagement with the concrete beyond the failure cone, meaning the residual thread-concrete interaction did not occur.

A cone failure mode was observed for all anchors in 2 in. thick concrete regardless of the brand or other variable. The size and shape of the cone failure were consistent in all tests; Fig. 3-14 shows the surface of the concrete after typical failures. Pullout failures did not occur because the thinness of the concrete layer could not provide enough resistance to prevent the concrete cone from developing.

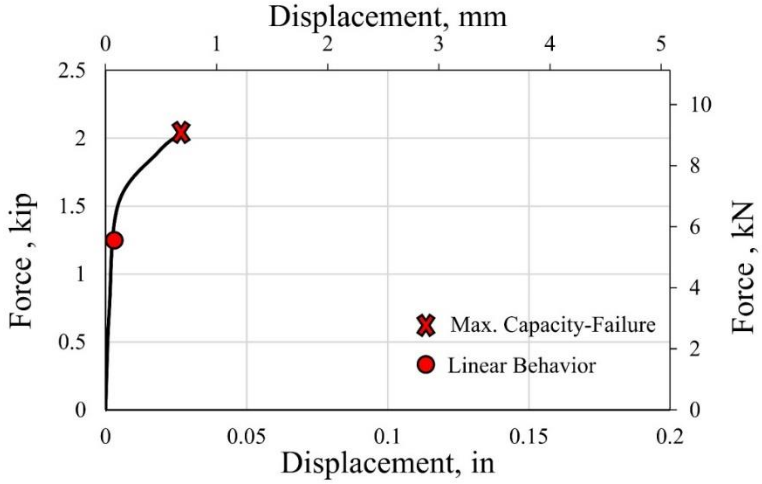

Fig. 3-13. Typical Load-displacement relationship for screw anchor embedded in 2-in. thick concrete.

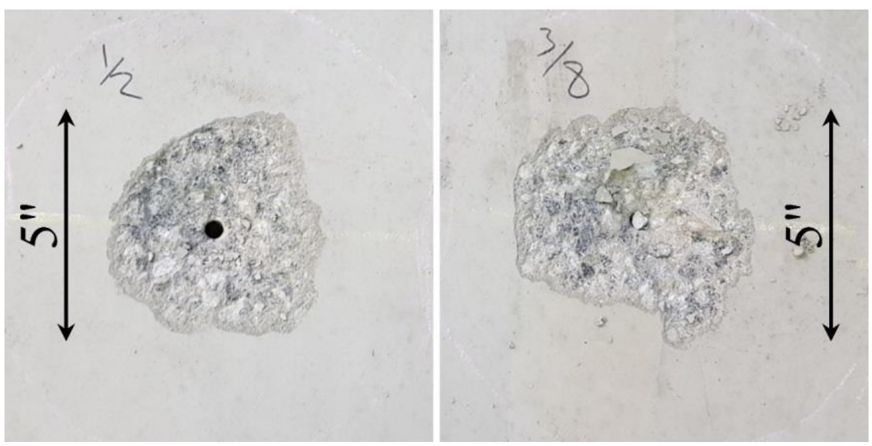

Fig. 3-14. Typical failure mode of screw anchors embedded in 2-in. thick concrete.

3.8.2 Statistical Analysis

A three-way ANOVA with a 95% confidence level was conducted to determine the effects of anchor diameter, concrete compressive strength, and brand on the capacity of anchors embedded in 2-in. thick concrete. There were no outliers in the data as assessed by inspection of a boxplot. The anchor capacities were normally distributed ($p > .05$) as assessed by Shapiro-Wilk's test of normality. The analysis showed that no statistically significant three-way nor two-way interaction between screw anchor diameter, concrete compressive strength and brand. In addition, there was no statistically significant main effect of anchor diameter (p = .755), concrete strength (p = .063), nor brand (p = .259) on the anchor capacity. The COV for the anchors tested in 2-in. concrete was 20%. Table 4 shows the mean capacity corresponding to each of the variables.

Table 3-5. Anchor pullout mean capacity corresponding to each of the variables for 2-in. thick concrete

Variable		*Mean Tested Capacity*
Diameter	*3/8 in.*	2.1 kip
	1/2 in.	2.1 kip
Concrete Compressive Strength	*6.7 ksi*	2.2 kip
	8.7 ksi	2.0 kip
Brand	*A*	2.1 kip
	B	2.2 kip
	C	2.0 kip

Note: 1 in. = 25.4 mm.;
1 ksi = 6.895 MPa.

3.9 Behavioral and Design Models for Screw Anchors in Thin Concrete Members

The screw anchor behavioral model by Kuenzlen (Fig. 3-15 left) was used as starting point for developing the proposed model, because concrete cone failure was present the theory of CCD is applicable. Kuenzlen considers the lack of thread engagement near the tip of the anchor; similarly, the proposed model accounts for lack of engagement, but due to back-face blowout (Fig. 3-15 right**)**. This proposed reduced effective embedment depth for screw anchors in thin concrete is calculated using Eq. (3-1), where h_b is the depth of the back-face blowout cone. A value of h_b equal to 0.95 in. (24.1 mm) is recommended based on fit with the experimental data. This value is also the maximum depth observed in the back-face blowout study. The proposed model uses Eq. 2-2 and Eq. 3-1 with k_c equal to 32 to determine tensile capacity. The factor 0.75 was determined by regression analysis of the experimental.

$$h_{ef} = 0.75\ (h_{nom} - h_b) \qquad \text{Eq. 3-1}$$

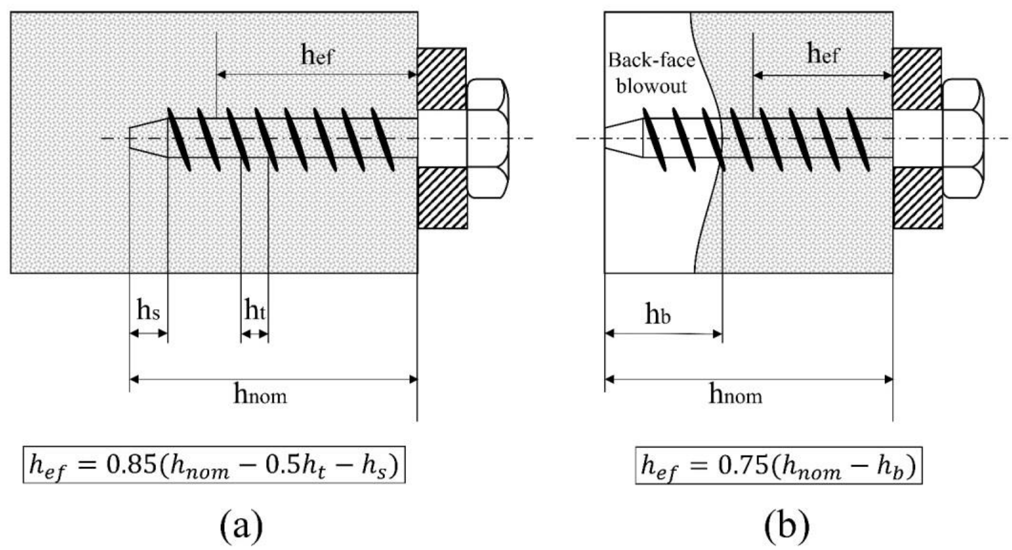

Fig. 3-15. (a) Effective depth by Kuenzlen and (b) proposed model.

Fig. 3-16 shows the experimental capacities (normalized to the concrete strength) of the tests with cone and shallow failures as a function of the effective embedment depth. Data associated with pullout failures were excluded from this figure. The figure also shows the theoretical capacity from the proposed model as calculated using Eq. 2-2 and Eq. 3-1. As can be observed in the figure the proposed model results in capacities that are within the experimental scatter. Overall, the model provides a good prediction for the average capacity with a bias (average experimental-to-model ratio) of 1.1 and a COV of 0.20. The increase in the COV value compared with the COV of 0.15 provided by Olsen et al. is due to the higher COV for anchors embedded in 2-in. concrete.

Experimental and theoretical results are also compared in Fig. 3-17 to Fig. 3-19 based on the ratio of tested to theoretical capacities ($N_{u\ test}/N_{cb}$.) These test-to-theoretical data are compared with nominal depth, anchor diameter, and concrete compressive strength to demonstrate accuracy with respect to each of these variables. The slope of the trend lines in these figures can be used to evaluate the impact of the variables on model accuracy. The downward slope of the trend line in Fig. 3-19 shows that conservatism of the model decreases with higher concrete strengths. The following paragraph describes how the value of k_c can be adjusted to create a design model that produces sufficient conservatism across all variables.

Fig. 3-17 to Fig. 3-19 compare the behavioral model to the 87 test data that failed in concrete breakout and shallow cone. For this data set and model, the overall mean value ratio (also referred to as the bias) was 1.1 and the COV was 0.2. The mean value ratio and COV are effectively unchanged when the entire data set including pullout failures (100 total data points) are considered. Accordingly, all data points were used to develop the design model for screw anchors in thin concrete.

When experimental data are available it is common practice for concrete anchorage designs to be based on the 5% lower fractile and 90% confidence level of the data (ACI 355.2). Eq. 3-2 is used to determine at value of k_c that achieves this level of conservatism, where F_m is the mean value, ν is the COV, and the K value is a factor for one-sided tolerance limits for normal distributions, corresponding to a 5% probability of non-exceedance with a confidence of 90%. Following this approach, the proposed design equation is given in Eq. 3-3. As shown in Fig. 3-20 the proposed design model produces conservative results for each of the experimental data points.

$$F_{5\%} = F_m\,(1 - K\,\nu) \qquad \text{Eq. 3-2}$$

$$N_{cb} = 19.5\,\sqrt{f'_c}\,h_{ef}^{1.5} \qquad \text{Eq. 3-3}$$

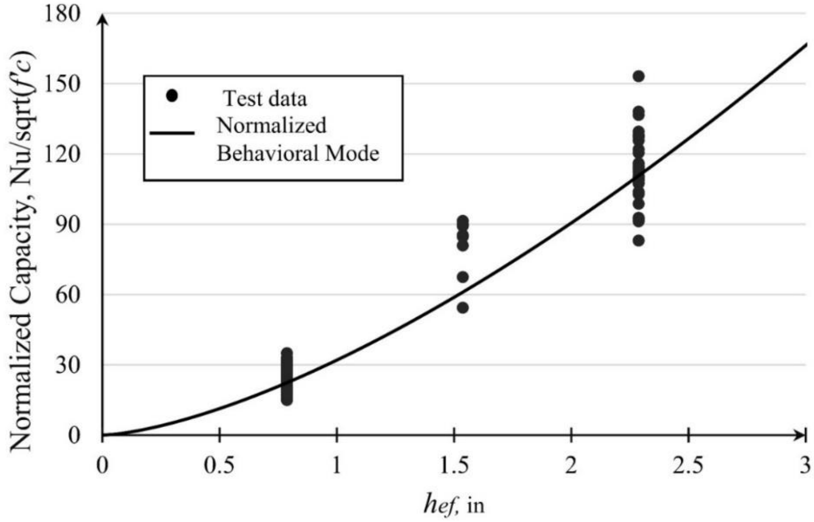

Fig. 3-16. Cone failure capacity of screw anchors in uncracked concrete as function of effective depth. (Note: 1 in. = 25.4 mm.; 1 ksi = 6.895 MPa).

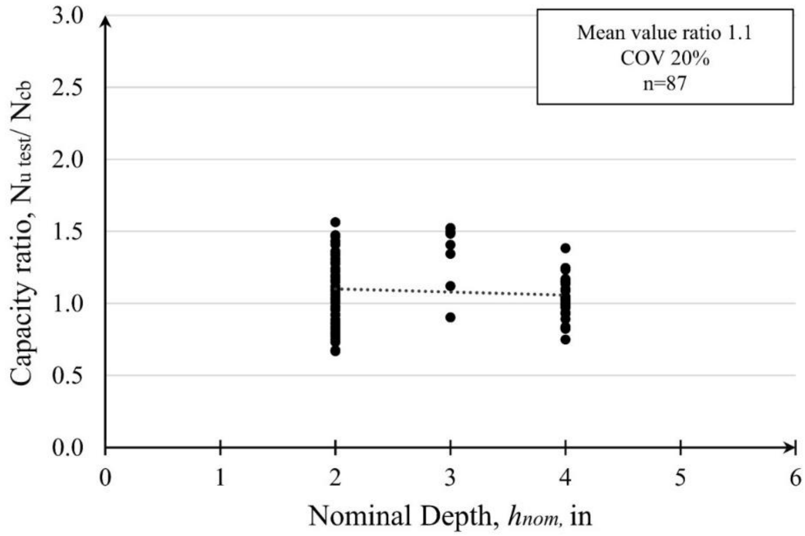

Fig. 3-17. Ratio of tested to predicted capacity versus concrete member thickness. (Note: 1 in. = 25.4 mm).

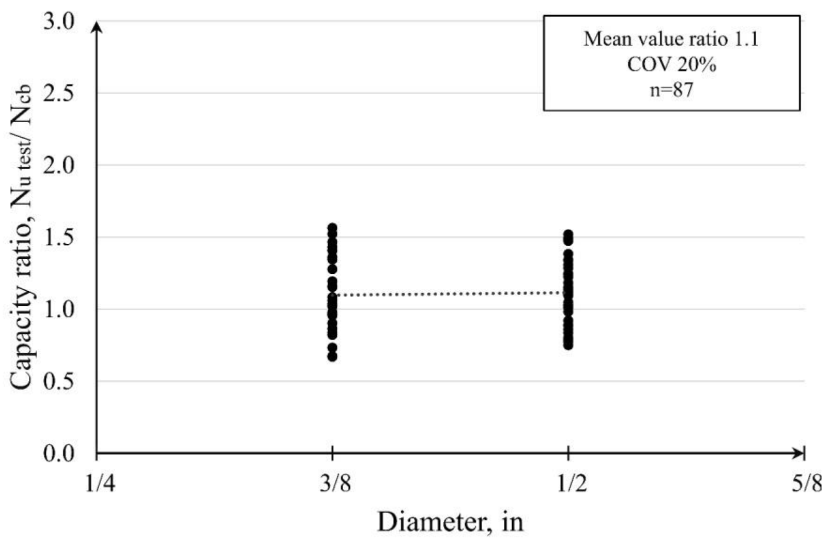

Fig. 3-18. Ratio of tested to predicted capacity versus diameter. (Note: 1 in. = 25.4 mm).

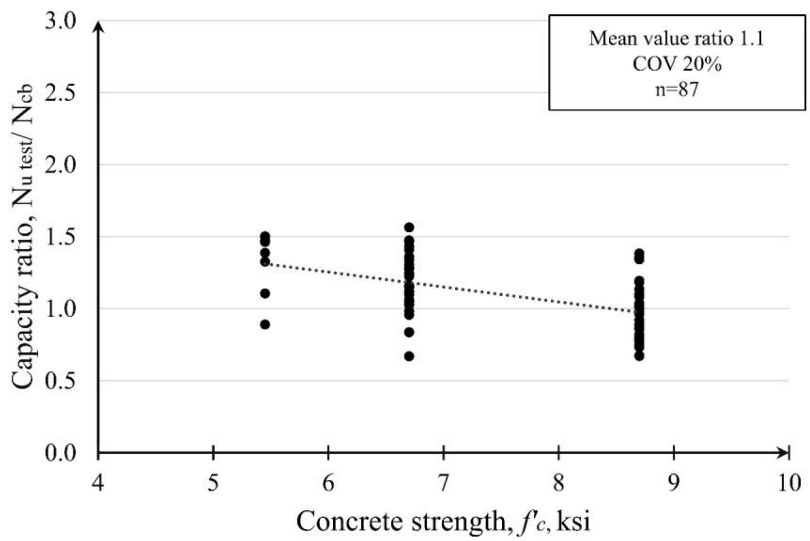

Fig. 3-19. Ratio of tested to predicted capacity versus concrete compressive strength. (Note: 1 ksi = 6.895 MPa).

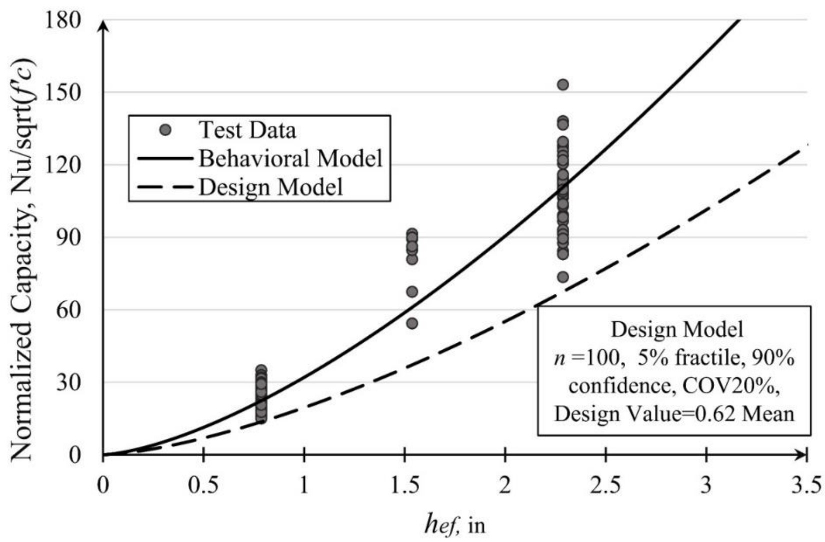

Fig. 3-20. Proposed Behavior and design models of screw anchors in uncracked concrete as function of effective depth. (Note: 1 in. = 25.4 mm.; 1 ksi = 6.895 MPa).

3.10 Comparison of Proposed Model Accuracy and Conservatism

Experimental data of screw anchors obtained in this study exhibit some degree of variability. Scatter in the experimental data is attributed to variations in concrete tensile capacity, variations in thread configurations between brands, and variations in back-face blowout depth. Of these parameters, variability of the tensile strength of concrete is likely the largest contributor to experimental scatter (Oslen et al. 2012). In order to assess the overall conservatism and accuracy of the proposed model it is useful to compare the results from the current experimental program with the results from other test programs. These comparisons are shown in Table 5; they provide context to the degree of scatter observed in the screw anchor tests and to the accuracy of the proposed model.

The bias and COV values for the other anchor types shown in Table 5 are based CCD and adhesive bond failure models. These models form the basis of the design models included in ACI 318-14. Bias and COV values from other anchor types are used as a threshold to compare the proposed model. Thus, it is inferred that the proposed model is adequate if it has a bias equal to or greater than 1.0 and the COV equal to or less than 23%. In all cases data from the current experiments and proposed model result in bias and COV values that are within the limits. These results suggest that the proposed model for screw anchors in thin concrete will provide a level conservatism and accuracy that are similar - if not better - than those resulting from models upon which the ACI code is based. Furthermore, the favorable comparison of bias and COV values suggest that the strength reduction factors in the ACI code are reasonable for use with the proposed design model for screw anchors in thin concrete. Recall that the screw anchor tests included failures from pullout. Thus, if the ACI strength reduction factors are used with the proposed design model, then condition B (pullout and pryout failures) factors should be used.

While the comparisons shown in Table 5 are encouraging, additional research is needed to confirm that findings of the current test program can be generally applied. It is recommended that future research include testing by multiple organizations and that testing include a wider range of variables. Variables in future research should include different concrete mixes (aggregate type and size, compressive strength, thickness), different hammer-drill models and users, and interactions between variables.

Table 3-6. Comparison of current and earlier tests programs.

Source of data	Database anchor type	Number of tests	Bias	COV (%)
Oslen, 2012	Screw anchors in thick concrete	402	1.1	15
Eligehausen et al. 1997	Headed studs	318	1.0	18
Fuchs et al. 1995	Expansion/undercut anchors	519	1.0	23
Cook et al. 1998	Adhesive anchors (bond failure)	888	1.0	20
Current test program	All tests	100	1.1	20
	Anchors in 4-in. concrete thick	48	1.0	14
	Anchors in 3-in. concrete thick	8	1.3	16
	Anchors in 2-in. concrete thick	44	1.1	23

Notes:
Bias = the average experimental-to-model capacity ratio
COV = the coefficient of variation of the bias
All data are from tensile tests of single anchors

3.11 Conclusions

This study investigated the tensile behavior of screw anchors embedded in thin concrete members. Experimental data were used to develop a design model for tension-loaded single screw anchors with full-thickness concrete embedment. The following conclusions are made:

1. Full-thickness drilling by a rotary-hammer drill causes concrete to blowout at the back-face. The range of blowout depth in the current study was 0.70 to 0.95 in. Futhermore, the depth of the cone in this study was not a function of the drill bit diameter, concrete compressive strength, or concrete thickness. These results are based on 31 test holes. A comprehensive study of back-face blowout, including additional test holes, is recommended for future research.
2. The effects of anchor diameter, anchor brand, and concrete compressive strength on screw anchor capacity are dependent on the thicknesses of concrete. Based on an ANOVA with 95% confidence, it is concluded that these variables had no effect on the capacity of screw anchors in 2in.-thick concrete. For anchors in 4 in.-thick concrete each of these variables had up to 20% effect on anchor capacity. The distinction is attributed to the small effective embedment depth and corresponding low concrete breakout strength of anchors installed in 2 in.-thick concrete; the low strength makes the capacity incentive to variables other than concrete thickness.
3. The proposed behavioral model, based on concrete capacity design and the work of Kuenzlen, can be used to calculate the tensile capacity of screw anchors with full-thickness installation in thin concrete members. The average experimental-to-calculated ratio for the test program was 1.1 with a COV of 0.2. The model considers the concrete cone breakout failure and uses a reduced effective embedment depth to account for back-face blowout.

4. The bias and the COV of the proposed model and experimental data are similar to the bias and COV reported for other anchor types the associated models. This suggests that the proposed model provides a similar level of accuracy and variability.

   The results and models in this paper are valid only for the limits of the variables tested. However, these limits are within a practical range values that are common in many in many applications.

   The following should be considered as the limits of the design model unless additional testing is provided:

   Anchor diameter = 3/8 to 1/2 in.

   Concrete strength = 5.5 to 8.7 ksi

   Concrete thickness = 2 to 4 in.

   Undercut degree =0.085 to 0.153 in.

3.12 References

ACI Committee 318. "Building Code Requirements for Structural Concrete (ACI 318-14): An ACI Standard: Commentary on Building Code Requirements for Structural Concrete (ACI 318R-14), an ACI Report." American Concrete Institute, 2015.

ACI Committee 355, "Qualification of Post-Installed Mechanical Anchors in Concrete (ACI 355.2-07) and Commentary," American Concrete Institute, Farmington Hills, MI, 2007, 35 pp.

ASTM E488/E488M-15 Standard Test Methods for Strength of Anchors in Concrete Elements, ASTM International, West Conshohocken, PA, 2015, https://doi.org/10.1520/E0488_E0488M-15

Cook, R.; Kunz, J.; Fuchs, W.; and Konz, R., "Behavior and Design of Single Adhesive Anchors under Tensile Load in Uncracked Concrete," *ACI Structural Journal*, V. 95, No. 1, Jan.-Feb. 1998, pp. 9-26.

Eligehausen, R.; Mallee, R.; and Silva, J., Anchorage in Concrete Construction, Ernst & Sohn, Berlin, Germany, 2006, 391 pp

Eligehausen, R.; Bouska, P.; Cervenka, V.; and Pukl, R., "Size Effect of the Concrete Cone Failure Load of Anchor Bolts," *Fracture Mechanics of Concrete Structures*, 1992, pp. 517-525.

Fuchs, W.; Eligehausen, R.; and Breen, J., "Concrete Capacity Design (CCD) Approach for Fastening to Concrete," ACI Structural Journal, V. 92, No. 1, Jan.-Feb. 1995, pp. 73-94.

ICC Evaluation Service AC193, "Acceptance Criteria for Mechanical Anchors in Concrete Elements," Whittier, CA, Feb. 2010.

Kuenzlen, J. H., "Load-Bearing Behavior of Screw Anchors under Axial Tension," doctoral thesis, the University of Stuttgart, Stuttgart, Germany, 2004. (in German).

Olsen, Jacob, Thilo Pregartner, and Anthony J. Lamanna. "Basis for design of screw anchors in concrete." ACI Structural Journal 109, no. 4 (2012): 559.

Owen, Donald B. Factors for one-sided tolerance limits and for variables sampling plans. No. SCR-607. Sandia Corp., Albuquerque, N. Mex., 1963.

TENSILE BEHAVIOR AND DESIGN OF ADHESIVE ANCHORS IN THIN CONCRETE MEMBERS

4.1 Introduction

Post-installed anchorage systems have seen increased use due to the growing demand for more flexible planning and construction (PCI Design Handbook 2017). Post-installed anchors have the advantage to be more flexible in job sites because its location can be easily adjusted to ensure proper alignment and for facilitating retrofits of buildings.

Adhesive anchors are commonly used in the concrete industry and are viewed as a practical and economical fastening system (Cook et al. 1998, Eligehausen et al. 2006). Accordingly, there is a desire to evaluate the capacity and behavior of adhesive anchors in precast concrete sandwich panels. This chapter presents experimental program that evaluates the effect of concrete member thickness, anchor diameter, concrete compressive strength, and anchor brand on the tensile behavior and capacity of adhesive anchors. The effect of full thickness drilling (penetration) on back-face blowout is also investigated. The experimental results are then used to verify a design approach for adhesive anchors in sandwich panels based on the 5% fractile of the mean value.

4.2 Experimental Program

An experimental program of 88 adhesive anchors pullout tests embedded in sandwich panels was conducted to evaluate the behavior, capacity, and failure modes of tension-loaded single adhesive anchors embedded in thin concrete members. All tests were conducted in plain uncracked concrete away from concrete edge. Variables in the experimental program include concrete thickness, anchor diameter, embedment depth, and anchor brand (Table 4-1). Four to five repetitions were tested for each combination of variables considered. Values of the variables were chosen based on common industry practice and on recommendations from precast concrete and anchor suppliers. Also based on supplier recommendations, the threaded rod in each test was extended to the insulation layer by approximately 1 in. Of the 88 tests, 39 were conducted using 2-in. thick concrete, 40 using 4-in. thick concrete, and 9 using 3-in. thick concrete. Anchors were typically installed and tested vertically; however, twelve additional tests of horizontally installed anchors were also conducted. The variables associated with the horizontal installation tests are reported later in chapter.

Table 4-1. Test matrix summary

Concrete Compressive Strength	5.5 ksi
Brands (unique threads)	3 (A, B, C)
Diameters	3/8 in., 1/2 in.
Embedment length	2 in., 3 in., 4 in.
Repetitions	4-5
Total number of tests	88

Note: 1 in. = 25.4 mm.;

1 ksi = 6.895 MPa.

4.3 Test Specimens

Eleven 3 ft. x 9 ft. x 8 in. thick concrete sandwich panels were fabricated by a precast concrete manufacturer. Concrete layers were either 42 in., or 3–3 in., and separated by a 2 in. insulation layer as shown in Fig. 4-1. Adhesive anchors were installed and tested in each of the sandwich panel concrete layers. After the tests on one side of a panel were completed, the panel was flipped and anchors were installed and tested on the other side. The testing area in the panels was unreinforced; however, reinforcement was provided at the perimeter to support the lifting points. All panels were casted with concrete compressive strength was 5.5 ksi (38 MPa) with aggregate size (#67).

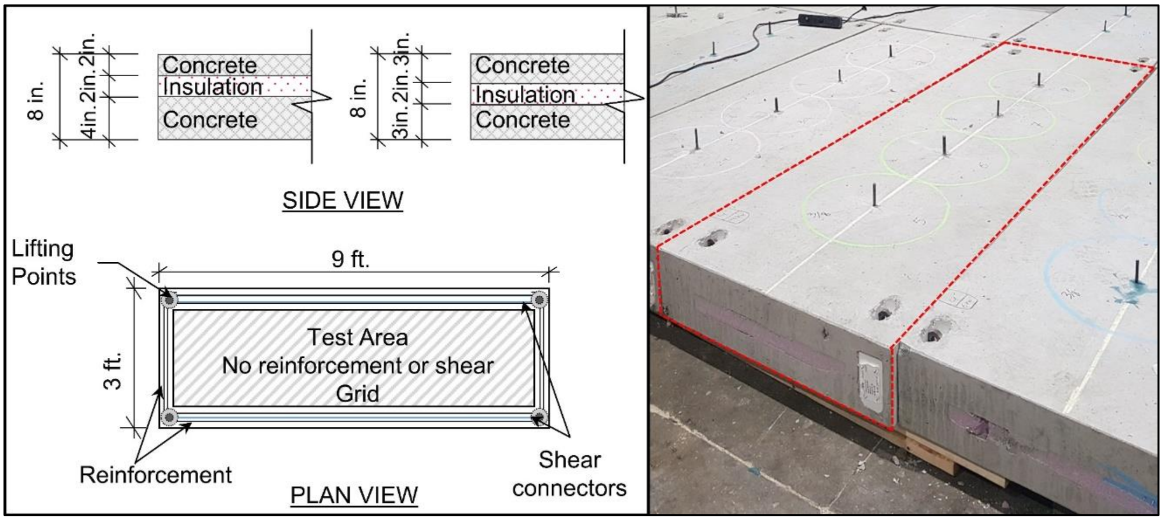

Fig. 4-1. Side and plan view for the tested panels.

Typically, four tests were conducted on each side of each panel. To prevent interaction between adjacent tests, the clear distance between tested anchors was at least five times the embedment depth. Thus, this distance exceeded the minimum distance specified by ASTM E488 *Standard Test Methods for Strength of Anchors in Concrete Elements* for unconfined pullout tests. The distance between the anchors and the perimeter reinforcement also complied with ASTM E488. Threaded rods were a grade B7 steel with tensile strength 125 ksi that met/exceeded ASTM A193. The B7 grade was chosen to mitigate the steel anchor failures.

4.4 Setup, Procedure and Measurements

Holes for anchors were drilled using carbide drill bits and a rotary-hammer drill. Because rotary-hammer drills combine the rotary mechanism with a hammering action that produces a pounding force, they are efficient and effective for drilling in concrete and masonry. Rotary-hammer drills also lead to the back-face blowout as discussed before. Holes were drilled through the entire thickness of the concrete layer

Before injecting the adhesive, the holes were cleaned with compressed air and brush according to the product specification. The hole was filled completely with the adhesive, and then the threaded rods were installed through the full thickness of concrete layer and extended for approximately 1 in. into the insulation layer as shown in Fig 4-2. The adhesive cured for at least 24 hours, which exceed the required time by the product specifications.

The testing apparatus shown in Fig 4-2 was designed to meet the requirements of ASTM E488, including the required distance between supporting points for unconfined pullout tests. The tension load was applied perpendicular to the panel by a hand operated hydraulic jack. Load was recorded using a calibrated load cell and checked using a pressure gage installed in the hydraulic line. The loading rate was adjusted to ensure that failure occurred within one to three minutes after the beginning of the test as specified by ASTM E488.

Two calibrated displacement transducers recorded the displacement of the anchor relative to the concrete surface and the average displacement was considered as recommended by ASTM E488. Data were continuously monitored and logged using a computer-based data acquisition system.

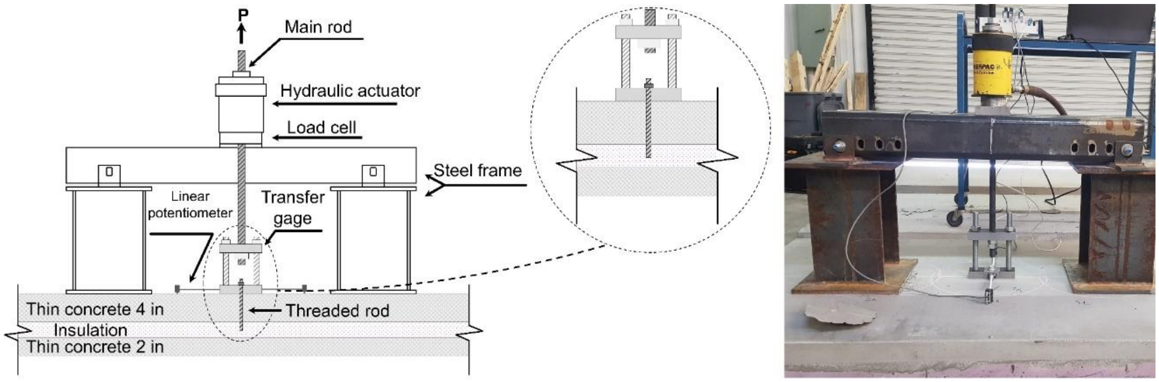

Fig. 4-2. Test apparatus.

4.5 Tests Results

The following section presents the results of 88 pullout tests. Results discussed in terms in terms of the failure mode and the associate load-deflection response, back-face blowout effect, and the effect of the variables on the capacity of adhesive anchors.

4.6 Failure Modes and Load-Displacement Response

Three failure modes were observed: steel anchor failure, concrete cone breakout, and concrete cone/pullout as shown in Fig. 4-3 a, b, and c respectively. Fig. 4-3 also shows the load-displacement response associated with each failure mode.

Anchors embedded in 2 and 3 in. concrete thickness layers failed in concrete cone breakout failure regardless the anchor diameter. The cone depth was equal to the concrete layer depth as will be discussed in the next section. Fig. 4-3a shows the load-displacement response for typical anchors embedded in 2 in. concrete layer. Load and displacement increased linearly until cracks began to form in the concrete cone. For the anchor in Fig. 4-3a cracks formed when the displacement reached approximately 0.05 in. (1.27 mm). Initial cracking in the concrete led to a reduction of stiffness but not to immediate failure. In the example, the load continued to increase until reached a peak near 9 kip (40 kN) with corresponding displacement of 0.1-0.15 in (3-4 mm).

Anchors embedded in 4 in. concrete experienced anchor steel failure for the 3/8 in. anchors and a combine failure concrete cone/pullout for 1/2 in. anchors (Fig. 4-3b). This general behavior is consistent with the adhesive anchors behavior described in Cook et. al 1998, where shallow embedment anchors typically fail in concrete cone failure, whereas anchors with deeper embedment depths experience combined failure mode.

The combined failure mode (1/2 in. anchors in 4 in. concrete thickness) experienced the smallest deformation (0.09 in. (2.3 mm)) and had the highest stiffness due to the higher bonded embedment depth (Fig. 4-3b).

It can be observed from Fig. 4-3c that anchor steel failure is a ductile leads the highest deformation of 0.2-0.25 in. (5-6.3 mm), which is almost twice the deformation associated with other failure modes. This behavior is due to the ductile nature of the steel.

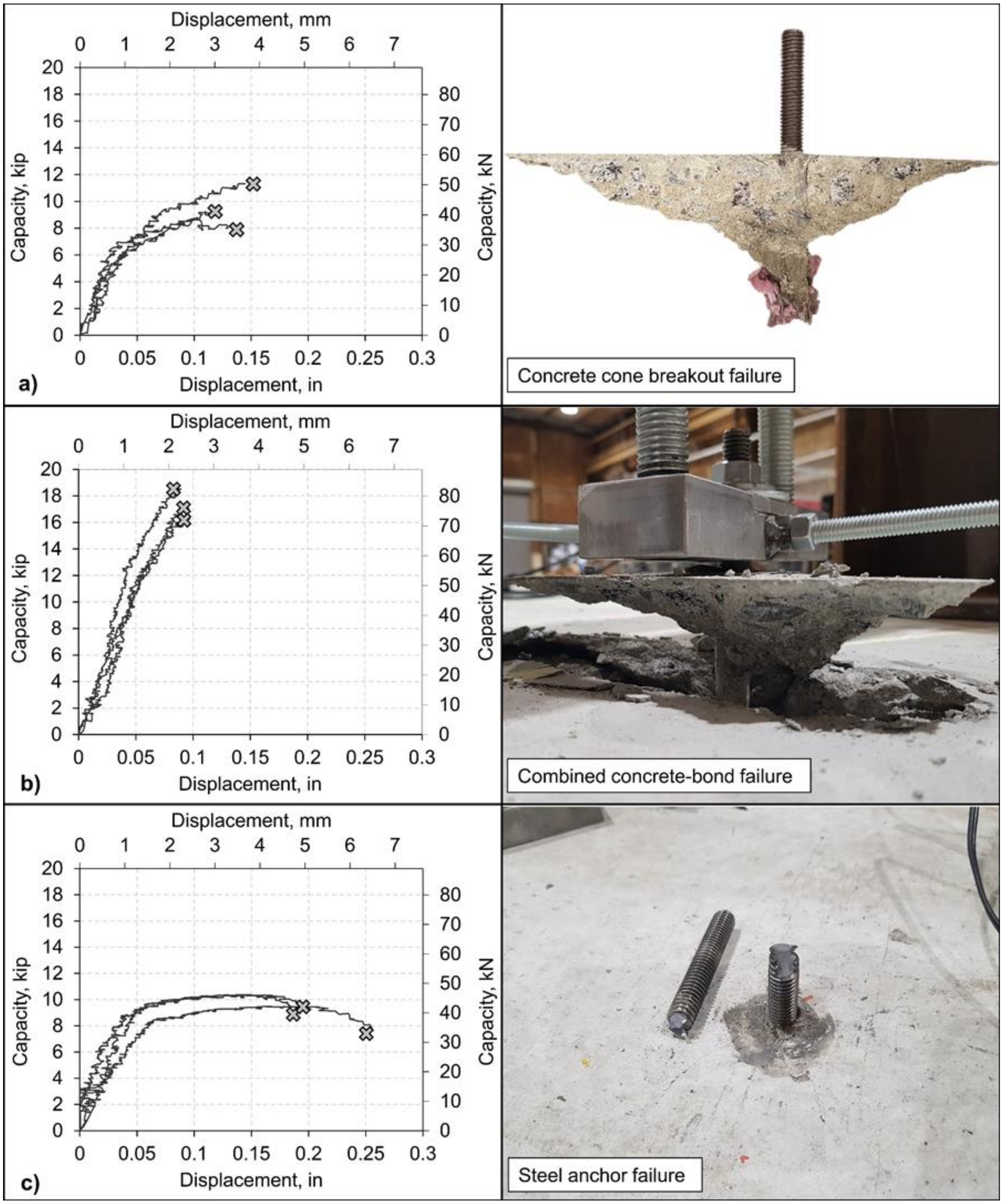

Fig. 4-3. Load-displacement and failure modes.

4.7 Effect of Variables

The experimental program includes two anchor diameters, 3/8 in. and 1/2 in. Fig. 4-4 presents the relationships between the capacity and the anchor diameter for each of the concrete thicknesses. The trend line shows that the effect of the diameter become more noticeable as the concrete thicknesses increase. This can be seen by the increase of the trend line slope, being the smallest at 2 in. concrete thickness and the highest at 4 in. concrete thickness. This behavior is consistent with the behavior of screw anchors embedded in thin concrete layers (chapter three) where the effect of anchor diameter, concrete strength was negligible in 2 in. concrete thickness and increase with increasing the thickness.

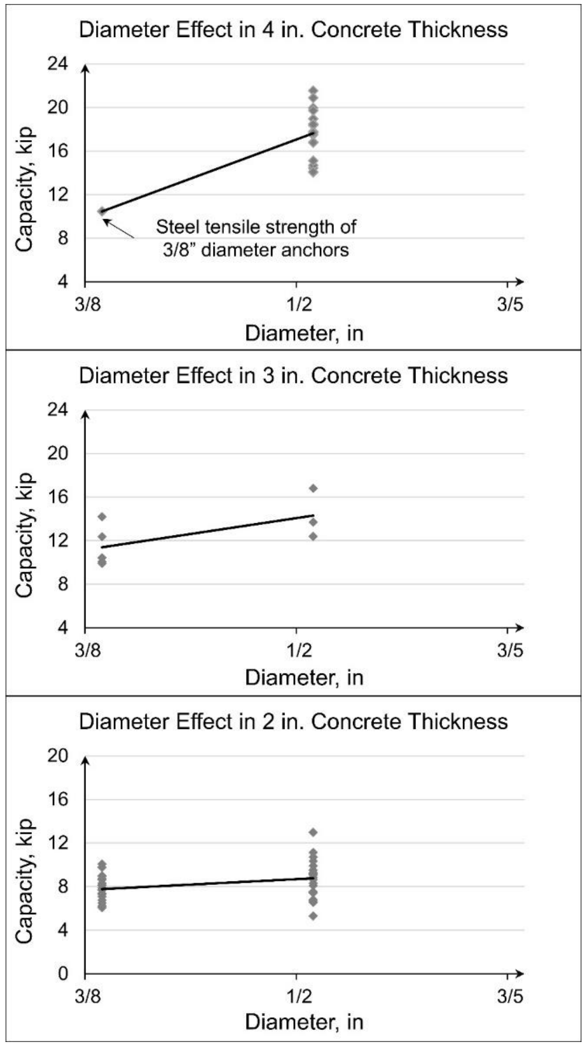

Fig. 4-4. Anchor diameter effect at different concrete thicknesses.

Fig. 4-5 shows the effect of the concrete thickness on the capacity. Anchor capacity versus thickness is plotted separately for 3/8 and 1/2 in. diameter anchors.

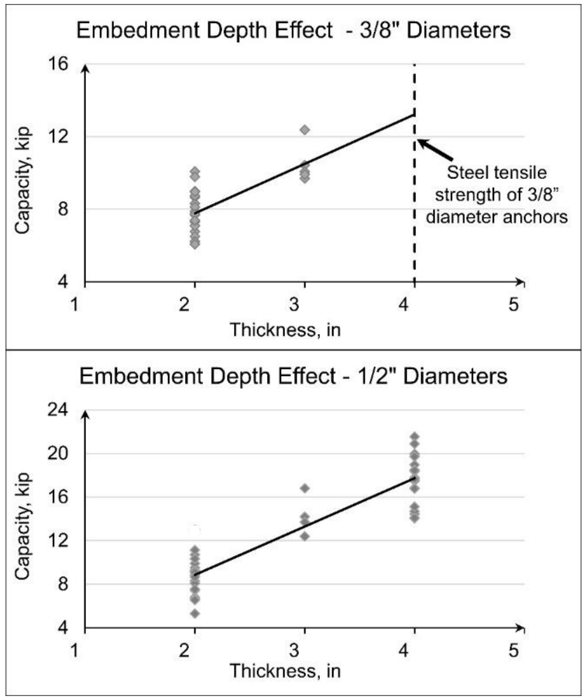

Fig. 4-5. Concrete thickness effect on anchor capacity.

A three-way ANOVA with 95% confidence level was conducted to determine the effects and the correlation of anchor diameter, concrete thickness, and the adhesive product manufacturer on anchor capacity. Table 4-2 shows the correlation coefficient for each variable. The coefficient of correlation ranges from -1 for maximum negative correlation to +1 for maximum positive correlation, while a 0 value represents no correlation. It can be seen that the adhesive product has no significant correlation to the capacity ($p < 0.671$) which means that changing the product manufacturer did not affect the capacity. Note that the same supplier was used for all the steel threaded rods but that the adhesive came from three different suppliers. The ANOVA results showed that there was a statistically significant main effect for anchor diameter ($p < .001$) and concrete thickness strength ($p < 0.001$), with highest correlation to the concrete thickness.

Table 4-2. Correlation coefficients

Anchor Diameter	Pearson Correlation	.535 (Correlation)
	p- value	< .001
Concrete Thickness	Pearson Correlation	0.910 (Highest correlation)
	p- value	< .001
Adhesive Product	Pearson Correlation	-0.052 (No correlation)
	p- value	0.671

Furthermore the ANOVA showed an interaction between the anchor diameter and concrete thickness, this interaction means that the effect of the diameter on the capacity is affected by the thickness. This interaction is supported by the results shown in Fig. 4-4 wherein the effect of anchor diameter (e.g. slope of the trend line) increases as the concrete thickness also increases.

4.8 Comparison between Adhesive and Screw Anchors

Adhesive anchors embedded in 2 and 3 in. concrete thicknesses in the test program always failed in concrete breakout. Back-face blowout did not impact the failure cone and the cone depth was equal to the concrete thickness. This result is attributed to the adhesive filling the cracks and fractures in the concrete which occurred due to the drilling. In addition, part of the injected adhesive entered the insulation foam layer and created a base or plug for the concrete cone; this adhesive base helped in creating full thickness cone. Fig. 4-6 shows a concrete cone breakout in 2 in. concrete thickness, the figure shows the injected adhesive between the cracks and the base created by the adhesive.

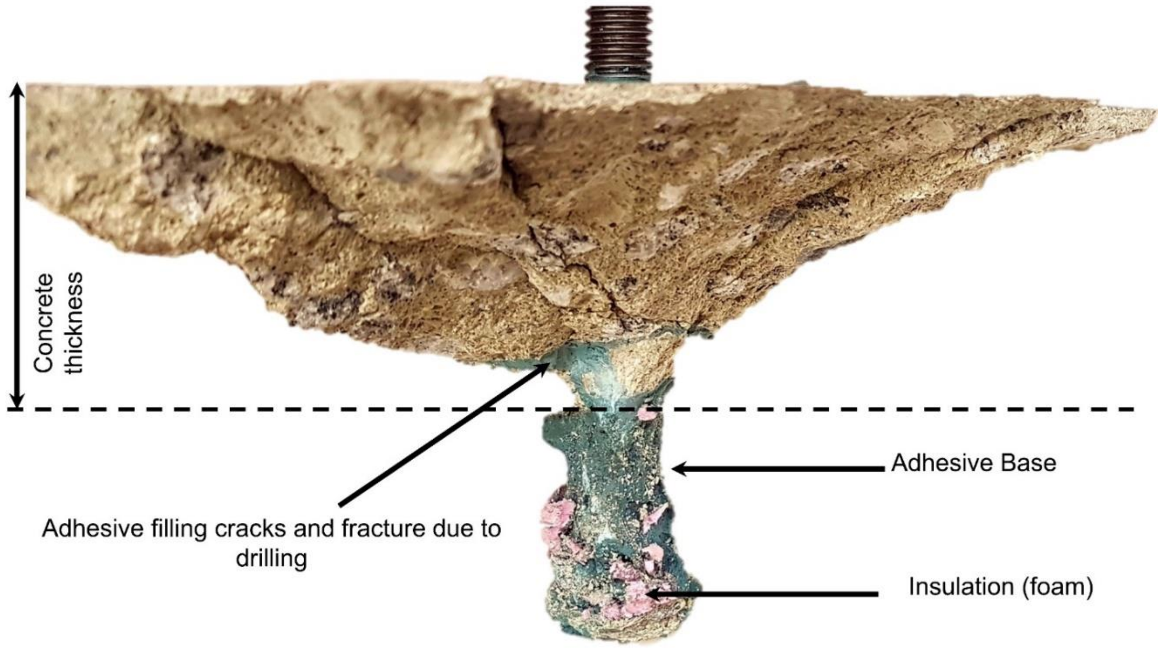

Fig. 4-6. Adhesive filled cracks due to back-face blowout and created a base in the foam layer.

Fig. 4-7 compares concrete cone breakout for screw and adhesive anchors embedded in 2 in. concrete thickness. The size of the breakout cone for the adhesive anchor is almost twice that of the screw anchor breakout cone. This increase in the size can be attributed to the adhesive that is filling the cracks and creating a base at the end of the anchor as explained earlier. This increase in cone size led to a significant increase in the capacity. Table 4-3 shows the average capacities of screw and adhesive anchors in 2, 3, and 4 in. concrete thicknesses. Adhesive anchors were tested in concrete with 5.5 ksi compressive strength while the screw anchors were testes in concrete with compressive strengths ranging from 5.5 to 8.7 ksi. For 2in. thick concrete the adhesive anchors have tensile capacity over four times the capacity of screw anchors. The additional strength is attributed to the increased effective depth and concrete blowout cone of adhesive anchors.

Table 4-3. Adhesive and screw anchors experimental mean capacities

Concrete thickness	Screw Anchors		Adhesive Anchors	
	3/8 Diameter	1/2 Diameter	3/8 Diameter	1/2 Diameter
2 in.	2.1 kip	2.0 kip	7.8	8.8 kip
3 in.	5.6 kip	6.2 kip	10.3 kip	14.1 kip
4 in.	9 kip	10.2 kip	-	17.5 kip

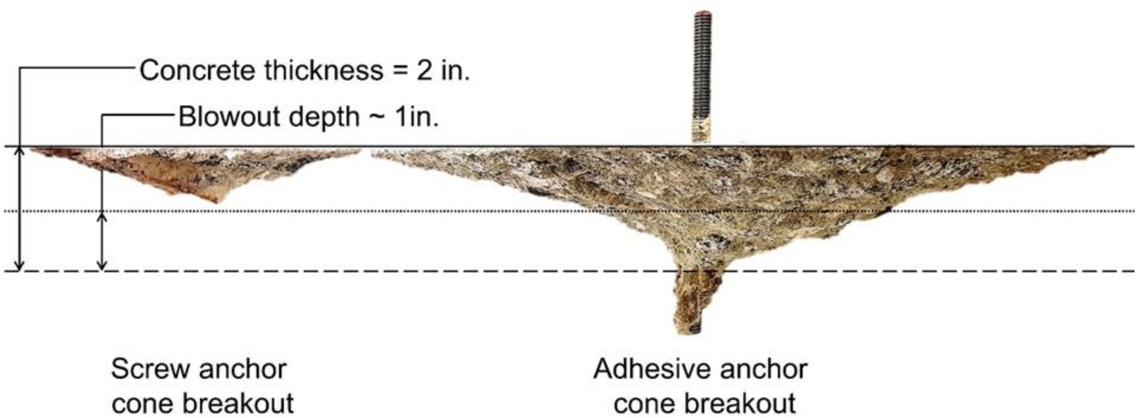

Fig. 4-7. Adhesive and screw anchors concrete cone breakout.

4.9 Behavioral and Design Models for Adhesive Anchors in Thin Concrete Members

The CCD model is used to evaluate the capacity of mechanical anchors failing in concrete cone breakout and has been adopted by buildings code and design standards. The capacity of single anchor fail in concrete cone is given in Eq. 2-2 with k_c =13.5 for SI units and k_c =32 for SI units (converted by the author).

The CCD model was used to evaluate the capacity of the adhesive anchors in the test program. For these calculations the effective depth of the anchor was set equal to the thickness of the concrete. This approach is in contrast with the approach used for evaluating screw anchor in thin concrete, wherein a reduced depth is recommended to account for the effects of back-face-blowout (Eq. 3-1). The experimental data are compared with CCD model ("behavioral model") in Fig. 4-8. Tests have shown that k_c values for adhesive and expansion mechanical anchors are approximately similar[8]. As shown in Fig. 4-8, the model has good agreement with the test data. The average strength ratio (tested capacity/ predicted capacity) was 1.1 with a coefficient of variation (COV) of 0.2. The accuracy and the fitting of the model can be checked by plotting the ratio between the tested capacity and ($N_{u\ test}$) and the predicted capacity (N_{cb}) with respect to thickness and diameter as shown in Fig. 4-9 and Fig. 4-10 respectively.

When experimental data are available it is common practice for concrete anchorage designs to be based on the 5% lower fractile with 90% confidence level of the data. Eq. 4-1 is used to determine the value of k_c that achieves this level of conservatism, where F_m is the mean value, ν is the COV, and the K value is a factor factors for one-sided tolerance limits for normal distributions corresponding to a 5% probability of non-exceedance with a confidence of 90% (Owen 1963). Following this approach, the proposed design equation is given in Eq. 4-2. As shown in Fig. 4-11 the proposed design model produces conservative results for each of the experimental data points.

$$F_{5\%} = F_m\ (1 - K\ \nu) \qquad \text{Eq. 4-1}$$

$$N_{cb} = 19.5\sqrt{f'_c}\ h_{ef}^{1.5} \qquad \text{Eq. 4-2}$$

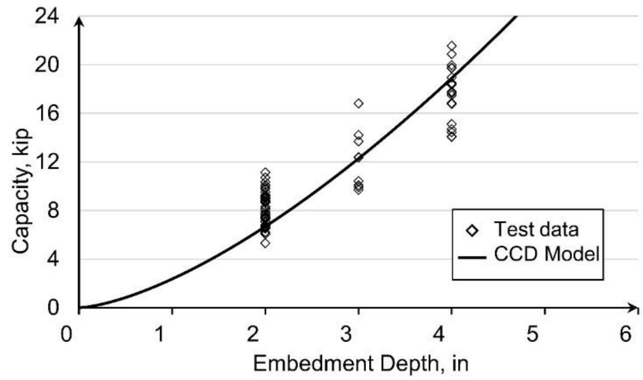

Fig. 4-8. Cone failure capacity of adhesive anchors in uncracked concrete as function of effective depth. (Note: 1 in. = 25.4 mm.; 1 ksi = 6.895 MPa).

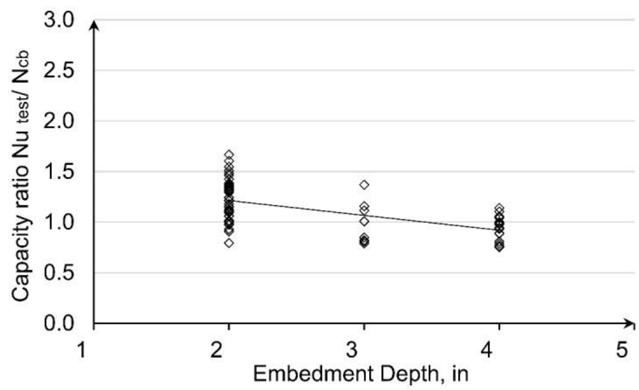

Fig. 4-9. Ratio of tested to predicted capacity versus concrete member thickness. (Note: 1 in. = 25.4 mm).

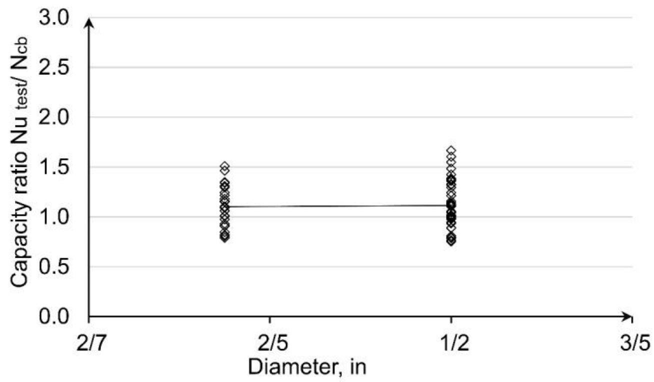

Fig. 4-10. Ratio of tested to predicted capacity versus diameter. (Note: 1 in. = 25.4 mm).

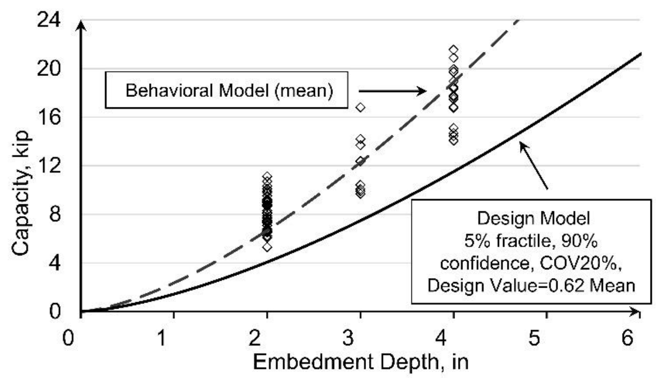

Fig. 4-11. Proposed Behavior and design models of adhesive anchors in uncracked concrete as function of effective depth. (Note: 1 in. = 25.4 mm.; 1 ksi = 6.895 MPa).

4.10 Horizontal Installation and Concrete Strength Effect

To verify the adequacy of the proposed model to predict the capacity for anchors installed in higher strength concrete and for anchors installed horizontally, twelve additional pullout tests were conducted in 2 in. and 4 in. thick concrete layers with 9.2 ksi concrete compressive strength. The anchors were installed horizontally in the panels as shown in Fig. 4-12. The panels were kept in the upright position as the adhesive cured and were then placed flat for testing of the anchors.

Fig. 4-13 shows the CCD model, steel tensile strength for 1/2" diameter anchor, and test data for anchors embedded in higher concrete strength with horizontal installation. Anchors embedded in 2 in. concrete thick showed a high agreement with the CCD model with tested/predicted ratio 1.0. All 1/2" Anchors embedded in 4 in. concrete thick reached their steel tensile capacity at 80% of the predicted capacity by CCD. The results indicate that changing the concrete strength neither the installing position of the anchor (vertical verses horizontal) affected the model prediction accuracy.

Fig. 4-14 shows the concrete strength effect on 1/2" anchors embedded in 2 and 4 in. concrete thick. The general trend for both concrete thicknesses is increased capacity as the concrete compressive strength. It is noted that the concrete strength effect become more noticeable with higher in thicker concrete layer which agrees with the screw anchors behavior.

Fig. 4-12. Horizontal installation of anchors.

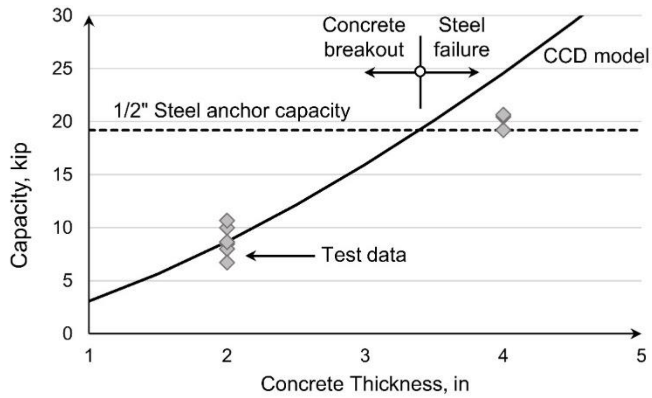

Fig. 4-13. Experimental and predicted capacities for anchors installed horizontally in higher concrete strength.

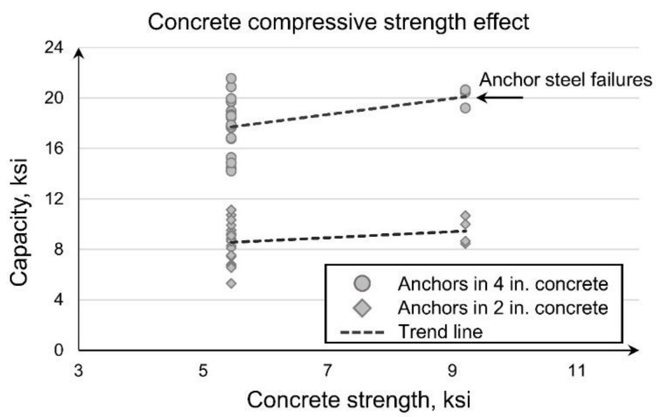

Fig. 4-14. Concrete strength effect for 1/2" anchors.

4.11 Comparison of Behavioral Model Accuracy and Conservatism

As would be expected experimental capacity of adhesive anchors obtained in this study exhibit a degree of variability. Scatter in the experimental data is primarily attributed to variations in concrete tensile capacity (Olsen et al. 2012). The experimental variability leads to variability in the accuracy of the proposed model. In order to assess the overall conservatism and accuracy of the proposed model it is useful to compare the current results with those of other test programs. These comparisons are shown in Table 4-4; they provide context to the degree of scatter observed in the adhesive anchor tests in thin concrete layers and to the accuracy of the behavior model.

Table 4-4. Comparison of current and earlier tests programs.

Source of data	Database anchor type	Number of tests	Bias	COV (%)
Chapter three	Screw anchors in thin concrete	100	1.1	20
Olsen et al. 2012	Screw anchors in thick concrete	402	1.1	15
Eligehausen, et al. 1993	Headed studs	318	1.0	18
Fuchs et al. 1993	Expansion/undercut anchors	519	1.0	23
Cook et al. 1998	Adhesive anchors (bond failure)	888	1.0	20
Current test program	All tests	100	1.1	20
	Anchors in 4-in. concrete thick	48	1.0	12
	Anchors in 3-in. concrete thick	8	1.3	19
	Anchors in 2-in. concrete thick	44	1.1	17

Notes:
Bias = the average experimental-to-model capacity ratio
COV = the coefficient of variation of the bias
All data are from tensile tests of single anchors

The bias and COV values for the other anchor types shown in Table 4-4 are based CCD and adhesive bond failure models. These models form the basis of the design models included in ACI 318-14. Bias and COV values from other anchor types are used as a threshold to compare the behavioral model. Thus, it is inferred that the behavior model for adhesive anchors in thin concrete is adequate if it has a bias equal to or greater than 1.0 and the COV equal to or less than 23%. In all cases data from the current experiments and model result in bias and COV values that are within these limits. This suggests that the model for adhesive anchors in thin concrete will provide a level conservatism and accuracy that are similar - if not better - than the leading models applied to other anchor types and conditions. Furthermore, the favorable comparison of bias and COV values suggest that the strength reduction factors in the ACI code are reasonable for use with the design model for adhesive anchors in thin concrete

While the comparisons shown in Table 4-4 are encouraging, additional research is needed to confirm that findings of the current test program can be generally applied. It is recommended that future research include testing by multiple organizations and that testing include a wider range of variables. Variables in future research should include different concrete mixes (aggregate type and size, compressive strength, thickness), different hammer-drill models and users, and interactions between variables. A reliability analysis is also recommended to confirm the validity of the ACI strength reduction factors.

4.12 Recommendation

Chapter three has shown that screw anchors in thin concrete members can support significant loads; however, it is clear from the current results that adhesive anchors provide superior tensile capacity under similar conditions. For example, in the case of anchors in 2 in. thick concrete, adhesive anchors provide approximately four times greater capacity than comparable screw anchors. The distinction can be seen in Fig. 4-15 that compares the tested capacities and prediction models for screw and adhesive anchors. In addition, adhesive anchors showed consistent performance independent of the adhesive supplier, unlike screw anchors wherein the failure mode and capacity were dependent on the product itself. Therefore, the authors recommend that adhesive anchors be used in lieu of screw anchors in most situations. Screw anchors are typically more efficient to install and may be reasonable for some temporary fixtures, non-structural elements, and lightly loaded connections.

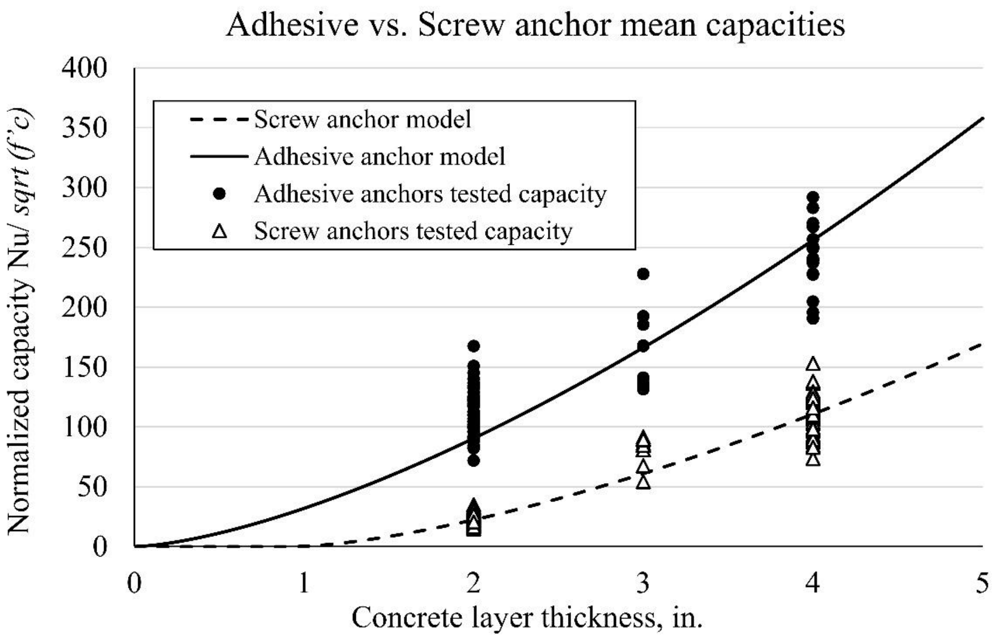

Fig. 4-15. Screw vs. adhesive anchors capacities.

4.13 Conclusions

This study investigated the tensile behavior of adhesive anchors embedded in thin concrete members. Experimental data were used to verify a design model for tension-loaded single adhesive anchors with full-thickness concrete embedment. Results were also compared and contrasted to a previous study on the use of screw anchors in thin concrete members. The following conclusions are made:

1. The CCD model with effective embedment depth equal to the concrete layer thickness can be used to calculate the tensile capacity of adhesive anchors with full-thickness installation in thin concrete members. The average experimental-to-calculated ratio for the test program was 1.1 with a COV of 0.2.

2. The bias and the COV of the proposed model and experimental data are similar to the bias and COV reported for widely accepted models applied to other anchor types and conditions. This suggests that the CCD model for adhesive anchors in thin concrete provides a similar level of accuracy and variability.
3. The depth of concrete cone breakout for adhesive anchors embedded in 2 and 3 in. concrete thickness was equal to the concrete layer thickness. The effect of back-face blowout was mitigated because the adhesive filled the cracks that occurred due to drilling. This phenomenon led to larger failure cone and significant higher capacity when compared to screw anchors.
4. The capacity of adhesive anchors was approximately 200% to 400% greater than the capacity of comparable screw anchors. Adhesive anchors exhibit a consistent failure mode in each concrete thickness that is independent of the adhesive product unlike screw anchors were the failure mode was affected the screw geometry.
5. The effect of anchor diameter and concrete strength on anchor capacity tend to increase by increasing the embedment depth. There was no significant effect for the adhesive products on anchor capacity. Although the test data for investigating the installation orientation (vertical verses horizontal installation) effect were limited, there is no evidence that the orientation affect the anchor capacity.

The results and models in this paper are valid only for the limits of the variables tested. However, these limits are within a practical range values that are common in many in many applications. The following should be considered as the limits of the design model unless additional testing is provided:

Anchor diameter = 3/8 to 1/2 in.

Concrete strength = 5.5 to 9.2 ksi

Concrete thickness = 2 to 4 in.

4.14 References

ACI Committee 318. "Building Code Requirements for Structural Concrete (ACI 318-14): An ACI Standard: Commentary on Building Code Requirements for Structural Concrete (ACI 318R-14), an ACI Report." American Concrete Institute, 2015.

ASTM E488/E488M-15 Standard Test Methods for Strength of Anchors in Concrete Elements, ASTM International, West Conshohocken, PA, 2015, https://doi.org/10.1520/E0488_E0488M-15

Cook, R. A.; Kunz, J.; Fuchs, W.; and Konz, R. C., 1998, "Behavior and Design of Single Adhesive Anchors under Tensile Load in Uncracked Concrete," ACI Structural Journal, V. 95, No. 1, Jan.-Feb., pp. 9-26.

Eligehausen, R.; Bouska, P.; Cervenka, V.; and Pukl, R., "Size Effect of the Concrete Cone Failure Load of Anchor Bolts," *Fracture Mechanics of Concrete Structures*, 1992, pp. 517-525.

Eligehausen, R.; Cook, R. A.; and Appl, J., 2006a, "Behavior and Design of Adhesive Bonded Anchors," ACI Structural Journal, V. 103, No. 6, Nov.-Dec., pp. 822-831.

Fuchs, W.; Eligehausen, R.; and Breen, J., "Concrete Capacity Design (CCD) Approach for Fastening to Concrete," ACI Structural Journal, V. 92, No. 1, Jan.-Feb. 1995, pp. 73-94.

Olsen, Jacob, Thilo Pregartner, and Anthony J. Lamanna. "Basis for design of screw anchors in concrete." ACI Structural Journal 109, no. 4 (2012): 559.

Owen, Donald B. Factors for one-sided tolerance limits and for variables sampling plans. No. SCR-607. Sandia Corp., Albuquerque, N. Mex., 1963.

PCI Design Handbook - Precast and Prestressed Concrete, eighth Edition, Precast/Prestressed Concrete Institute, Chicago, IL, 2017.

SHEAR BEHAVIOR AND DESIGN OF SCREW AND ADHESIVE ANCHORS IN THIN CONCRETE MEMBERS

5.1 Introduction

Chapter three and four discuss the tensile capacity and behavior of screw and adhesive anchors in thin concrete members with full embedment depth. This chapter describes an experimental program that was conducted to evaluate the behavior of post-installed screw and adhesive anchors in thin concrete members subjected to shear loads towards the free edge. Variables included in the experimental program include concrete member thickness, concrete compressive strength, anchor diameter, anchor type, and edge distance. The effects of full thickness drilling (penetration) on back-face and its implications on anchor shear capacity were also investigated. The experimental results have been used to test the applicability and suggest changes to the current shear design provisions for anchors in ACI 318-14.

5.2 Anchor Shear Capacity According to CCD

Anchors close to the concrete edge and subjected to shear load towards the edge may fail by semi-conical concrete breakout originating at the bearing point (Fig. 5-1a). If the concrete breakout mechanism has sufficient strength (typically due to being far from the free edge) then the steel anchor will fail due to the shear load. The capacity of anchor embedded in thick uncracked concrete member away from corner is determined by the Concrete Capacity Design (CCD) method (Fuchs et al. 1995) given in Eq. 5-1.

$$V_b = 13\left(\frac{l_e}{d_o}\right)^{0.2}\sqrt{d_o}\ \sqrt{f'_c}\,(c_1)^{1.5} \qquad \text{Eq. 5-1}$$

where

l_e = effective load transfer length, in.

d_o = outside diameter of anchor, in.

f'_c = concrete compressive strength

c_1 = edge distance, in.

The derivation of the CCD shear equation is similar to the CCD equation in tension (Fig. 2-8) were the surface area of the fracture surface is multiplied by the concrete tensile strength (represented by the square root of the of the concrete compressive strength). The failure load is proportional to the edge distance (c_1) which is analogous to the embedment depth in tension-loaded anchors (Eligehausen et al. 2006). The area of the fractured conical shape is proportional to ${c_1}^2$, however the failure load is proportional to $c_1^{1.5}$ due to the size effect discussed in Fuchs, 1990. In addition, the CCD shear equation takes into account the flexural stiffness and the anchor diameter using the first two terms in the equation respectively.

Eq. 5-1 is applicable for anchors where the full semi-conical fractured surface can form (Fig. 5-1a). Based on 35^o angle cone, this condition can met if the depth of the concrete member exceed 1.5c_1 and the width exceed 3c_1. The capacity of anchors embedded in thin concrete members or close to corner, where the fractured area is truncated, is reduced. The capacity of such anchors can be evaluated using Eq. 5-2 based on the ratio of the projected of full fractured surface, A_{vo}, (Fig. 5-1b) and the projected area of a truncated fractured surface, A_v, (Fig. 5-1c and 5-1d).

$$V_{cb} = \left({}^{A_v}/_{A_{vo}}\right)\ V_b \qquad \text{Eq. 5-2}$$

However, shear tests of anchors in thin concrete members (Zhao et al. 1989 reported in Eligehausen et al. 2006) demonstrated that the CCD approach tends to underestimate experimental capacity of anchors in thin concrete members. To avoid unnecessarily high conservatism, Eligehausen et al. (2004) proposed a modification factor to be applied to CCD where $h < 1.5c_1$. This modification factor is currently implemented in ACI 318-14 code:

$$\psi_{h,v} = \sqrt{1.5c_1 / h} \qquad \text{Eq. 5-3}$$

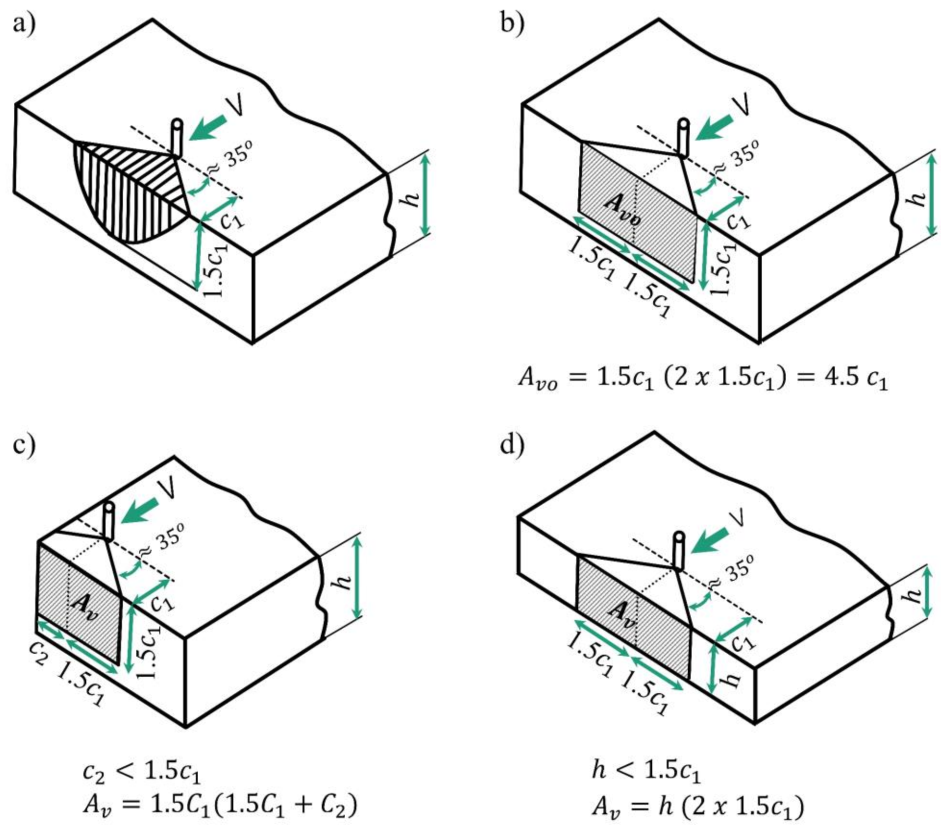

Fig. 5-1. Anchors subjected to shear load a) Idealized failure surface for single anchor per CCD b) projected area for single anchor in thick concrete c) projected area for single anchor close to corner d) projected area for single anchor in thin concrete member.

5.3 Experimental Program

An experimental program of 149 screw and adhesive shear tests performed in 12 precast sandwich panel specimens was conducted to evaluate the behavior, capacity and failure modes of shear-loaded single anchors embedded in thin concrete members. All tests were conducted in plain uncracked concrete away from concrete edge where the full width of fracture surface could develop. Variables in the experimental program included concrete thickness, concrete compressive strength, anchor type, anchor diameter, and edge distance. The test program resulted in an 86 different combination of variables with one or two (mostly two) repetitions of for each combination (Table 5-1). Variables were selected in consultation with precast concrete and anchor suppliers. In each test, the embedment depth of the screw anchor was equal to the thickness of the concrete member. For adhesive anchors, the threaded rod was extended almost 1 in. to the insulation layer as discussed in chapter four to increase the tensile capacity of the anchor. Of the 149 tests, 48 were conducted using 2-in. thick concrete, 54 using 3-in. thick concrete, and 47 using 4-in. thick concrete.

Table 5-1. Test variables

Tested concrete Compressive Strength	5.1 ksi, 9.2 ksi
Concrete thickness	2 in., 3 in., 4 in.
Anchor Diameters	3/8 in., 1/2 in.
Edge distance	2 in., 3 in., 5 in., 8in
Anchor type	Screw, adhesive
Repetitions	1-2*
Total number of tests	149
Combination of variables	86

Note: 1 in. = 25.4 mm.;
1 ksi = 6.895 MPa.
* most combinations have 2 repetitions

5.4 Test Specimens

Twelve concrete sandwich panels were fabricated by a precast concrete manufacturer; concrete layers for a given panel were 4 and 2 in., or 3 and 3 in. Layers were separated by a 2 in. insulation layer as shown in Fig. 5-2. Anchors were installed and tested in each of the sandwich panel concrete layers. After the tests on one side of a panel were completed, the panel was flipped and anchors were installed and tested on the other side. The testing area in the panels was unreinforced. Corners were solid concrete without insulation to support the lifting points and provide integrity to the panel for lifting, shipping, and flipping. Two concrete mixes were used for the panels, resulting in a well-separated concrete compressive strengths (Table 1). Maximum aggregate size in all panels was 3/4" (i.e. #67 stone).

Sandwich panels were 5.5 ft. long by 3.5 ft. wide. Typically, seven tests were conducted on each side of each panel (Fig. 5-3). To prevent interaction between adjacent tests, the clear distance between tested anchors was more than four times the edge distance. As such, the anchors spacing exceeded the minimum distance specified by ASTM E488 *Standard Test Methods for Strength of Anchors in Concrete Elements* for shear tests. For adhesive anchors, B7 grade threaded rods were used.

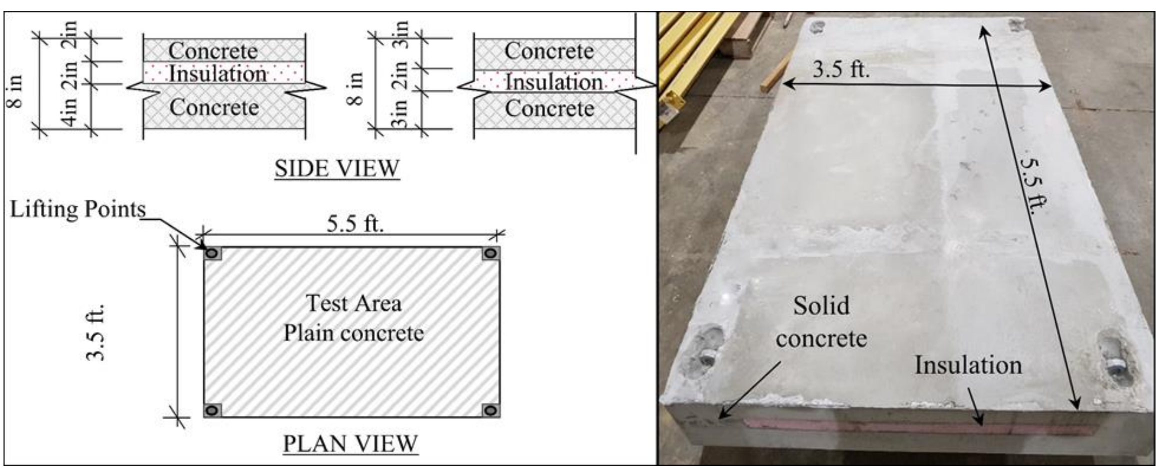

Fig. 5-2. Test specimens.

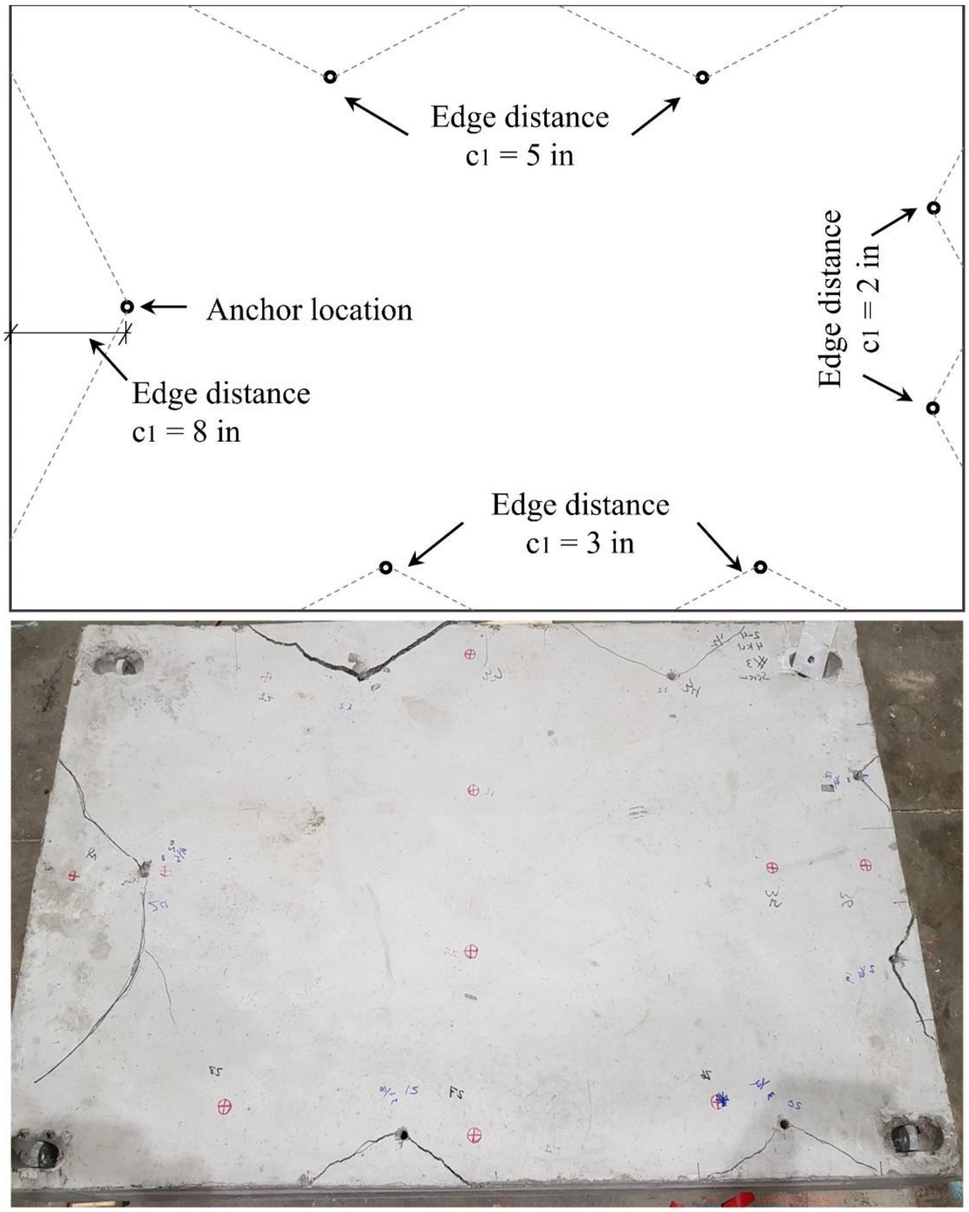

Fig. 5-3. Shear tests layout.

5.5 Setup, Procedure and Measurements

Holes were drilled through the entire thickness of the concrete layer using carbide drill bits and a rotary-hammer drill. Hole diameter, hole cleaning, and anchor placement followed the manufacturers' installation instructions.

The testing apparatus is shown in Fig. 5-4, and was designed to comply with ASTM E488, including the required distance between supporting points. The loading frame was oriented parallel to the panel edge, while shear load was applied perpendicular to the panel edge by a hand operated hydraulic jack. Load was recorded using a calibrated load cell and checked using a pressure gage. The loading rate was adjusted to ensure that failure occurred within 1 to 3 minutes after the beginning of the test as specified by ASTM E488.

The loading plate was designed according to ASTM E488. A polyethylene layer was always inserted between the loading plate and the concrete surface to reduce the friction. Two calibrated displacement transducers recorded the displacement of the loading plate relative to the concrete surface. Data were continuously monitored using a computer-based data acquisition system.

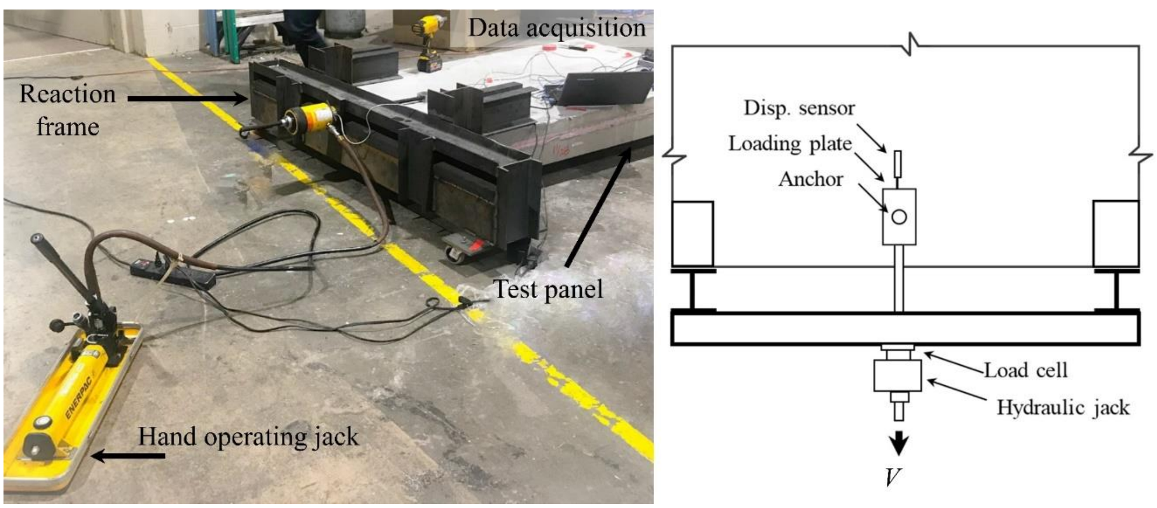

Fig. 5-4. Test apparatus.

5.6 TEST RESULTS

5.6.1 Failure Mode and Load-Displacement Behavior

Concrete edge breakout failure originating at the anchor bearing was the dominant failure mode exhibited throughout the experimental program. The failure surface extended through the full thickness due to concrete thinness and the full thickness embedment of the anchors (Fig. 5-5). Similar failure mode was exhibited for adhesive and screw anchors. The average breakout angle was 28^{o} degrees.

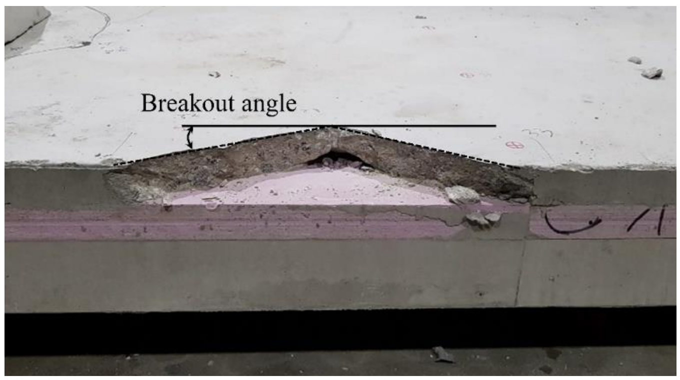

Fig. 5-5. Concrete edge breakout in shear.

Steel anchor failure occurred when the edge distance and the concrete thickness were sufficiently large leading to a concrete breakout strength that exceeded that the steel shear capacity. The variables were selected to promote breakout failure; hence, steel failure only occurred in 10% of the tests.

Fig. 5-6 shows a typical load-displacement response of an adhesive anchor embedded in thin concrete member with full embedment depth. The overall behavior shown in the figure was typical for both screw and adhesive anchors and is similar to the shear behavior anchors described in Eligehausen et al. (2006). At the beginning of the test load is transferred by friction between the loading plate and the concrete surface. When the applied load exceeded the friction resistance, the plate slipped resulting in the semi-flat plateau at the bottom of the figure. With additional displacement, the plate engaged the anchor in bearing resulting in an increase in stiffness of the system. Load and displacement continued to increase until concrete edge breakout failure occurred at peak load.

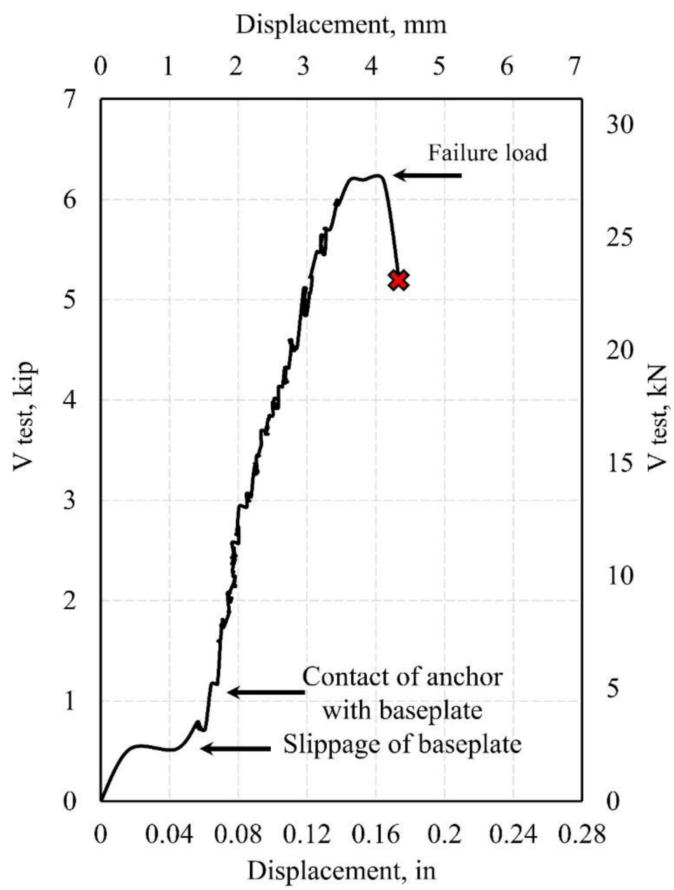

Fig. 5-6. Typical load-displacement curve for shear loaded anchors in thin concrete members.

5.6.2 Screw vs. Adhesive Anchors

The effects of back-face blowout were evaluated by examining the concrete failure surfaces after testing. For screw anchors the back-face cone blowout was easily identified and its depth in the direction of the anchor was measured (Fig. 5-7a). Blowout depth values ranged from 0.65 to 0.96 in. Blowout depth values were similar to those reported in chapter three. Blowout depth could not be readily measured in adhesive anchor specimens because the adhesive filled any cracks and damage in the blowout region (Fig. 5-7b). This phenomenon gave adhesive anchors higher stiffness due to restraint over the entire embedment depth. In contrast, screw anchors were unrestrained in the blowout region which led to lower stiffness with respect to the adhesive anchors. It is reasoned that the higher stiffness for adhesive anchors provided greater stress distribution and resulted in the higher capacities observed in the test program (Fig. 5-8). This rationale is consistent with the CCD procedure wherein anchor stiffness is accounted by the ratio of the shear transfer length to the diameter (Eq. 5-1).

Fig. 5-8 compare the average capacities of screw and adhesive anchors at each edge distance and member thickness. The capacities shown in the figure are normalized to 5 ksi concrete compressive strength by multiplying the experimental capacity by the ratio $\sqrt{5/f'_{c,\ actual\,(ksi)}}$. Each bar represent the average of multiple replicates. Adhesive anchors had higher capacity than comparable screw anchors because of the higher stiffness that resulted from adhesive filling the blowout region as mentioned earlier. On average, the adhesive anchors had 17% more capacity than screw anchors tested under the same variables. However, the difference in capacity between screw and adhesive anchors was a function of concrete layer thickness. The greatest difference, 31%, was observed in 2 in. concrete thickness. The change is attributed to the relative impact of the blowout with respect to the member thickness. To account for back-face blowout and its implication on the shear capacity of screw anchors, a depth (Eq. 3-1) is used in the next section of the paper to calculate the shear load transfer length (l_e). Adhesive anchors are relatively less impacted by blowout and the shear load transfer length was set equal to the concrete member thickness.

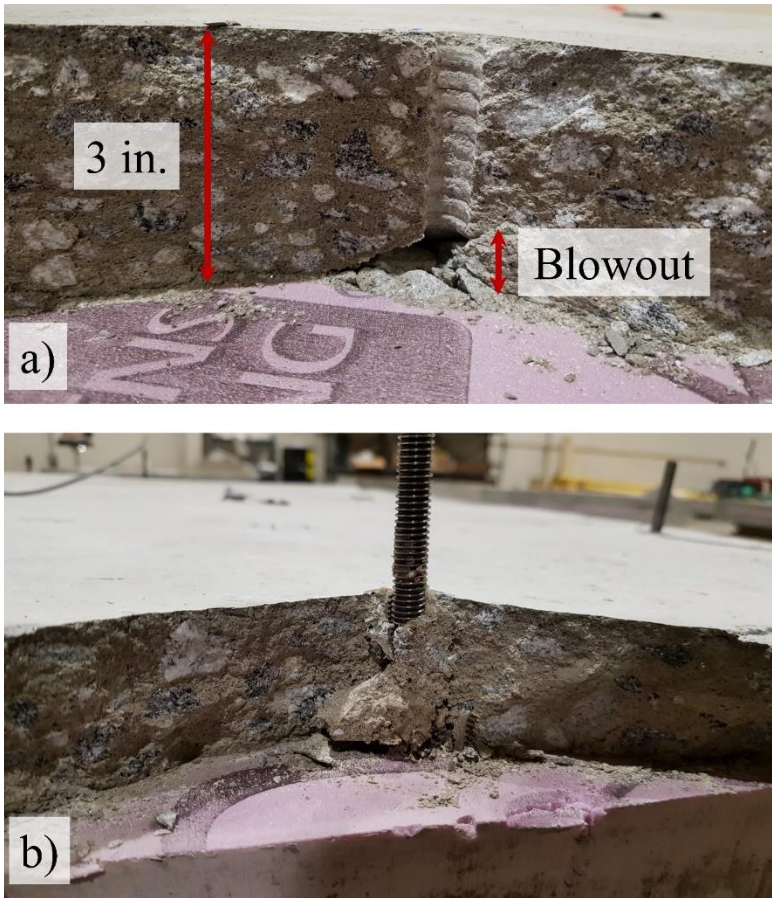

Fig. 5-7. Back-face blowout in a) screw anchors b) adhesive anchors.

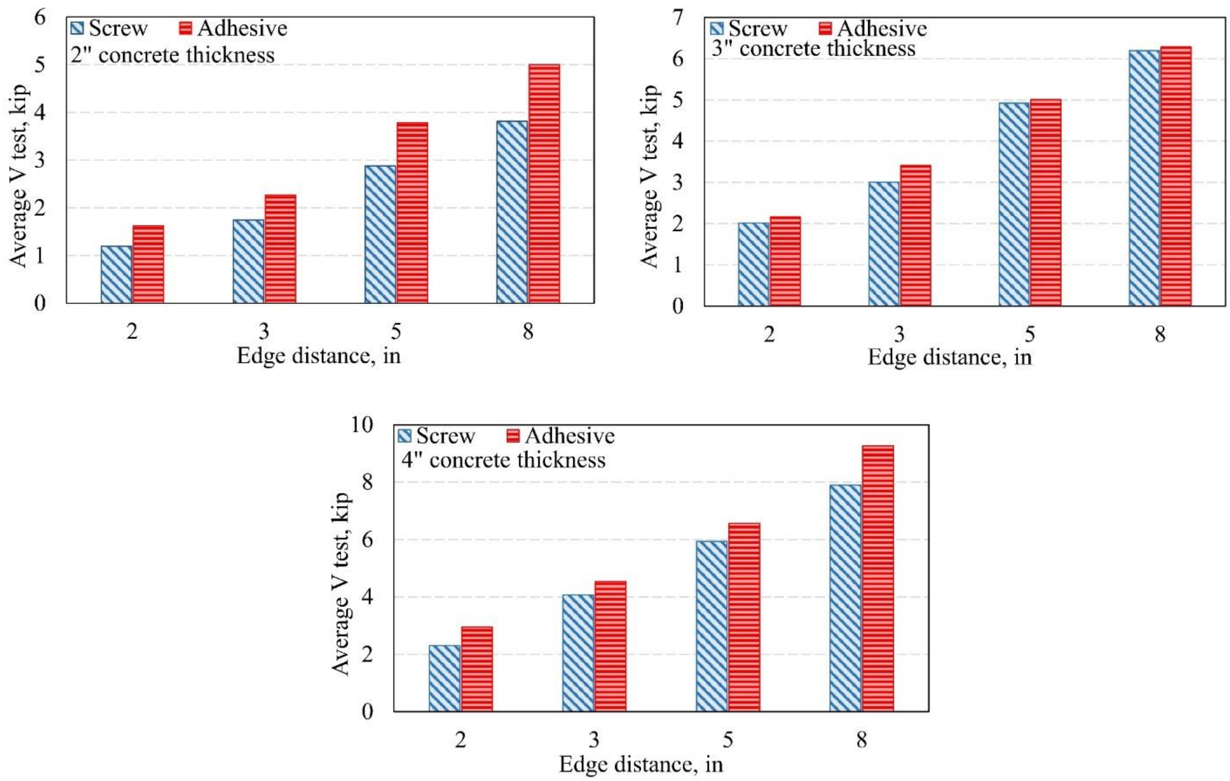

Fig. 5-8. Comparison between screw and adhesive average capacities concrete (Note: 1 ksi = 6.895 MPa).

5.6.3 Evaluation of CCD Model

Fig. 5-9 shows the experimental capacities for anchors in 2", 3", and 4" concrete thickness under shear load. The data is normalized to concrete strength 5 ksi, 1/2" anchor diameter, l_e = concrete thickness. Recall that reduced effective depth (Eq. (3-1)) is used to calculate the load transfer length (l_e) for screw anchors.

Although Eq. 5-1 expresses a nonlinear relationship between failure loads and edge distance, Fig. 5-9 shows that failure loads tends to increase nearly linearly with the edge distance. This behavior was also observed by Zhao et al. for anchors in thin concrete members (reported in Eligehausen et al. (2006)). For purposes of this discussion "thin" refers to members wherein the projected failure is rectangular (Fig 5-1d) rather than semi-conical (Fig 5-1a). The linear relationship observed in the tests is attributed to the change in fracture surface from a semi-conical surface that is proportional to c_1^2 to rectangular (truncated) surface that is proportional to c_1. A correction factor to address this change in relationship will be discussed later in the paper.

In addition, Eq. 5-2 determine the capacity of an anchor based on the failure projected area, which imply that the capacity is directly proportional to the member thickness. However, this was not confirmed by the test results. Fig. 5-9 shows the trend line of the capacity in each thickness, it can be seen that the slope become steeper as the member thickness increases. This behavior indicate an interaction between the edge distance and the thickness instead of directly proportional relationship.

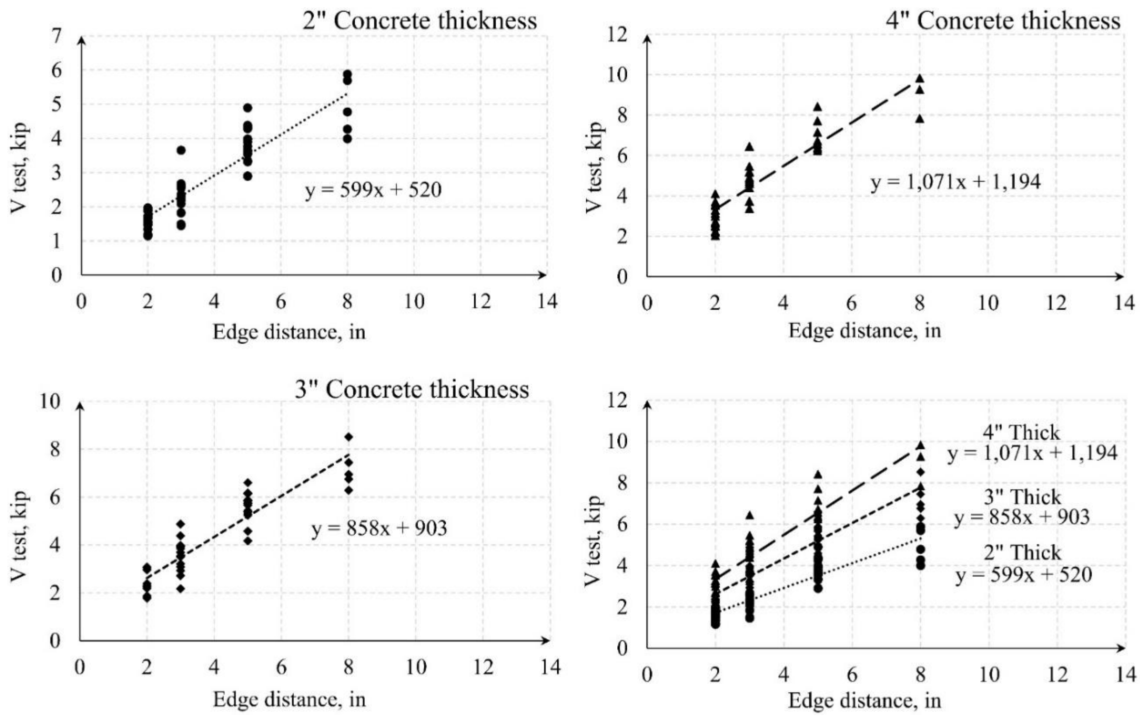

Fig. 5-9. Experimental shear loads as function of edge distance for different concrete thicknesses (Note: 1 in. = 25.4 mm; 1 ksi = 6.895 MPa).

The theoretical CCD strength of each anchor was calculated using Eq. 5-1 and Eq. 5-2. For screw anchors the shear transfer depth was calculated using Eq. 3-1, whereas for adhesive anchors the depth was taken as the concrete layer thickness. Fig. 5-10 shows the ratio of tested-to-calculated capacity verses the edge distance. The figure shows that the conservatism of the CCD model increases with the greater edge distance. The figure also shows that increased concrete member thickness has an impact on the level conservatism. This can be observed by comparing the slope of the trend lines for the different concrete thicknesses. The steepest slope is for the 2 in. thick concrete, suggesting that the model accuracy is not directly proportional to the member thickness and there is an interaction between the member thickness and the edge distance.

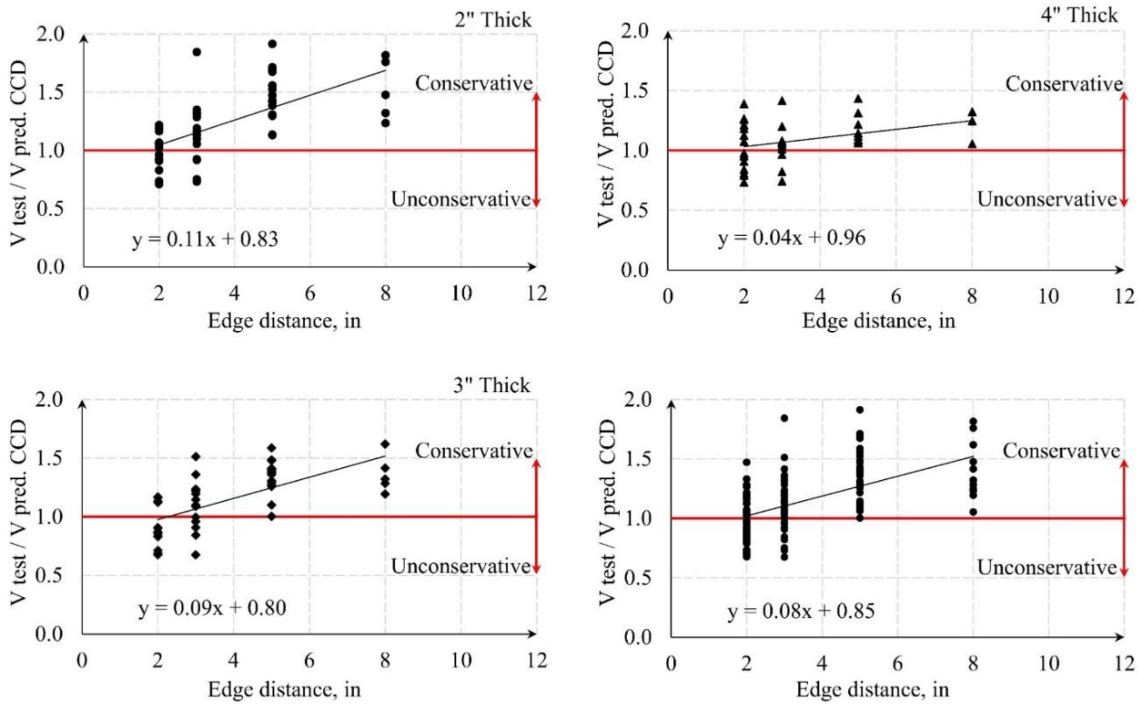

Fig. 5-10. Ratio of tests to predicted capacity by CCD verses edge distance (Note: 1 in. = 25.4 mm).

The interaction between member thickness and edge distance is more clearly demonstrated in Fig. 5-11. In this figure, the ratio of the tested capacity to CCD-predicted capacity is plotted against the ratio of the thickness to the edge distance (h/c_1). A nonlinear trend line is shown to illustrate the change in model conservatism as a function of h/c_1. The figure shows that CCD underestimates anchor capacities (has increasing conservatism) as the ratio h/c_1 becomes smaller than 1.5. For ratios less than 1.5 the member depth is insufficient for the full semi-conical fracture surface to develop. For values of h/c_1 greater than 1.5 the full semi-conical fracture surface can develop and the model shows better prediction accuracy.

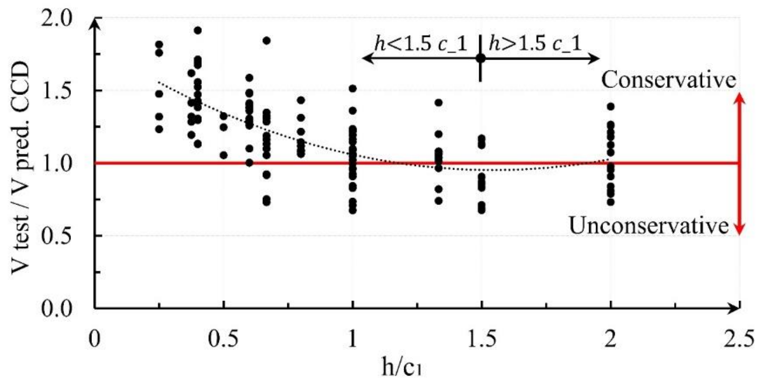

Fig. 5-11. Ratio of tests to predicted capacity by CCD verses depth to edge distance ratio.

A similar trend has been observed in other anchor shear tests in thin members. Eligehausen et al. (2004) proposed a modification factor ($\psi_{h,v}$) for anchors where h < 1.5 c_1. (without full thickness embedment depth) as discussed in the background section. Fig. 5-12 shows the ratio of the tested capacity to the predicted capacity by the CCD adjusted by the thickness modification factor (Eq. 5-3) verses edge distance and the thickness to edge distance ratio (h/c_1). The figure shows that the thickness modification factor leads to an overestimation (unconservative) of anchor capacity. Possible reasons for this overestimation are that the thickness modification factor was not intended for full embedment anchors, and that the tested members in this program were very thin.

Based on the comparisons shown in Fig. 5-10, 5-11, and 5-12 the CCD model does not have a consistent level of accuracy or conservatism for the given test data. Fitness of the model changes with edge distance and member thickness. The next section presents an alternative thickness modification factor that addresses this issue.

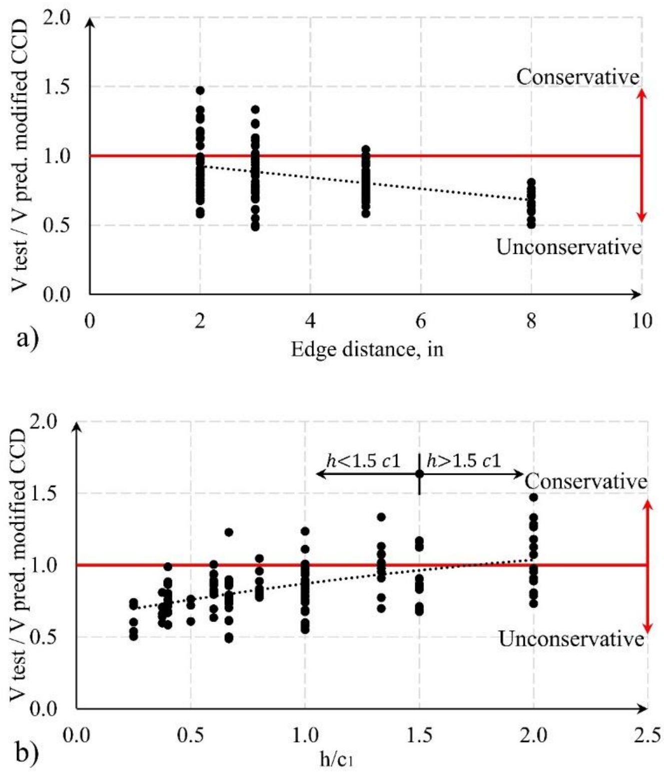

Fig. 5-12. Ratio of tests to predicted capacity by CCD verses a) edge distance b) depth to edge distance ratio (Note: 1 in. = 25.4 mm).

5.7 Proposed Thickness Modification Factor for Anchor with Full Embedment Depth

A nonlinear regression analysis with the form presented in Eq. 5-4 was conducted to determine a more suitable thickness modification factor. This equation has the same form as the factor proposed by Eligehausen et al. 2006. The regression results for the factors A and B are 1.48 and 0.213 respectively. The estimate of the factor A is very close the 1.5 value proposed in Eligehausen whereas the value for B is less than the 0.5 value. The proposed modification factor based on nonlinear regression of the test data is shown in Eq. 5-5.

$$\psi_{h,v} = \left(\frac{A\, c_{a1}}{h}\right)^{B} \qquad \text{Eq. 5-4}$$

$$\psi_{h,v} = \left(\frac{1.5\, c_{a1}}{h}\right)^{0.2} \qquad \text{Eq. 5-5}$$

Overall, the CCD model with the revised modification factor provides a good with the experimental data; the bias (average experimental-to-model ratio) is 1.0 and the coefficient of variation (COV) is 18%. The COV value is close to the 17% COV for anchors in shear reported by Eligehausen et al. 2006.

Experimental to theoretical ($V_{u\ test}/V_{cb}$) ratios are plotted in Fig. 5-13 with respect to anchor diameter, concrete compressive strength, concrete thickness, and anchor type to demonstrate accuracy with respect to each of these variables. The slope of the trend lines in these figures can be used to evaluate the impact of the variables on model accuracy. The model accuracy is relatively consistent over the range of variables.

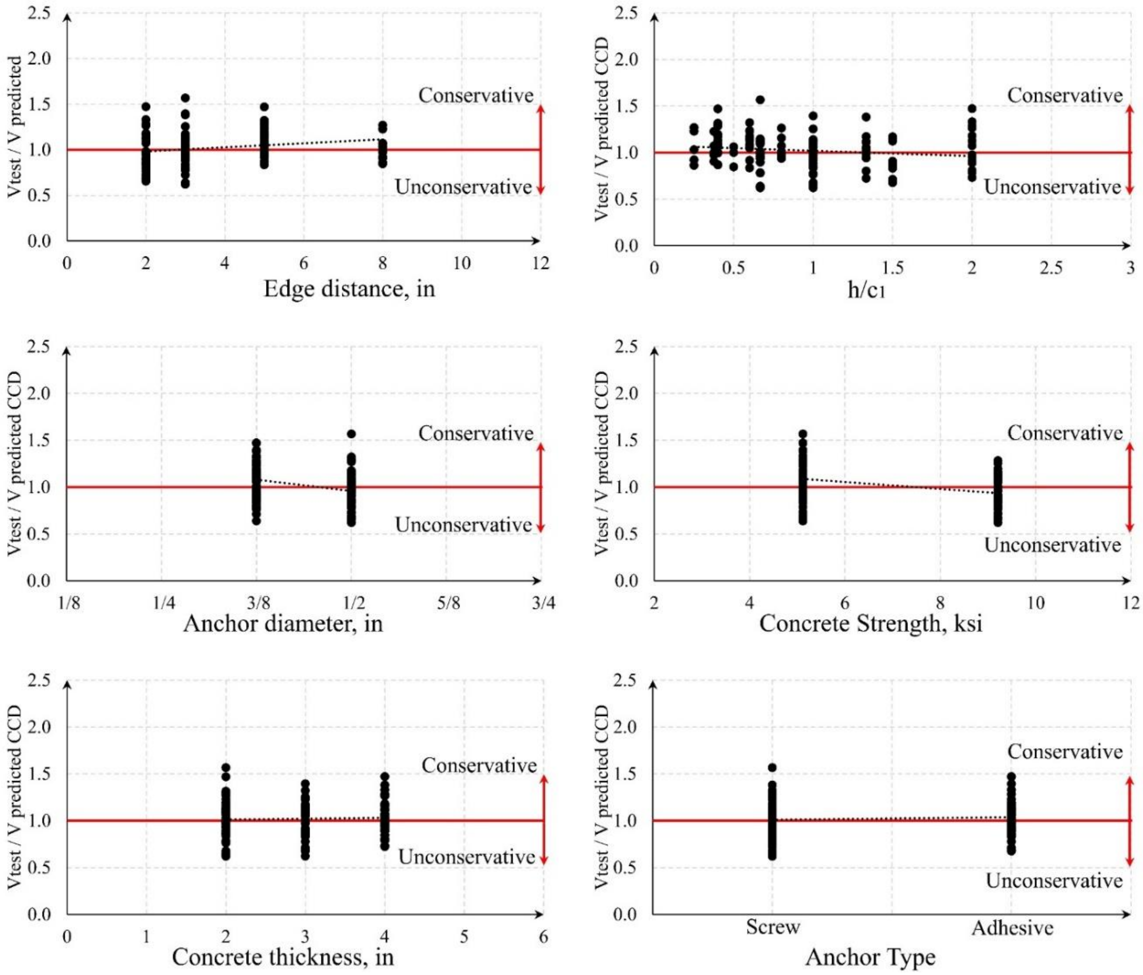

Fig. 5-13. Ratio of tested to predicted capacity versus experimental variables (Note: 1 in. = 25.4 mm; 1 ksi = 6.895 MPa).

5.8 Design Model

When experimental data are available it is common practice for concrete anchorage designs to be based on the 5% lower fractile and 90% confidence level of the data. Eq. 5-6 is used to determine 5% fractile factor, where F_m is the mean value equation, ν is the COV, and the K value is a factor factors for one-sided tolerance limits for normal distributions, corresponding to a 5% probability of non-exceedance with a confidence of

90% (Owen 1963). Following this approach, the proposed design equation for shear-loaded through-thickness single anchors is given in Eq. 5-7. Fig. 5-14 shows the ratio of tested capacity to the 5% fractile predicted capacity. The figure demonstrating that the design model produces conservative results for all data in the test program.

$$F_{5\%} = F_m\,(1 - K\,\nu) \qquad \text{Eq. 5-6}$$

$$V_b = 8.6\left(\frac{l_e}{d_o}\right)^{0.2}\sqrt{d_o}\ \ \sqrt{f'_c}\,(c_1)^{1.5} \qquad \text{Eq. 5-7}$$

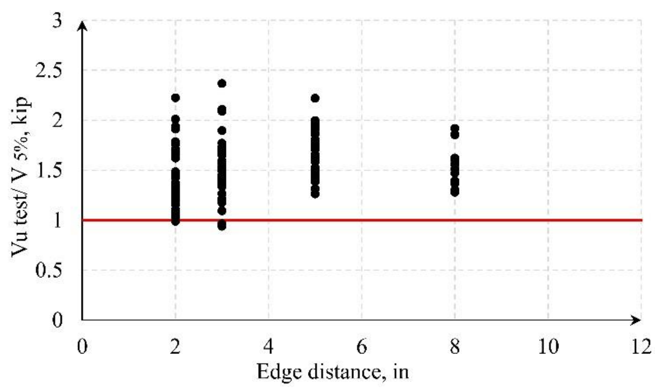

Fig. 5-14. Ratio of tested to design model based on 5% fractile.

5.9 Conclusions

This study investigated the behavior and capacity of screw and adhesive anchors embedded in thin concrete members subjected to shear load towards the free edge. Experimental data were compared to the Concrete Capacity Design method and a thickness modification factor was proposed to improve the model fit. A design model based on 5% lower fractile and 90% confidence was also developed.

The CCD method can be applied to design the single screw and adhesive anchors with full embedment depth in thin concrete members by considering the following:

1. Full thickness drilling by rotary- hammer drill causes the concrete to blow at the back-face. This phenomena will result in a reduction in the capacity of screw anchors relative to adhesive anchors. Adhesive anchors were not affected by blowout as the adhesive fills the cracks and fractures that form due to drilling. To account for this difference between the screw and adhesive anchors, the shear load transfer length for screw anchors should be calculated according the reduced embedment depth given in Eq. 3-1. For adhesive anchors, the shear load transfer length should be set equal to the concrete member thickness.
2. Anchor capacities in the test program were not directly proportional to the member thickness which resulted in an underestimation of the anchor capacity when utilizing the CCD method. The thickness modification factor in ACI-318 is intended to correct for this underestimation, however, for the anchors in the experimental program the factor overcorrected leading to unconservative theoretical values. The revised thickness modification factor presented in Eq. 5-5 should be used for anchors in thin concrete member with full thickness embedment depth.
3. By modifying CCD according to items 1 and 2 above, the average experimental-to-calculated ratio (bias) becomes 1.0 with a COV of 0.18. The same modifications have been considered in the 5% fractile design model presented in Eq. 5-7.

   The following should be considered as the limits of the design model unless additional testing is provided:

   Anchor diameter = 3/8 to 1/2 in.

Concrete strength = 5.5 to 8.7 ksi

Concrete thickness = 2 to 4 in.

5.10 References

ASTM E488/E488M-15 Standard Test Methods for Strength of Anchors in Concrete Elements, ASTM International, West Conshohocken, PA, 2015, https://doi.org/10.1520/E0488_E0488M-15.

Eligehausen, R.; Fuchs, W.; Hofmann, J. (2004): Shear towards the free edge – an example using ACI 318-02, Appendix D. Discussion of the paper by Burdette, E. G. and Zisi, N. in Concrete International, March 2004.

Eligehausen, R.; Mallee, R.; and Silva, J., Anchorage in Concrete Construction, Ernst & Sohn, Berlin, Germany, 2006, 391 pp.

Fuchs, W.; Eligehausen, R.; and Breen, J., "Concrete Capacity Design (CCD) Approach for Fastening to Concrete," ACI Structural Journal, V. 92, No. 1, Jan.-Feb. 1995, pp. 73-94.

Fuchs, W., "Tragverhalten von Befestigungen unter Querlast im ungerissenen Beton (Behaviour of Fastenings under Shear Load in Uncracked Concrete)," Mitteilungen No. 1990/2, Institut fiir Werkstoffe im Bauwesen, Universitlit Stuttgart, 1990

Owen, Donald B. Factors for one-sided tolerance limits and for variables sampling plans. No. SCR-607. Sandia Corp., Albuquerque, N. Mex., 1963.

SUMMARY AND CONCLUSIONS

6.1 Summary of Research

This dissertation is motivated by the desire for using post-installed anchors in thin concrete members, such as sandwich panels. Current design standards and specifications have limitations on the minimum embedment depths and minimum member thickness that prevent engineers from designing post-installed anchors in thin concrete members (Fig. 6-1). In addition, these limitations do not allow full thickness embedment anchors.

To investigate the capacity and behavior of single screw and adhesive anchors embedded in uncracked thin concrete members with full embedment depth (Fig. 6-1), three experimental programs were conducted. Experimental programs one and two investigate the tensile capacity and behavior of screw and adhesive anchors respectively. Variables included are concrete strength, concrete member thickness, anchor diameter, and anchor manufacturer. The obtained data were used to develop and verify behavioral models and design models based on the 5% fractile. The third experimental program investigated the capacity and behavior of screw and adhesive anchors subjected to shear loads towards the free edge. Variables included concrete strength, concrete thickness, anchor type, anchor diameter, and edge distance. Similarly, the obtained data were used to develop a design procedure for anchors with full embedment depth under shear loads.

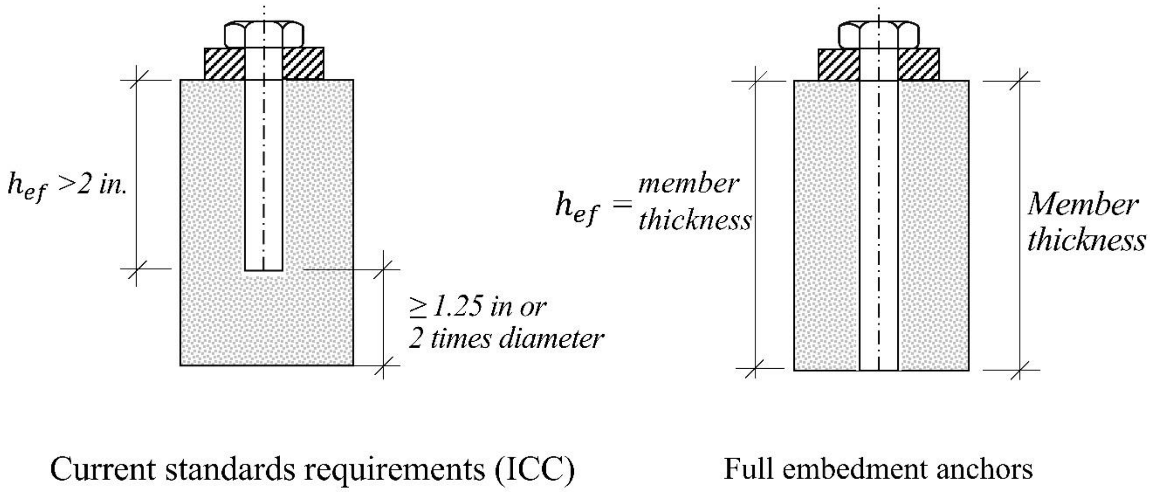

Fig. 6-1. Full embedment anchors vs. current standards requirements on embedment depth.

6.2 Back-face Blowout

Back-face blowout is cited as a reason for prohibiting the embedment of anchors in the full thickness of a concrete member. This phenomenon occurs when the hammering action of a rotary-hammer drill breaks a cone out of the concrete as the drill bit approaches the back-face (Fig. 6-2). A total of 50 holes were drilled and investigated to evaluate the size of blowout cones. It was observed that holes drilled with smaller drill bits tended to have narrower blowout cones. Blowout widths range from 3.5-5.0 in. (89-127 mm). Depth of the blowout cones ranged from 0.65 to 0.95 in. (17.78-24.13 mm). Critically, it was observed that for these tests that blowout depth and was not a function of the drill bit diameter.

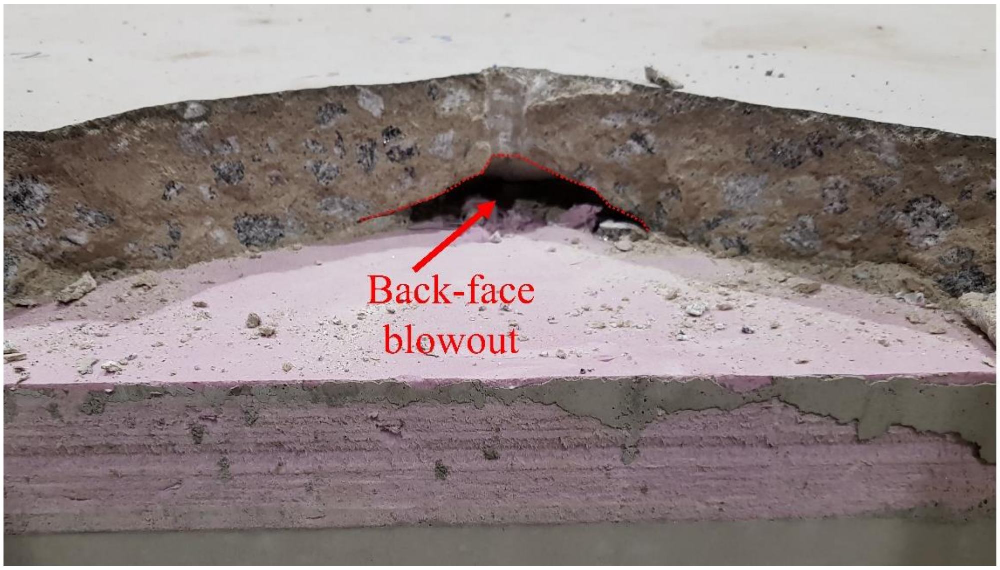

Fig. 6-2. Back-face blowout due to drilling through the concrete layer thickness.

6.3 Tensile Capacity of Single Screw and Adhesive Anchors with Full Thickness Embedment

Screw anchors (n=100) and adhesive anchors (n=101) were subjected to tensile loading while being embedded in the full thickness of the concrete members. For screw anchors the back-face blowout phenomenon resulted in a reduction in the tensile capacity because the blowout reduced the effective embedment depth of the anchor. The proposed behavioral and design models for screw anchors utilize the Concrete Capacity Design (CCD) method with reduced embedment depth to account for the blowout effect (Fig. 6-3).

For adhesive anchors, the threaded rod were embedded the full thickness of the concrete member and extended into the insulation layer by one inch. While back-face blowout occurred in adhesive anchor specimens it did not negatively impact the capacity. This is because the adhesive filled the cracks and fractures due to drilling and effectively repaired the blown-out portion of the back face. In addition, the adhesive formed a base in the insulation layer that increased the breakout cone size. The proposed behavioral and design models for adhesive anchors are similar to those for screw anchors except that the reduced embedment is not applied. Instead, the embedment depth for adhesive anchors is equal to the concrete member thickness. Fig. 6-3 illustrate the application of the design model for screw an adhesive anchors. Fig. 6-4 and 6-5 show the experimental data along with the behavioral and design models for screw and adhesive anchors respectively. These figures demonstrate that the behavioral models are within the experimental scatter and that the design models are conservative in all cases relative to the experiments.

It was observed that the capacity and failure mode of screw anchors was affected by the threads geometry. Anchors with high undercut degree (a dimension representing the degree of interlock between threads and concrete) have a higher capacity and fail in concrete breakout, while anchors with small undercut degree have lower capacity and tend to fail in pullout.

Adhesive anchors provided superior tensile capacity under similar conditions as compared to screw anchors. Adhesive anchors provided consistent performance independent of the adhesive supplier, unlike screw anchors wherein the failure mode and capacity were dependent on the undercut degree which varied by product.

Therefore, the author recommends that adhesive anchors be used in lieu of screw anchors in most situations. Screw anchors are typically more efficient to install and may be reasonable for some temporary fixtures, non-structural elements, and lightly loaded connections.

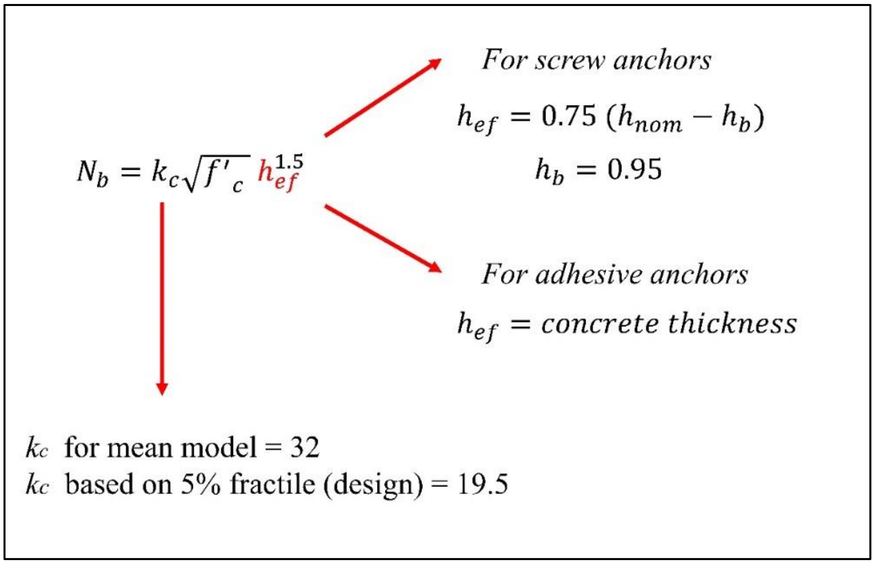

Fig. 6-3. Proposed tensile design model for screw and adhesive anchors with full embedment depth. Variables as defined in chapter 3.

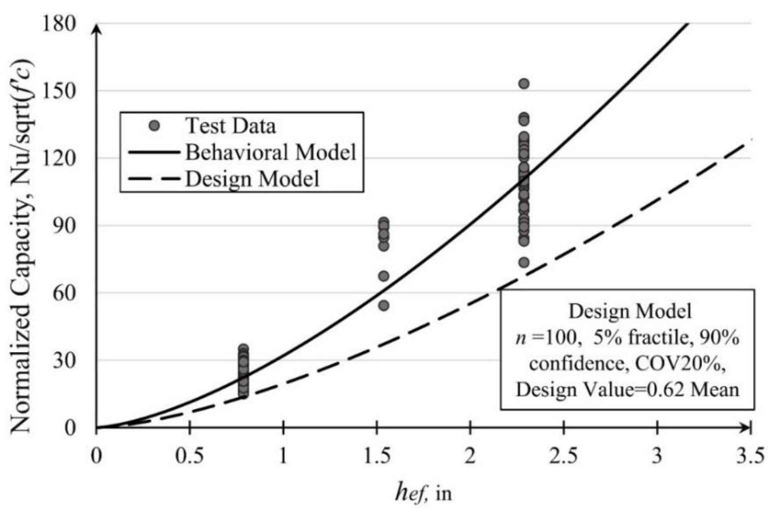

Fig. 6-4. Proposed behavior and design models for screw anchors in uncracked concrete as function of effective depth. (Note: 1 in. = 25.4 mm.; 1 ksi = 6.895 MPa).

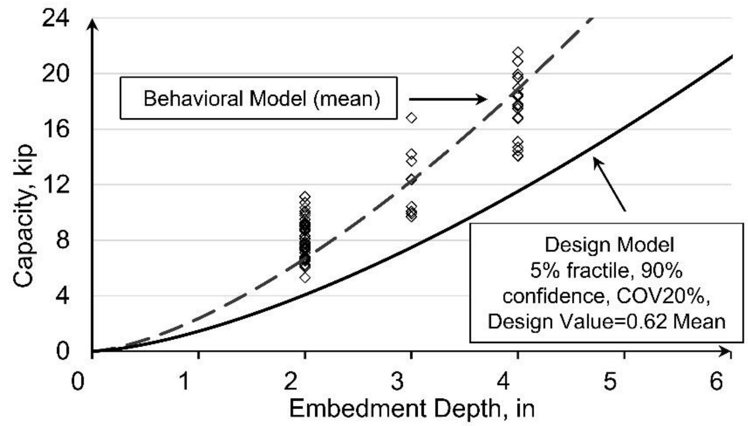

Fig. 6-5. Proposed behavior and design models for adhesive anchors in uncracked concrete as function of effective depth. (Note: 1 in. = 25.4 mm.; 1 ksi = 6.895 MPa).

6.4 Shear Capacity of Single Screw and Adhesive Anchors with Full Thickness Embedment

Concrete back-face blowout effect is also present in shear loaded anchors with full thickness embedment. Because adhesive repairs the blowout adhesive anchors have higher stiffness than screw anchors as the anchor is restrained along the entire member thickness. In contrast, screw anchors are unrestrained in the blowout region which leads to lower stiffness. This higher stiffness enables adhesive anchors to distribute stresses over a larger area and hence have higher capacity. The increased shear capacity of adhesive anchors relative to screw anchors is more subtle than for tensile capacity. On average adhesive anchors shear capacity are 17% higher than screw anchors

It is proposed to utilize the CCD method for designing anchors subjected to shear loads with some modifications. First, in consideration of the effect of back-face blowout it is proposed to use a reduced shear transfer length for screw anchors. The reduced transfer length for shear is the same as the reduced embedment depth for tension. The thickness modification factor is also revised. Fig. 6-6 summarizes the proposed modifications on CCD method. Fig. 6-7 shows the ratio of the test-to-predicted data. As shown in Fig. 6-7 the proposed modifications result in a consistent level of accuracy for the range of tested edge distances.

Shear capacity $$V_{cb} = \frac{A_{Vc}}{A_{Vco}} \boldsymbol{V_b} \ \boldsymbol{\psi_{h,v}}$$

$$V_b = kc\left(\frac{l_e}{d_a}\right)^{0.2} \sqrt{d} \ \lambda \sqrt{f'c} \ (C_{a1})^{1.5}$$

$l_e \ for \ screw \ anchors = 0.75 * (h_{ef} - 0.95)$

$l_e \ for \ adhesive \ anchors = concrete \ thickness$

kc for mean model = 13

kc based on 5% fractile (design) = 8.6

Revised thickness modification factor $$\psi_{h,v} = \left(\frac{1.5 \ c_{a1}}{h}\right)^{\frac{1}{5}}$$

Fig. 6-6. Proposed shear design model for screw and adhesive anchors with full embedment depth.

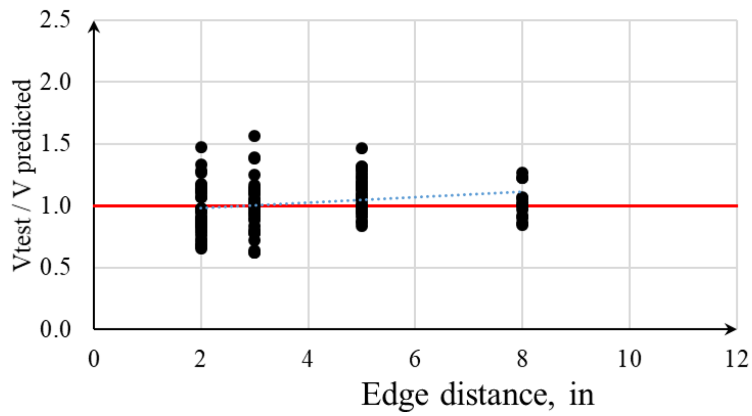

Fig. 6-7. Experimental to predicted shear capacity for anchors fully embedded in thin concrete.

6.5 Future Work

This dissertation elucidates the behavior and capacity of single screw and adhesive anchors fully embedded in thin concrete members under tensile and shear loads. Future studies can be built upon this work to achieve a more comprehensive understanding of anchors in thin concrete members with full embedment depth. The following are suggested for future research:

- Future study can investigate the capacity and behavior of multi-anchor groups with different spacing between anchors to verify the generality of the 35^{o} angle cone assumption to other situations.
- Future research may expand the range of the tested variables in this dissertation.
- Future researches may investigate the capacity of anchors embedded in prestressed concrete members. This is particularly relevant because sandwich panels are often prestressed.

- Future study may consider the behavior of anchors in thin concrete members under dynamic loading.
- Future studies may investigate the behavior of anchors under combined loading (tension and shear).
- Further study on installation orientation (horizontal and overhead) of screw anchors., It is suspected that installation orientation will not affect screw anchors behavior and capacity, however, this opinion should be confirmed through testing.

APPENDICES

7.1 Appendix A

Screw Anchors Pullout Tests Data

Test ID	Anchor Brand	Diameter (in)	Concrete Thickness (in)	Concrete Strength (Psi)	Load (lbs.)	Failure mode
1	A	0.375	4	6700	7515	Breakout/pullout
2	A	0.5	4	6700	9400	Breakout/pullout
3	C	0.375	4	6700	8115	Pullout failure
4	C	0.5	4	6700	10480	Breakout/pullout
5	B	0.375	4	6700	7588	Concrete Breakout
6	B	0.5	4	6700	11296	Concrete Breakout
7	C	0.375	4	6700	6898	Pullout failure
8	C	0.5	4	6700	9127	Pullout failure
9	A	0.375	4	6700	8710	Pullout failure
10	A	0.5	4	6700	10142	Pullout failure
11	B	0.375	4	6700	11180	Breakout/pullout
12	B	0.5	4	6700	9487	Concrete Breakout
13	A	0.375	4	6700	8411	Breakout/pullout
14	A	0.5	4	6700	6792	Breakout/pullout
15	B	0.375	4	6700	10453	Concrete Breakout
16	B	0.5	4	6700	10404	Concrete Breakout
17	C	0.375	4	6700	7913	Pullout failure
18	C	0.5	4	6700	9314	Concrete Breakout
19	A	0.375	4	8700	8645	Breakout/pullout
20	A	0.5	4	8700	9205	Concrete Breakout
21	C	0.375	4	8700	8172	Pullout failure

22	C	0.5	4	8700	10149	Breakout/pullout
23	B	0.375	4	8700	10324	Breakout/pullout
24	B	0.5	4	8700	10470	Concrete Breakout
25	C	0.375	4	8700	6858	Pullout failure
26	C	0.5	4	8700	10272	Breakout/pullout
27	A	0.375	4	8700	10039	Breakout/pullout
28	A	0.5	4	8700	10669	Breakout/pullout
29	B	0.375	4	8700	11933	Breakout/pullout
30	B	0.5	4	8700	11723	Concrete Breakout
31	A	0.375	4	8700	10013	Concrete Breakout
32	A	0.5	4	8700	11230	Breakout/pullout
33	B	0.375	4	8700	10599	Concrete Breakout
34	B	0.5	4	8700	14281	Concrete Breakout
35	C	0.375	4	8700	8682	Pullout failure
36	C	0.5	4	8700	9167	Pullout failure
37	C	0.375	4	8700	8506	Breakout/pullout
38	C	0.5	4	8700	11541	Pullout failure
39	A	0.375	4	8700	9680	Breakout/pullout
40	A	0.5	4	8700	10287	Breakout/pullout
41	B	0.375	4	8700	10527	Concrete Breakout
42	B	0.5	4	8700	11367	Concrete Breakout
43	C	0.375	4	6700	7322	Pullout failure
44	C	0.5	4	6700	9491	Pullout failure
45	A	0.375	4	6700	9483	Breakout/pullout
46	A	0.5	4	6700	8899	Concrete Breakout
47	B	0.375	4	6700	8980	Breakout/pullout
48	B	0.5	4	6700	10599	Breakout/pullout
49	A	0.375	2	8700	2260	Concrete Breakout

50	A	0.5	2	8700	2100	Concrete Breakout
51	A	0.375	2	8700	1804	Concrete Breakout
52	C	0.375	2	8700	2007	Concrete Breakout
53	C	0.5	2	8700	1794	Concrete Breakout
55	B	0.375	2	8700	1529	Concrete Breakout
57	B	0.375	2	8700	2165	Concrete Breakout
58	A	0.5	2	8700	1612	Concrete Breakout
59	A	0.375	2	8700	1400	Concrete Breakout
60	A	0.5	2	8700	1671	Concrete Breakout
61	C	0.5	2	8700	1564	Concrete Breakout
62	C	0.375	2	8700	1407	Concrete Breakout
63	C	0.5	2	8700	2467	Concrete Breakout
64	B	0.5	2	8700	1851	Concrete Breakout
65	B	0.375	2	8700	2837	Concrete Breakout
66	B	0.5	2	8700	2105	Concrete Breakout
67	A	0.375	2	6700	1752	Concrete Breakout
68	A	0.5	2	6700	1530	Concrete Breakout
69	A	0.375	2	6700	2862	Concrete Breakout
70	C	0.375	2	6700	1940	Concrete Breakout
71	C	0.5	2	6700	1881	Concrete Breakout
72	C	0.375	2	6700	1225	Concrete Breakout
74	B	0.5	2	6700	2270	Concrete Breakout
76	A	0.5	2	6700	2242	Concrete Breakout
77	A	0.375	2	6700	2683	Concrete Breakout
78	A	0.5	2	6700	2698	Concrete Breakout
79	C	0.5	2	6700	2047	Concrete Breakout
80	C	0.375	2	6700	2338	Concrete Breakout
81	C	0.5	2	6700	2005	Concrete Breakout

82	B	0.5	2	6700	2110	Concrete Breakout
83	B	0.375	2	6700	2619	Concrete Breakout
84	B	0.5	2	6700	2354	Concrete Breakout
85	A	0.375	2	8700	1712	Concrete Breakout
86	A	0.5	2	8700	1642	Concrete Breakout
87	C	0.375	2	8700	2041	Concrete Breakout
88	C	0.5	2	8700	1922	Concrete Breakout
89	B	0.375	2	8700	2489	Concrete Breakout
90	B	0.5	2	8700	2288	Concrete Breakout
91	A	0.375	2	6700	2489	Concrete Breakout
92	A	0.5	2	6700	2044	Concrete Breakout
93	C	0.375	2	8700	2579	Concrete Breakout
94	C	0.5	2	6700	2450	Concrete Breakout
95	B	0.375	2	6700	2125	Concrete Breakout
96	B	0.5	2	6700	2394	Concrete Breakout
97	A	0.375	3	5450	5972	Breakout/pullout
98	A	0.5	3	5450	4977	Breakout/pullout
99	C	0.375	3	5450	4011	Breakout/pullout
100	C	0.5	3	5450	6589	Breakout/pullout
102	B	0.5	3	5450	6748	Concrete Breakout
103	C	0.375	3	5450	6249	Breakout/pullout
104	A	0.5	3	5450	6636	Breakout/pullout
105	A	0.375	3	5450	6364	Concrete Breakout

7.2 Appendix B

Adhesive Anchors Pullout Tests Data

Test ID	Adhesive Brand	Anchor Diameter	Member Thickness	Concrete Strength (Psi)	Load (lbs.)	Failure mode
1	A	3/8	4	5450	10369	Steel Yield
2	A	1/2	4	5450	18951	Breakout/pullout
3	A	3/8	4	5450	10345	Steel Yield
4	A	1/2	4	5450	17657	Breakout/pullout
5	C	3/8	4	5450	11738	Steel Yield
6	C	1/2	4	5450	16770	Breakout/pullout
7	C	3/8	4	5450	10359	Steel Yield
8	C	1/2	4	5450	18445	Breakout/pullout
9	B	3/8	4	5450	10821	Steel Yield
10	B	1/2	4	5450	19712	Breakout/pullout
11	B	3/8	4	5450	9480	Steel Yield
12	B	1/2	4	5450	16831	Breakout/pullout
13	A	3/8	4	5450	N/A	Steel Yield
14	A	1/2	4	5450	19742	Breakout/pullout
15	C	3/8	4	5450	N/A	Steel Yield
16	C	1/2	4	5450	20881	Breakout/pullout
17	B	3/8	4	5450	N/A	Steel Yield
18	B	1/2	4	5450	21548	Breakout/pullout
19	A	3/8	4	5450	N/A	Steel Yield
20	A	1/2	4	5450	19954	Breakout/pullout
21	A	3/8	4	5450	10252	Steel Yield
22	A	1/2	4	5450	14445	Breakout/pullout

23	A	3/8	4	5450	11470	Steel Yield
24	A	1/2	4	5450	17777	Breakout/pullout
25	C	3/8	4	5450	10288	Steel Yield
26	C	1/2	4	5450	14241	Breakout/pullout
27	C	3/8	4	5450	10404	Steel Yield
28	C	1/2	4	5450	15279	Breakout/pullout
29	B	3/8	4	5450	10785	Steel Yield
30	B	1/2	4	5450	18683	Breakout/pullout
31	B	3/8	4	5450	10306	Steel Yield
32	B	1/2	4	5450	18566	Breakout/pullout
33	A	3/8	4	5450	11848	Steel Yield
34	A	1/2	4	5450	17683	Breakout/pullout
35	C	3/8	4	5450	11377	Steel Yield
36	C	1/2	4	5450	17862	Breakout/pullout
37	B	3/8	4	5450	9244	Steel Yield
38	B	1/2	4	5450	14210	Breakout/pullout
39	A	3/8	4	5450	8380	Steel Yield
40	A	1/2	4	5450	14850	Breakout/pullout
41	A	3/8	3	5450	9698	Concrete Breakout
42	A	1/2	3	5450	14206	Concrete Breakout
43	C	3/8	3	5450	10067	Concrete Breakout
44	C	1/2	3	5450	16808	Concrete Breakout
45	B	3/8	3	5450	10419	Concrete Breakout
46	A	3/8	2	5450	8653	Concrete Breakout

47	A	1/2	2	5450	6794	Concrete Breakout
48	A	3/8	2	5450	10081	Concrete Breakout
49	A	1/2	2	5450	10717	Concrete Breakout
50	C	3/8	2	5450	8960	Concrete Breakout
51	C	1/2	2	5450	8308	Concrete Breakout
52	C	3/8	2	5450	7690	Concrete Breakout
53	C	1/2	2	5450	8101	Concrete Breakout
54	B	3/8	2	5450	6503	Concrete Breakout
55	B	1/2	2	5450	9518	Concrete Breakout
56	B	3/8	2	5450	8313	Concrete Breakout
57	B	1/2	2	5450	8866	Concrete Breakout
58	A	3/8	2	5450	6763	Concrete Breakout
59	A	1/2	2	5450	6674	Concrete Breakout
60	C	3/8	2	5450	6068	Concrete Breakout
61	C	1/2	2	5450	7431	Concrete Breakout
62	B	3/8	2	5450	6082	Concrete Breakout
63	B	1/2	2	5450	5307	Concrete Breakout
64	B	3/8	2	5450	8131	Concrete Breakout

65	B	1/2	2	5450	6558	Concrete Breakout
66	A	3/8	2	5450	7092	Concrete Breakout
67	A	1/2	2	5450	8823	Concrete Breakout
68	A	3/8	2	5450	7303	Concrete Breakout
69	A	1/2	2	5450	9095	Concrete Breakout
70	C	3/8	2	5450	9777	Concrete Breakout
71	C	1/2	2	5450	11135	Concrete Breakout
72	C	3/8	2	5450	7729	Concrete Breakout
73	C	1/2	2	5450	7532	Concrete Breakout
74	B	3/8	2	5450	7079	Concrete Breakout
75	B	1/2	2	5450	9913	Concrete Breakout
76	B	3/8	2	5450	8741	Concrete Breakout
77	B	1/2	2	5450	10342	Concrete Breakout
78	A	3/8	2	5450	7883	Concrete Breakout
79	A	1/2	2	5450	9197	Concrete Breakout
80	C	3/8	2	5450	7375	Concrete Breakout
81	C	1/2	2	5450	8656	Concrete Breakout
82	B	3/8	2	5450	6221	Concrete Breakout

83	B	1/2	2	5450	9258	Concrete Breakout
84	B	3/8	2	5450	9000	Concrete Breakout
85	B	1/2	2	5450	9083	Concrete Breakout
86	B	3/8	3	5450	12366	Concrete Breakout
87	B	1/2	3	5450	13690	Concrete Breakout
88	C	3/8	3	5450	9914	Concrete Breakout
89	C	1/2	3	5450	12396	Concrete Breakout
90	C	1/2	2	9209.6	9990	Concrete breakout
91	C	1/2	2	9209.6	8470	Concrete breakout
92	C	3/8	2	9209.6	8000	Concrete breakout
93	C	3/8	2	9209.6	6714	Concrete breakout
94	C	1/2	2	9209.6	8654	Concrete breakout
95	C	1/2	2	9209.6	10668	Concrete breakout
96	C	1/2	4	9209.6	19200	Steel Yield
97	C	1/2	4	9209.6	20458	Steel Yield
98	C	1/2	4	9209.6	20644	Steel Yield
99	C	1/2	4	9209.6	N/A	Steel Yield
100	C	1/2	4	9209.6	N/A	Steel Yield
101	C	1/2	4	9209.6	N/A	Steel Yield

7.3 Appendix C

Anchors Shear Tests Data

Test ID	Anchor Type	Anchor Dia. (in)	Member Thickness (in)	Concrete Strength (psi)	Load (lbs.)	Load (lbs.)
0	Screw	3/8	2	5117.2	1450	1449.7
2	Screw	3/8	2	5117.2	2573	2573.0
4	Screw	3/8	2	5117.2	3374	3374.0
5	Screw	3/8	2	5117.2	1773	1773.0
6	Screw	3/8	2	5117.2	1147	1147.0
8	Screw	3/8	2	5117.2	2788	2788.0
11	Screw	3/8	2	9209.6	1384	1384.0
12	Screw	3/8	2	9209.6	1610	1610.0
13	Screw	3/8	2	9209.6	1877	1877.0
14	Screw	3/8	2	9209.6	2680	2680.0
15	Screw	3/8	2	9209.6	3424	3424.0
16	Screw	3/8	2	9209.6	3772	3772.0
17	Screw	3/8	2	9209.6	4411	4411.0
18	Screw	1/2	2	5117.2	1388	1387.7
19	Screw	1/2	2	5117.2	1423	1423.3
20	Screw	1/2	2	5117.2	3065	3064.6
21	Screw	1/2	2	5117.2	1977	1976.6
22	Screw	1/2	2	5117.2	3636	3635.8
23	Screw	1/2	2	5117.2	3595	3594.7
24	Screw	1/2	2	5117.2	4932	4932.2
25	Screw	1/2	2	9209.6	1293	1292.9
26	Screw	1/2	2	9209.6	1339	1339.0
27	Screw	1/2	2	9209.6	1631	1630.8

28	Screw	1/2	2	9209.6	2060	2060.3
29	Screw	1/2	2	9209.6	3266	3266.4
30	Screw	1/2	2	9209.6	3255	3254.9
31	Screw	1/2	2	9209.6	4493	4493.2
32	Screw	3/8	3	5117.2	1857	1857.3
33	Screw	3/8	3	5117.2	2400	2399.9
34	Screw	3/8	3	5117.2	3215	3215.4
35	Screw	3/8	3	5117.2	2874	2873.6
36	Screw	3/8	3	5117.2	5013	5012.5
37	Screw	3/8	3	5117.2	4991	4991.2
38	Screw	3/8	3	5117.2	6915	6914.9
39	Screw	3/8	3	9209.6	2599	2598.6
40	Screw	3/8	3	9209.6	3334	3333.6
41	Screw	3/8	3	9209.6	4775	4774.8
42	Screw	3/8	3	9209.6	4334	4333.8
43	Screw	3/8	3	9209.6	6354	6354.2
44	Screw	3/8	3	9209.6	5923	5922.8
45	Screw	3/8	3	9209.6	8110	8110.2
46	Adhesive	3/8	2	5117.2	1826	1826.4
47	Adhesive	3/8	2	5117.2	1599	1599.2
48	Adhesive	3/8	2	5117.2	2021	2020.7
49	Adhesive	3/8	2	5117.2	1938	1938.3
50	Adhesive	3/8	2	5117.2	4541	4540.9
51	Adhesive	3/8	2	5117.2	3284	3284.3
52	Adhesive	3/8	2	5117.2	5281	5281.0
53	Adhesive	3/8	2	9209.6	1865	1864.6
54	Adhesive	3/8	2	9209.6	2400	2400.2

55	Adhesive	3/8	2	9209.6	2790	2790.2
56	Adhesive	3/8	2	9209.6	3326	3325.6
57	Adhesive	3/8	2	9209.6	4958	4958.1
58	Adhesive	3/8	2	9209.6	4954	4953.9
59	Adhesive	3/8	2	9209.6	Steel Yield	Steel Yield
60	Adhesive	1/2	2	5117.2	1737	1736.8
61	Adhesive	1/2	2	5117.2	1486	1486.3
62	Adhesive	1/2	2	5117.2	2574	2574.4
63	Adhesive	1/2	2	5117.2	2652	2652.2
64	Adhesive	1/2	2	5117.2	3941	3941.5
65	Adhesive	1/2	2	5117.2	3809	3808.7
66	Adhesive	1/2	2	5117.2	4831	4830.6
74	Adhesive	3/8	3	5117.2	2856	2856.1
75	Adhesive	3/8	3	5117.2	2765	2764.8
76	Adhesive	3/8	3	5117.2	3643	3643.4
77	Adhesive	3/8	3	5117.2	4523	4522.9
78	Adhesive	3/8	3	5117.2	5250	5250.0
79	Adhesive	3/8	3	5117.2	4915	4915.0
80	Adhesive	3/8	3	5117.2	Steel Yield	Steel Yield
81	Adhesive	3/8	3	9209.6	2721	2720.9
82	Adhesive	3/8	3	9209.6	2334	2333.9
83	Adhesive	3/8	3	9209.6	4364	4363.7
84	Adhesive	3/8	3	9209.6	3847	3846.7
85	Adhesive	3/8	3	9209.6	Steel Yield	Steel Yield
86	Adhesive	3/8	3	9209.6	Steel Yield	Steel Yield
87	Adhesive	3/8	3	9209.6	Steel Yield	Steel Yield

88	Screw	3/8	4	5117.2	2925	2925.1
89	Screw	3/8	4	5117.2	2730	2729.7
90	Screw	3/8	4	5117.2	5345	5345.5
91	Screw	3/8	4	5117.2	4530	4530.4
92	Screw	3/8	4	5117.2	6986	6985.8
93	Screw	3/8	4	5117.2	6400	6399.6
94	Screw	3/8	4	5117.2	Steel Yield	Steel Yield
95	Screw	3/8	4	9209.6	3491	3491.4
96	Screw	3/8	4	9209.6	2961	2961.4
97	Screw	3/8	4	9209.6	4160	4160.4
98	Screw	3/8	4	9209.6	5471	5470.7
99	Screw	3/8	4	9209.6	7485	7484.6
100	Screw	3/8	4	9209.6	7955	7955.3
101	Screw	3/8	4	9209.6	Steel Yield	Steel Yield
102	Screw	1/2	4	5117.2	1846	1846.2
103	Screw	1/2	4	5117.2	1990	1989.7
104	Screw	1/2	4	5117.2	4373	4373.1
105	Screw	1/2	4	5117.2	4264	4264.5
106	Screw	1/2	4	5117.2	5649	5648.8
107	Screw	1/2	4	5117.2	5786	5785.9
108	Screw	1/2	4	5117.2	8891	8891.2
109	Screw	1/2	4	9209.6	3072	3072.4
110	Screw	1/2	4	9209.6	2733	2732.8
111	Screw	1/2	4	9209.6	4093	4092.9
112	Screw	1/2	4	9209.6	5592	5591.5
113	Screw	1/2	4	9209.6	7720	7720.2
115	Screw	1/2	4	9209.6	9506	9505.6

116	Screw	1/2	3	5117.2	2103	2103.2
117	Screw	1/2	3	5117.2	1576	1576.2
118	Screw	1/2	3	5117.2	3407	3406.6
119	Screw	1/2	3	5117.2	3502	3501.8
120	Screw	1/2	3	5117.2	5094	5094.5
121	Screw	1/2	3	5117.2	5843	5843.1
122	Screw	1/2	3	5117.2	6153	6152.6
123	Adhesive	3/8	4	5117.2	3593	3593.0
124	Adhesive	3/8	4	5117.2	3249	3249.3
125	Adhesive	3/8	4	5117.2	4564	4563.6
126	Adhesive	3/8	4	5117.2	4534	4534.3
127	Adhesive	3/8	4	5117.2	Steel Yield	Steel Yield
128	Adhesive	3/8	4	5117.2	Steel Yield	Steel Yield
129	Adhesive	3/8	4	5117.2	Steel Yield	Steel Yield
130	Screw	1/2	3	9209.6	2680	2680.0
131	Screw	1/2	3	9209.6	2610	2610.5
132	Screw	1/2	3	9209.6	3475	3474.9
133	Screw	1/2	3	9209.6	2581	2580.9
134	Screw	1/2	3	9209.6	6811	6811.0
135	Screw	1/2	3	9209.6	6215	6215.3
136	Screw	1/2	3	9209.6	8018	8017.8
137	Adhesive	3/8	4	9209.6	2913	2913.0
138	Adhesive	3/8	4	9209.6	4203	4202.9
139	Adhesive	3/8	4	9209.6	Steel Yield	Steel Yield
140	Adhesive	3/8	4	9209.6	Steel Yield	Steel Yield
141	Adhesive	3/8	4	9209.6	Steel Yield	Steel Yield

142	Adhesive	3/8	4	9209.6	Steel Yield	Steel Yield
143	Adhesive	3/8	4	9209.6	Steel Yield	Steel Yield
144	Adhesive	1/2	4	5117.2	2754	2753.8
145	Adhesive	1/2	4	5117.2	3025	3025.4
146	Adhesive	1/2	4	5117.2	4444	4443.6
147	Adhesive	1/2	4	5117.2	4782	4781.8
148	Adhesive	1/2	4	5117.2	6641	6641.1
150	Adhesive	1/2	4	5117.2	9371	9370.5
159	Adhesive	1/2	3	5117.2	1833	1833.4
160	Adhesive	1/2	3	5117.2	3734	3733.8
161	Adhesive	1/2	3	5117.2	3573	3572.8
162	Adhesive	1/2	3	5117.2	5447	5446.7
163	Adhesive	1/2	3	5117.2	5943	5942.8
165	Adhesive	1/2	3	9209.6	2415	2415.1
166	Adhesive	1/2	3	9209.6	3071	3071.4
167	Adhesive	1/2	3	9209.6	4356	4355.8
168	Adhesive	1/2	3	9209.6	3686	3686.4
169	Adhesive	1/2	3	9209.6	5664	5663.5
170	Adhesive	1/2	3	9209.6	6212	6211.5
171	Adhesive	1/2	3	9209.6	8530	8529.8

7.4 Appendix D

Coefficient of variation of pullout experimental data

The following graphs show the coefficient of variation of the pullout data at each concrete thickness for each data set. This COV is not to be confused of the COV of the bias which is used to select kc value. COV data is presented here for documentation.

1- Screw anchors in tension

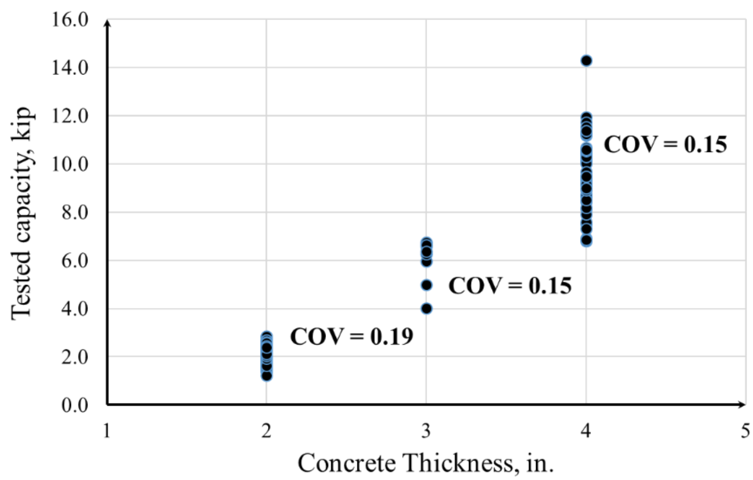

2- Adhesive anchors in tension